國立臺灣師範大學文學院地理學系

博士論文

Department of Geography
College of Liberal Arts
National Taiwan Normal University

Doctoral Dissertation

宜蘭縣環境災害脆弱度與恢復力之研究

A RESEARCH OF VULNERABILITY AND RESILIENCE TO ENVIRONMENTAL HAZARDS IN YILAN COUNTY

宋健豪

Sung, Chien-Hao

指導教授：廖學誠 博士

Advisor：Liaw, Shyue-Cherng, Ph.D.

中華民國 111 年 7 月

July 2022

摘要

本研究旨在探討台灣東北區域宜蘭縣境內,環境災害脆弱度與恢復力之空間分布模式,受到地形與降雨型態之影響,洪患與土石流為本研究區中最為常見之自然災害,本研究應用社會脆弱度指數(Social Vulnerability Index,SoVI)、社區恢復力基線指數(Baseline Resilience Indicator of Community,BRIC)、回復力-脆弱度空間剖析模式(Spatially Explicit Resilience-Vulnerability model; SERV)模式量化研究區域中對於洪患與土石流之災害脆弱度與恢復力,本研究應用主成分分析整合具相關性、共線性之變數,已提供更為簡潔之成果,除此之外,本研究應用空間自相關探討脆弱度以及恢復力之空間分布模式以及空間差異,並透過空間落遲迴歸、空間誤差迴歸以及地理加權回歸驗證 SoVI、BRIC 以及 SERV 模式之效力;,空間自相關成果顯示研究區域中之山區為極度脆弱並缺乏恢復力之區域,反之,平原中之都市區域為低脆弱度及高恢復力之區域,根據空間落遲迴歸、空間誤差迴歸以及地理加權回歸成果顯示 SoVI、BRIC 以及 SERV,就全縣尺度三項指標具尚可接受之判定係數均及解釋能力,並無顯著偏誤;就平原區域而言,三項指標均具備較佳之判定係數均及解釋能力,並無顯著偏誤;就山區而言,整體有待提升;本研究發現,宜蘭縣境內山區與平原之存在顯著之空間差異,地形條件為造成顯著空間差異的主要因素之一,研究區域內山區之海拔高度與陡峭坡度為主要影響其社、經發展障礙的主因,由於山區不利於社、經發展的因素,而使其成為極度脆弱並缺乏恢復力之區域,其他地區如平原城市地區,由於其有利於社會經濟發展的地形,而使其具備低脆弱度及高恢復力。

關鍵字:脆弱度;恢復力;社會脆弱度指數;社區恢復力基線指數;回復力-脆弱度空間剖析模式;空間自相關;空間落遲模式;空間誤差模式;地理加權迴歸;空間差異

ABSTRACT

This research aims to explore the spatial pattern of vulnerability and resilience to environmental hazards in Yilan County, northeastern Taiwan. We apply the Social Vulnerability Index (SoVI), Baseline Resilience Indicator of Community (BRIC), and Spatially Explicit Resilience-Vulnerability model (SERV) to quantify the vulnerability and resilience to environmental hazards, including flood and debris flow events, which are the most common environmental hazards in our case study area due to the features of topography and precipitation. We apply the Principal Component Analysis (PCA) to aggregate the variables with correlation and collinearity. Moreover, we use spatial autocorrelation analysis to analyze the spatial pattern and spatial difference. To validate the effectiveness of SoVI, BRIC, and SERV, we also adopted the authentic debris flow and flood events as dependent variables and also applied the Spatial Lagged Model (SLM), Spatial Error Model (SEM), and Geographically Weighted Regression (GWR). The result of spatial autocorrelation analysis shows that the mountain areas are extremely vulnerable and lack enough resilience. In contrast, the urban regions in plain areas show low vulnerability and high resilience. According to the results of SLM, SEM, and GWR, on the county-wide scale, the three indexes adopted in this research have relatively acceptable R^2, which means these three indexes have an acceptable ability to explain the occurrence of authentic events of debris flow and flood without significant bias. In plain areas, the three indexes adopted in this research have relatively higher R^2 and the ability to explain the occurrence of authentic events of debris flow and flood without significant bias. In mountain areas, overall, the R^2 and the ability to explain the occurrence of authentic events are poor. This research found that the spatial difference between the mountain and plain areas is significant. The topography is the most significant factor in the spatial difference. The high elevation and steep slopes in mountain areas are significant obstacles to socioeconomic development. This situation

causes consequences of high vulnerability and low resilience. The other regions, the urban regions in the plain areas, have favorable topography for socioeconomic development.

Keywords: Vulnerability; Resilience; Social Vulnerability Index (SoVI); Baseline Resilience Indicator of Community (BRIC); Spatially Explicit Resilience-Vulnerability model (SERV); Spatial Autocorrelation Analysis; Spatial Lagged Model (SLM); Spatial Error Model (SEM); Geographically Weighted Regression (GWR); Spatial Difference

師大

TABLE OF CONTENTS

LIST OF FIGURES

LIST OF TABLES

CHAPTER 1
INTRODUCTION

1.1 Background

The frequency of extreme climate events has increased dramatically, causing tremendous damage worldwide since the late 20th century, and these events are predicted to increase. The United Nations (UN) defined the 1990s as the International Decade for Natural Disaster Reduction, and environmental hazards have become a crucial issue for national governments. Internationally, there has been much effort has to cope with environmental hazards, such as the United Nations International Strategy for Disaster Reduction (UNISDR) or the Intergovernmental Panel on Climate Change (IPCC). In the United States, the Federal Emergency Management Agency (FEMA) announced a series of projects in the 1990s for building disaster-resistant communities in order to reduce losses due to environmental hazards.

Taiwan passed the Disaster Prevention and Protection Act in July 2000, following the notorious Jiji earthquake. This disaster leads to the establishment of the National Science and Technology Center for Disaster Reduction (NCDR) as the responsible agency for disaster reduction and management. Subsequently, there has been considerable planning and research on preventing and mitigating environmental hazards in Taiwan.

Due to Taiwan's geographic location, both typhoons and seismic events frequently occur. Typhoons are one of the most devastating environmental hazards to property and human life (Wang, 2004), and in the Western Pacific region, they typically occur from July to September. Because of climate change, both the strength and frequency of typhoons have recently increased substantially; for example, the famed typhoon Morakot triggered a rotational slide that caused the Siaolin Village event. Seismic events are another common environmental hazard in Taiwan, and, unlike typhoons, they occur with little warning. As a result, they have enormous costs to both property and human life in Taiwan, such as the 1999 ML 7.3 Jiji earthquake, 2016 ML 6.4 Meinong earthquake, and 2018 ML7.0 Hualien earthquake.

Environmental hazard and disaster management are essential to implementing disaster reduction and emergency management. Since the late 2000s, the terms 'vulnerability' and 'resilience' have been widely used in the field of environmental hazards and disaster management. The former denotes potential losses due to environmental hazards, while the latter represents the ability to recover, adapt, and evolve during or after the hazards. (Adger, 2004; Cutter, 1996; Cutter *et al.,* 2003; Cutter *et al.,* 2008; Holling, 1973; Doorn, 2015; Norris *et al.,* 2008). Both vulnerability and resilience are profoundly affected by inherent social characteristics. Based on the characteristics of vulnerability and resilience, several quantifiable indicators have been developed to measure and visualize the problem. For instance, there are the Social Vulnerability Index (SoVI), Baseline Resilience Indicator for Community (BRIC), Community Disaster Resilience Indicator (CDRI), and others.

Yilan County is in northeastern Taiwan, where it frequently bears the brunt of typhoons and seismic events. After the completion of the Hsuehshan Tunnel, connecting Yilan County to the Taipei metropolitan area, the number of tourists has grown remarkably over the past decade, increasing the exposure to environmental hazards. Consequently, environmental hazards and disaster management is a significant issues for the county government. As a result, in this research, we aim to provide a holistic and profound analysis of the social vulnerability to environmental hazards and the community's inherent resilience to environmental hazards. Furthermore, since most of the indices used in this research were built up by the socioeconomic variables, another goal is to explore the relationship between authentic environmental hazard events and socioeconomic status through multivariate regression. Moreover, a hypothesis proposes in this research is that individuals or groups with poor socioeconomic status have no choice but to select the areas where is high exposure to the environmental hazard. As a result, areas with high social vulnerability will have to encounter more environmental hazard events. On the other hand, the areas with high inherent resilience because of the better socioeconomic status will have more opportunity or selection to avoid the areas with high exposure to the environmental hazards or even alter the areas they dwell into less exposure to the environmental hazard.

1.2 Objective

This study uses quantifiable indicators to measure social vulnerability to environmental hazards and resilience at the sub-county level. Furthermore, we utilize spatial autocorrelation analysis to analyze the distribution of disaster risk areas. Last but not least, we adopt spatial multivariate regression to verify the performance and effectiveness of these indicators. The primary contributions of this study are:

(1) Most of the studies regard an administration as a single study unit. However, they ignore the difference in topography in the administration unit. Therefore, In this research, we import the concept of topography.

(2) Based on the literature review, the validation of social vulnerability and community inherent resilience to environmental hazards is lacking. As a result, this research aims to provide an integrated validation and verify the social vulnerability to environmental hazards and the community's inherent resilience to environmental hazards. Through this approach, the decision-maker will have reliable indices for further decisions formulated. The dependent variables we used are the authentic flood and debris flow events.

1.3 Organization

This study has four sections. In the first, we introduce the background, objectives, and organization of this research. The second chapter reviews some of the most relevant research on the social vulnerability to environmental hazards and resilience, along with definitions for vulnerability, resilience, SoVI, and BRIC. The third chapter explains the materials, approach, methods, and variables used. The fourth presents the results, including:

(1) Spatial distribution and spatial clusters of the SoVI;

(2) Spatial distribution and the spatial clusters of the BRIC;

(3) Through the matrix of risk combines the potential of environmental hazards and social vulnerability to environmental hazards.

(4) Results of the spatial multivariate regression.

Fig 1.1 outlines the process of this study.

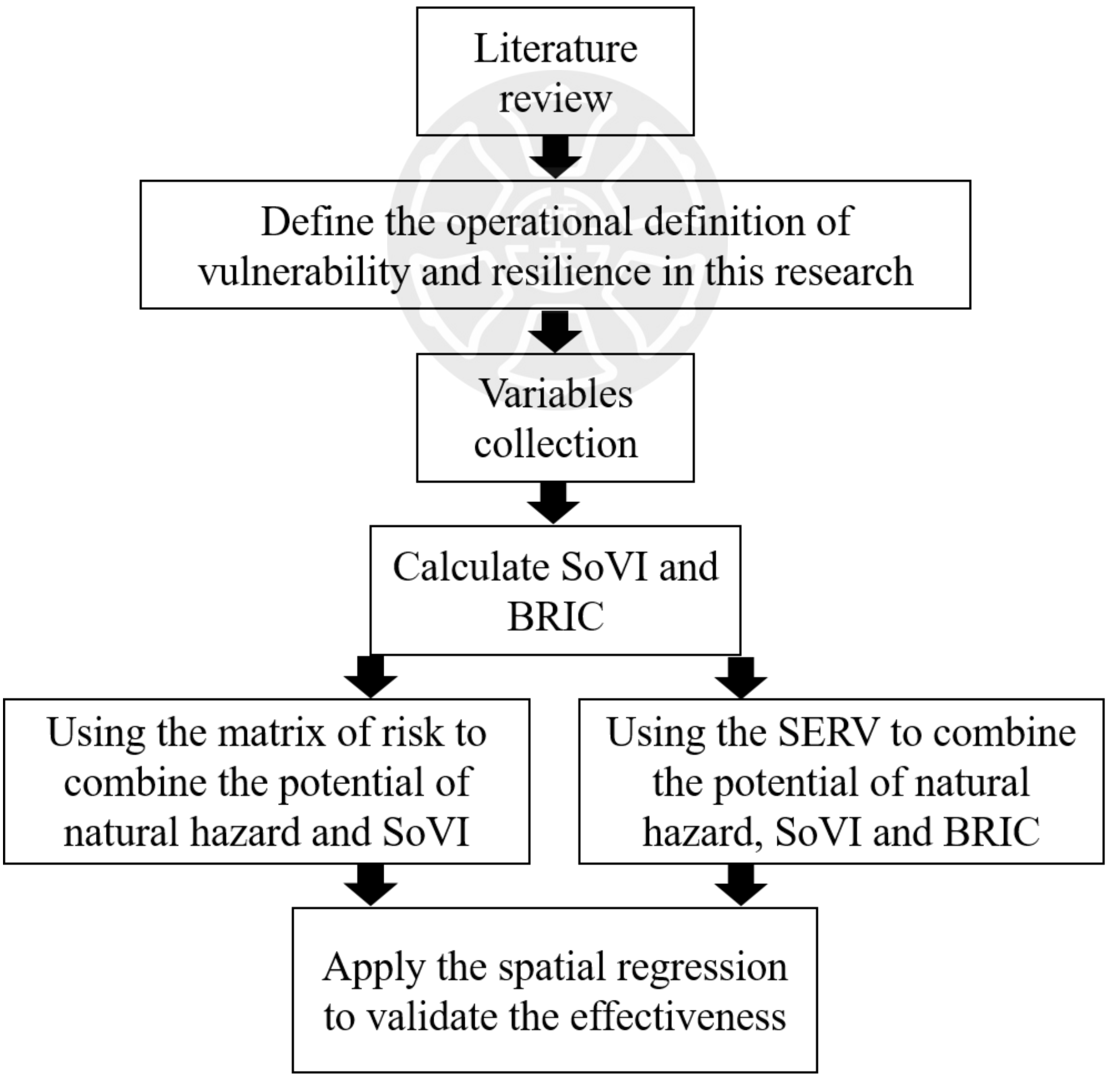

Fig. 1.1 Research process

CHAPTER 2
LITERATURE REVIEW

2.1 Vulnerability

This study applies the concept of social vulnerability to environmental hazards and the matrix of risk to investigate the potential loss of an environmental hazard in Yilan County. Although these concepts have been widely used in environmental hazard and disaster management over the past several decades, their definitions vary, and the definitions are clarified below for this study.

In general, the vulnerability can be considered pre-environmental event characteristics with an essential influence on potential loss from environmental hazards (Cutter, 1996; Cutter *et al.,* 2003; Cutter *et al.,* 2008; Doorn, 2015). These pre-event characteristics are clearly related to social aspects (Cutter, 1996) and socioeconomic conditions. Uitto (1998) defined vulnerability as an individual's trait that affects their ability to face the impacts of an environmental event and can be represented by variables such as socioeconomic indicators, age, wealth, and ethnicity. Also, according to McCarthy *et al. (2001), vulnerability is the degree to which a system is susceptible to sustaining damage from climate change,* which can characterize sensitivity, exposure, and adaptive capacity. Adger *et al.* (2004) suggest that "The vulnerability of a system, population or individual to a threat relates to its capacity to be harmed by that threat." Alternatively, vulnerability is a combination of exposure to environmental hazards and social vulnerability (Rygel *et al.,* 2006).

In this research, the concept of bringing by Cutter (1996), Cutter *et al.* (2003), and Cutter *et al.* (2008) is applied.

2.2 Quantifying and visualizing vulnerability

Summing up previous studies, we take social vulnerability to environmental hazards as potential losses from environmental hazards, and its quantification is discussed below. Most studies divide vulnerability into exposure, sensitivity, and adaptive capacity to environmental hazards (McCarthy *et al.,* 2001; Adger, 2006; Wang and Yarnal, 2012; Frazier *et al.,* 2014). Also, social fabric significantly influences sensitivity and adaptive capacity. Undoubtedly, vulnerability is clearly related to both environmental characteristics and the social context (Cutter, 1996).

The social vulnerability index (SoVI), developed by Cutter *et al.* (2003), is composed of a broad set of social fabric variables, including socioeconomic status, wealth, ethnicity, gender, disability, and age, which reflect the social fabric characteristics of an area. As a result, most of the studies applied SoVI as the concept of social vulnerability to environmental hazards. Furthermore, since the SoVI is quantifiable, it can be demonstrated in figures and analysis by the geographic information system (GIS) and cartographic techniques.

Originating from a different schema of the socioeconomic fabric variables, therefore, the variables are transformed into the same scale or measurement for further analysis. Standardization is the most common approach to transforming variables. (Rygel *et al.,* 2006; Lee, 2014; Frazier *et al.,* 2014; Frigerio *et al.,* 2016; Frigerio and Amicis, 2016), transforming the units of variables by dividing the difference between the mean value and the raw value by the standard deviation. Thus the value becomes the distance between the raw value and the mean value in units of standard deviation so that variables can be compared across different measurements.

When the variables have been transformed, multicollinearity between variables is considered by testing with the Pearson correlation analysis or by calculating the variance inflation factor (VIF) value (Cutter *et al.,* 2010; Cutter *et al.,* 2014; Frigerio and Amicis, 2016). If the Pearson correlation coefficient is more substantial than 0.7 or the VIF value is greater than 5, there is multicollinearity between the variables. Factor analysis is the most common approach to solve this problem by summarizing and reducing. Principal component analysis (PCA) is the most widely used approach for factor analysis (Rygel *et al.,* 2006; Cutter and Finch, 2008; Fekete, 2009; Khan, 2012;

Tate, 2012; Wang and Yarnal, 2012; Zebardast, 2013; Frazier *et al.,* 2013; Frazier *et al.,* 2014; Hung *et al.,* 2016; Wood *et al.,* 2010; Frigerio *et al.,* 2016; Frigerio and Amicis, 2016). Most studies apply the varimax orthogonal rotation with Kaiser normalization, then extract components that have eigenvalues higher than 1.0. The percentage of explained variance is also an essential component. Although there may be no evidence to indicate that the variables have different weights, some studies use the percentage of variance as the weight to calculate the weighted arithmetic mean of the index (Siagian *et al.,* 2014; Frigerio *et al.,* 2016; Frigerio and Amicis, 2016).

Numerous researchers have used socioeconomic fabric variables to construct a vulnerability index and GIS visualization. (Cutter *et al.,* 2003; Khan, 2012; Fekete, 2009; Działek *et al.,* 2016; Lee, 2014; Rygel *et al.,* 2006; Wood *et al.,* 2010). Most of these studies used GIS as a platform to visualize and quantify social vulnerability. But in addition to visualizing and quantifying social vulnerability, GIS can also perform the spatial statistic technique for further analysis (Frazier *et al.,* 2014; Frigerio *et al.,* 2016; Frigerio and Amicis, 2016; Chang and Huang, 2015; Hung *et al.,* 2016; Wang and Yarnal, 2012).

2.3 Resilience

Vulnerability represents potential losses, whereas resilience refers to the ability to "bounce forward" during or after environmental hazards. Environmental hazard and disaster management researchers have increasingly applied the concept of 'resilience' as the key to recovery ability. The most common definition of resilience is that of Holling (1973), who considered resilience the 'measure of the persistence of systems and their ability to absorb change and disturbance and still maintain the same relationships between populations or state variables.' Resilience also has various definitions. In this section, we review previous research to capture the essence of resilience and the difference between resilience and adaptive capacity.

According to Prior and Hagmann (2014), in the context of ecology, resilience refers to the ability of a system to return quickly to normal functioning following a disturbance. In the field of global climate change, the IPCC (2007) defined resilience as 'the ability of a social or ecological system to absorb disturbances while retaining the same basic structure and ways of functioning, the capacity for self-organization, and the capacity to adapt environmentally to stress and change.' Resilience is also defined as 'a system's capacity which not only absorbs disturbance and reorganizes into a fully functioning system but also advances the state through learning and adaptation' (Cutter *et al.,* 2008). Norris *et al.* (2008) take resilience as a process that links a set of capacities with a positive trajectory of functioning and adaptation after a disturbance. From a social-ecological perspective, Carpenter *et al.* (2001) described resilience as (1) the ability to maintain the same function and structure when a certain amount of change takes place, (2) the extent to which a system that can self-organize when the system encounters a disturbance, or (3) the ability of the system to co-evolve with the disturbance. Wardekker *et al.* (2010) considered resilience the ability of a system to stand with the various trends of disturbance and to co-evolve with it. Resilience also can be regarded as a transformative process that strengthens the capacity of a specific social unit by recovering from and transforming aftershocks, stresses, and change (Winderl, 2014).

Although the concept of resilience has many aspects analogous to adaptive capacity, the relationship which is still far from unarticulated (Cutter *et al.,* 2008; Doorn, 2015); some researchers have defined resilience as an element of vulnerability (Doorn, 2015; Costa and Kropp, 2013; Balica *et al.,* 2012; McLaughlin and Cooper, 2010). Moreover, Thomalla *et al.* (2006) also denoted vulnerability as composed of exposure, sensitivity, and resilience.

Another open issue is whether resilience represents the ability to 'bounce back' or to 'bounce forward.' The former is the ability to adapt and recover from a disturbance to the original conditions (Klein *et al.,* 2003; Doorn, 2015). In this aspect, some scholars consider the term 'bounce back' to be insufficient in the longer term (Twigger-Ross *et al.,* 2014; Jordan and Javernick, 2013). Due to the uncertainty of environmental hazards, simple recovery may be insufficient in the long run and might lead to the reproduction of other critical crises. Bounce forward, on the other hand, is the ability not only to adapt but also to evolve with each environmental event (Wardekker *et al.,* 2010), and to learn from the disturbance (Cutter *et al.,* 2008; Carpenter *et al.,* 2001; Norris *et al.,* 2008; Wardekker *et al.,* 2010). Consequently, the system does not merely recover but evolves by learning from environmental hazards.

In this research, we apply the definition of Cutter *et al.* (2008), considering resilience not only the bounce forward processes but also a moving forward circulation.

2.4 Disaster resilience of the community

According to UNDP (2014), the assessment of disaster resilience can be distinguished into global, national, sub-national, and household/individual levels by geographic scale. In this study, the target is disaster resilience on the community scale. Based on UNDP (2014), "another common measurement uses a sub-national region - a 'community' - as the smallest unit of analysis," which means our research is at the sub-nation level. Cutter (2016) divided the research methodology for disaster resilience into assessment tools and methodological approaches. The assessment tools for community disaster resilience include indices, scorecards, and tools based on their characteristics. The indices are a statistical approach that aggregates multiple indicators into a single value to give an overall result. The scorecards are an evaluation toolset that evaluates performance or progress. The model or toolkits involve mathematical formulas or assessing procedures and survey instruments.

The methodological approach for disaster resilience assessment can be considered top-down or bottom-up (Cutter, 2016). The former usually includes statistics and quantification methodology, while the latter usually focuses on characteristics of the systems or community or their capacities. Due to the requirements of quantification and visualization, we prefer the index and top-down approach. Four different disaster resilience indexes from previous studies are summarized in Table 2.1. Similar to SoVI, all of these indexes are also composed of social fabric variables.

This research applies the baseline resilience indicators for communities (BRIC) as the tool to measure and quantify the community's inherent resilience to environmental hazards in Yilan City.

Table. 2.1 Quantifiable indices for measuring community disaster resilience

Index	**Resources of references**
Community disaster resilience indicators (CDRI)	Peacock *et al.,* 2010; Yoon *et al.,* 2015
Baseline Resilience Indicators for Communities (BRIC)	Cutter *et al.,* 2008; Cutter *et al.,* 2010; Cutter *et al.,* 2014; Cutter *et al.,* 2016; Burton, 2015
Community disaster resilience index (CDRi)	Sherrieb *et al.* (2010)
Community resilience index (CRI)	Mayunga (2007)

2.5 Constructing the BRIC

This section explains the construction of the BRIC, which is based on the disaster resilience of place (DROP) model (Cutter *et al.,* 2008) and focuses on the community's inherent resilience to environmental hazards. The inherent resilience is the most fundamental component of community disaster resilience since it is how the community responds to environmental hazards (Cutter *et al.,* 2008). The BRIC model includes the six subcomponents of society, economy, infrastructure, institutions, community, and environment (Cutter *et al.,* 2010; Cutter *et al.,* 2014; Burton, 2015; Cutter *et al.,* 2016). Each of these subcomponents contains different social fabric variables. The variables processing procedure is very similar to the SoVI since all the social fabric variables in BRIC also have a different schema. To adjust the variables to the same measurement, they are transformed into a ratio scale, and min-max normalization is applied (Cutter *et al.,* 2010; Cutter *et al.,* 2014). After normalization, the value of each variable is rescaled from zero to one. The Pearson correlation test is applied to detect multicollinearity between each variable (Burton, 2015; Cutter *et al.,* 2010), and highly correlated variables are removed. The arithmetic average calculates each subcomponent's value, so the subcomponent's value will also vary between zero to one. Finally, the BRIC score is the sum of six subcomponents, so the BRIC score is between 0-6 (Burton, 2015; Cutter *et al.,* 2016). The spatial statistic is applied to investigate the distribution pattern.

2.6 Indicator validation

After constructing the SoVI and BRIC, some studies apply multiple regression analysis to validate the results. The most common approach for validating the indices is the ordinary least squares (OLS) (Yoon *et al.,* 2015; Bakkensen *et al.,* 2016). While the OLS can provide a holistic perspective, spatial non-stationarity is another crucial issue. Derived from the difference between the spatial units, hence the spatial non-stationarity view is a widespread phenomenon across the overall study area. Yoon *et al.* (2015) applied the geographically weighted regression (GWR) to investigate the spatial difference of CDRI across Korea, and they found that the R^2 and AIC (Akaike Information Criterion) of GWR are better than the OLS. Since Yilan County has 234 villages, spatial non-stationarity might affect the outcome of OLS. Thus we applied geographical weight regression to evaluate differences in the overall area and resolve the spatial non-stationarity.

CHAPTER 3
MATERIALS AND METHODS

3.1 Study area

The study area, Yilan County, is located in northeastern Taiwan (Fig 3.1), with 106 km of shoreline, a total area of 2,144 km^2, and a population of approximately 460,000. The average elevation of our study areas is 830 m, and the southeastern part is mountainous, rising to 3000 m. The northwestern part of Yilan County is a floodplain and the most populated area.

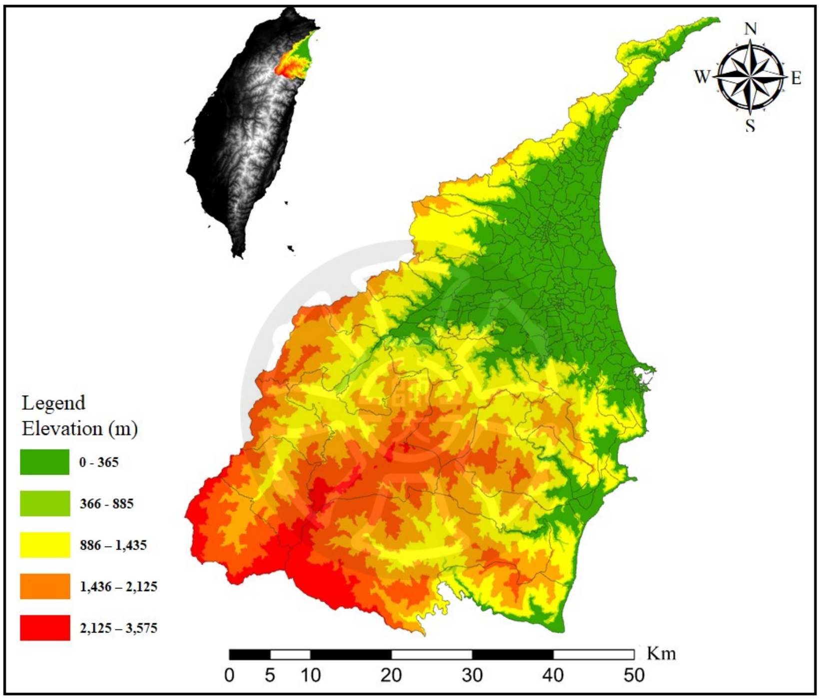

Fig. 3.1 Study area

Yilan County is more prosperous than other administrative divisions in eastern Taiwan. It remains primarily agricultural, though the county government considers tourism the primary means for economic development, and the number of tourists has grown markedly within the past two decades. This change was supported by the revision of the Agricultural Development Act in 2000, which relieved restrictions on developing farmland, so private residences on large plots of land referred to as farmhouses are now ordinary in Yilan.

Indeed, the county government successfully transformed its industrial pattern;

however, this also created not only large areas of land use and land cover change but traffic problem as well. Because of the rapid change in the social environment, characteristics of topography, and success of industry transformation, it has become urgent to furnish a holistic evaluation of its social vulnerability to environmental hazards and the community's inherent resilience to environmental hazards.

One of the aims is to validate the indicator with the authentic flood and debris flow event. Owing to its distinct topographic characteristics and the spatial features of flood and debris flow, the separation of the study area is essential since the chance of debris flow occurring in the floodplain areas is tremendously insignificant, and vice-versa, the chance of a flood occurring in the mountain areas is also salient low. Therefore, if we take the entire Yilan county as a single unit to conduct the spatial multivariate regression, there will be some bias in the result. Thus, in this study, we divide the study area into the mountain and plain areas based on the elevation. According to the Soil and Water Conservation Act, the threshold dividing the mountain and floodplain area is 100 m. Therefore, we also apply the same elevation threshold. Fig 3.2 demonstrates the spatial distribution of mountain and floodplain areas in Yilan county.

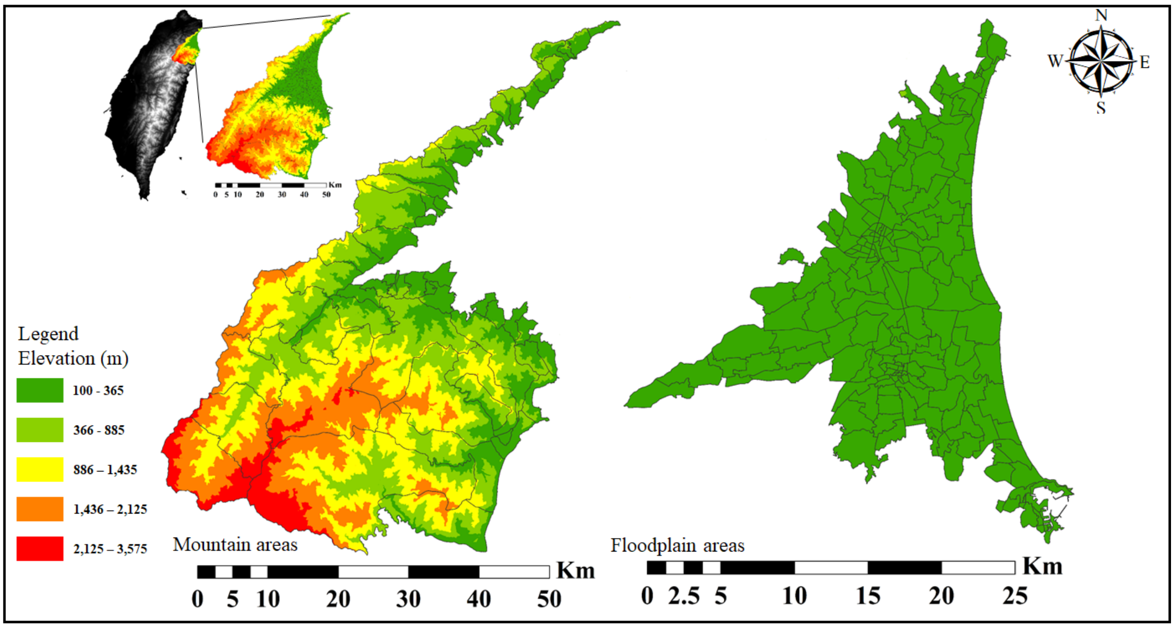

Fig. 3.2 Mountain and floodplain sub-study areas.

3.2 Resilience and vulnerability model

3.2.1 Social vulnerability index

Here we regard vulnerability as potential losses from environmental hazards (Cutter *et al.,* 2003). Potential losses from environmental hazards are highly related to socioeconomic conditions (Cutter *et al.,* 2003). Most of the research also applied the SoVI to demonstrate the social vulnerability to environmental hazards, meaning it can regard as the potential loss to environmental hazards. This study applies the Social Vulnerability Index (SoVI) of Cutter *et al*. (2003). SoVI is a combination of socioeconomic variables that has been widely used to estimate and quantify potential losses from environmental hazards. Here, the SoVI is computed by the following equation, where X_i is the socioeconomic variable.

$$X_i = \frac{\overline{X_v} - X_v}{\sigma_{X_v}} \tag{1}$$

$$\text{SoVI} = \sum_{1}^{i=n} X_i \tag{2}$$

3.2.2 Baseline resilience indicator for a community

According to Holling (1973), resilience is the ability of a system to absorb disturbances and still maintain full function. Since this study quantifies community disaster resilience, the Baseline Resilience Indicator for Community (BRIC) extends the disaster resilience of place model (DROP) model developed by Cutter *et al.* (2014). Similar to the SoVI, the BRIC model has a sequence of socioeconomic variables that can effectively quantify and visualize the community's inherent resilience to environmental hazards. The BRIC separates socioeconomic variables into six different dimensions of resilience: social, economic, community, institutional, housing/infrastructural, and environmental (Cutter *et al.,* 2014; Cutter, 2016; Cutter *et* *al.,* 2016; Burton, 2015). Bric is calculated by the following equation:

$$X_i = \frac{X_V - X_{(V\,MIN)}}{X_{(V\,MAX)} - X_{(V\,MIN)}} \tag{4}$$

$$X_d = \frac{1}{n}\left(\sum_{1}^{i=n} X_i\right) \tag{5}$$

$$X_d = \frac{1}{n}\left(\sum_{1}^{i=n} X_i\right) \tag{6}$$

3.2.3 The matrix of risk

In order to integrate the social vulnerability to environmental hazards with the potential of flood and debris flow, we apply the matrix of risk. In this research, we define risk as the interplay of social vulnerability to the environmental hazard (SoVI) and the potential of a environmental hazard (Blaikie *et al.,* 2014; Frigerio *et al.,* 2016). Fig 3.3 and the equation demonstrate the concept of the matrix of risk.

$$\text{Risk} = \text{SoVI} \times \text{Potential of environmental hazard} \tag{3}$$

Risk		Potential of Flood					Potential of Debris Flows				
		-1.5SD<	-1.5 SD To -0.5 SD	-0.5 SD To 0.5 SD	0.5 SD To 1.5 SD	>1.5 SD	-1.5SD<	-1.5 SD To -0.5 SD	-0.5 SD To 0.5 SD	0.5 SD To 1.5 SD	>1.5 SD
		1	2	3	4	5	1	2	3	4	5
Social Vulnerability Index											
-1.5SD<	1	1	2	3	4	5	1	2	3	4	5
-1.5 SD To -0.5 SD	2	2	4	6	8	10	2	4	6	8	10
-0.5 SD To 0.5 SD	3	3	6	9	12	15	3	6	9	12	15
0.5 SD To 1.5 SD	4	4	8	12	16	20	4	8	12	16	20
>1.5 SD	5	5	10	15	20	25	5	10	15	20	25

Fig. 3.3 the matrix of risk

3.2.4 The spatially explicit resilience-vulnerability model

Both SoVI and BRIC are composed of a series of socioeconomic variables. However, the concept is very different. Frazier *et al.* (2014) developed the spatially explicit resilience-vulnerability model (SERV). SERV was performed in this study to combine the SoVI and BRIC. SERV model also can import the concept of the environmental hazard. The concept of SERV is shown as the following equation:

$$V=E+S-AC$$

The S represents the social vulnerability, which is SoVI. The AC in this research represents the community's inherent resilience to environmental hazards, which is the BRIC. E in the equation stands for exposure to environmental hazard, which is the potential of an environmental hazard.

3.3 Variable selection and study material

3.3.1 Variable selection

Many studies have already identified specific socioeconomic variables that have a direct impact related to the community's social vulnerability to environmental hazards and resilience (Adger *et al.,* 2004; Adger, 2006; Cutter, 1996; Cutter *et al.,* 2003; Frazier *et al.,* 2013;). Based on the former studies (Cutter, 1996; Cutter *et al.,* 2003; Cutter *et al.,* 2014; Frazier *et al.,* 2013; Cutter *et al.,* 2016; Burton, 2015), specific indicators such as economic vitality, household status, education, race, ethics, infrastructure, age, and sex are broadly used to build the quantitative index of the social vulnerability to environmental hazard and resilience. We have chosen 21 variables from previous studies as the most relevant to SoVI and BRIC, as presented in Table 3.1 and Table 3.2. Variables used in this study are from the Socioeconomic Geography Information

System (SEGIS, http://segis.moi.gov.tw/).

Table. 3.1 The socioeconomic variables for constructing SoVI

Variable	**Resources of references**
Population Density	Cutter 1996; Cutter *et al.*, 2003
Ratio of Female Population	Cutter 1996; Cutter *et al.*, 2003
Dependency Ratio	Cutter 1996; Cutter *et al.*, 2003
Ratio of Solitary Elderly	Cutter 1996; Cutter *et al.*, 2003
Ratio of Physical and Mentally Challenged	Cutter 1996; Cutter *et al.*, 2003
Aging Index	Cutter 1996; Cutter *et al.*, 2003
Ratio of Population Younger than 5 Years Old	Cutter 1996; Cutter *et al.*, 2003
Ratio of Population Older than 65 Years Old	Cutter 1996; Cutter *et al.*, 2003
Ratio of the Indigenous Population	Cutter 1996; Cutter *et al.*, 2003
Ratio of Foreign Laborer	Cutter 1996; Cutter *et al.*, 2003
Ratio of Low-Income Households	Cutter 1996; Cutter *et al.*, 2003
Population of Without High School Diploma	Cutter 1996; Cutter *et al.*, 2003

Table. 3.2 The socioeconomic variables for constructing BRIC

Variable	Resources of references
Standardized Income	Cutter *et al.,* 2014; Cutter, 2016; Cutter *et al.,* 2016; Burton, 2015
Number of Hospital Beds	Cutter *et al.,* 2014; Cutter, 2016; Cutter *et al.,* 2016; Burton, 2015
Number of Licensed Medical Personnel	Cutter *et al.,* 2014; Cutter, 2016; Cutter *et al.,* 2016; Burton, 2015
Presidential Election Vote Rate	Cutter *et al.,* 2014; Cutter, 2016; Cutter *et al.,* 2016; Burton, 2015
Number of Pharmacies	Cutter *et al.,* 2014; Cutter, 2016; Cutter *et al.,* 2016; Burton, 2015
Number of Clinics and Hospitals	Cutter *et al.,* 2014; Cutter, 2016; Cutter *et al.,* 2016; Burton, 2015
Number of Ambulances	Cutter *et al.,* 2014; Cutter, 2016; Cutter *et al.,* 2016; Burton, 2015
Number of Fire Stations	Cutter *et al.,* 2014; Cutter, 2016; Cutter *et al.,* 2016; Burton, 2015
Number of Police Stations	Cutter *et al.,* 2014; Cutter, 2016; Cutter *et al.,* 2016; Burton, 2015
Capacity of Emergency Shelters	Cutter *et al.,* 2014; Cutter, 2016; Cutter *et al.,* 2016; Burton, 2015
Number of the Population With a College Diploma	Cutter *et al.,* 2014; Cutter, 2016; Cutter *et al.,* 2016; Burton, 2015
Number of Population Between 20 to 50 Years Old	Cutter *et al.,* 2014; Cutter, 2016; Cutter *et al.,* 2016; Burton, 2015

3.3.2 Disaster potential of the study area

This study combines the SoVI, BRIC, and the exposure to environmental hazards through the SERV model, and this section introduces the exposure to chosen environmental hazards and how the exposure is calculated. Since flood and debris flow is the most common environmental hazards in the study area, these two hazards are the exposure element. The potential of these environmental hazards is acquired from the government's open data provided by the Water Resources Agency and the Soil and Water Conservation Bureau.

The Water Resources Agency defines the flood potential as a scenario simulating a particular pattern of daily precipitation, physiography conditions, and flood control facilities. The SOBEK ver2.13 model simulates the flood potential, and the Water Resources Agency provides four flood potential scenarios based on daily precipitation. Fig 3.4 to 3.7 will demonstrate the different flood potentials.

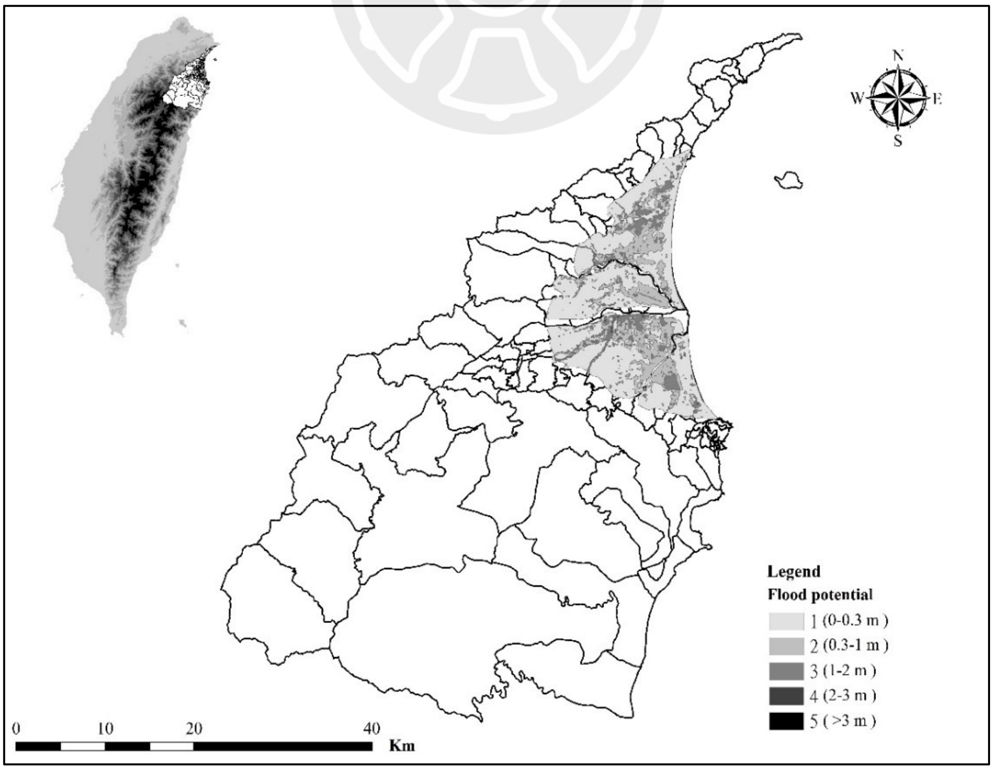

Fig. 3.4 Flood potential when daily precipitation is 200 mm

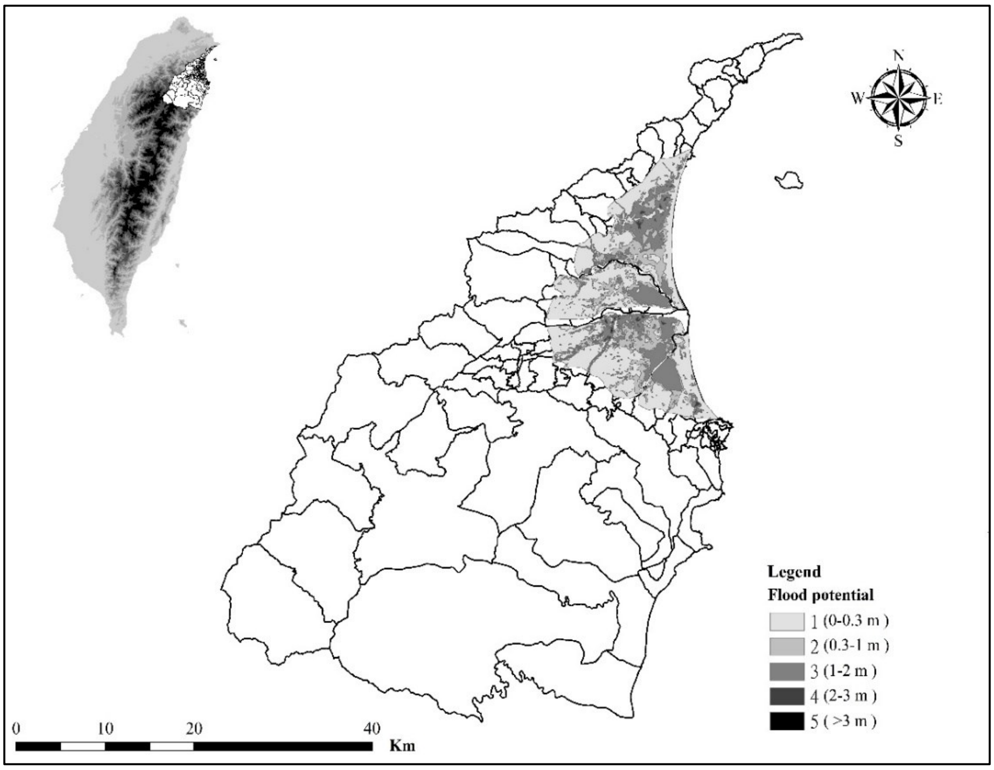

Fig. 3.5 Flood potential when daily precipitation is 350 mm

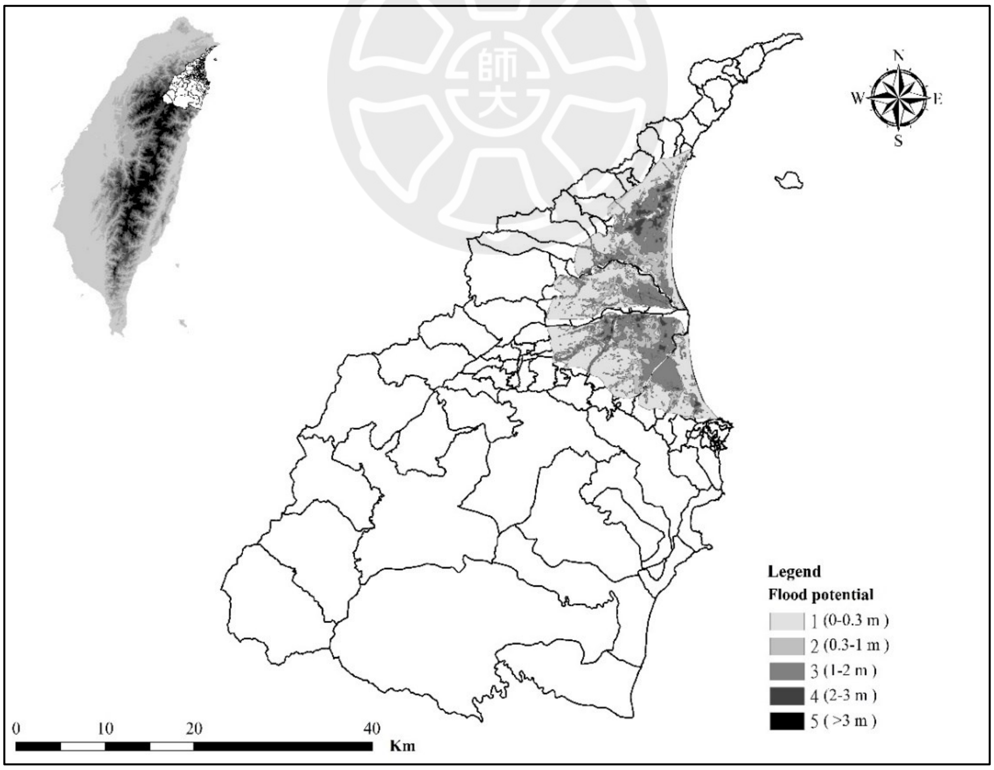

Fig. 3.6 Flood potential when daily precipitation is 450 mm

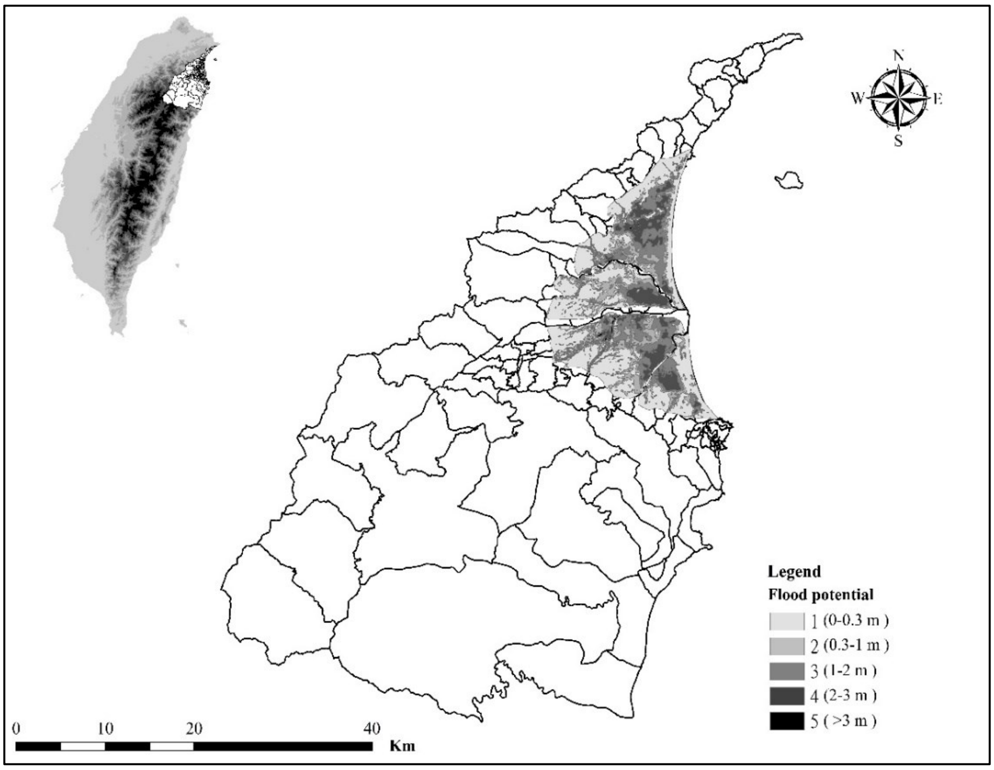

Fig. 3.7 Flood potential when daily precipitation is 600 mm

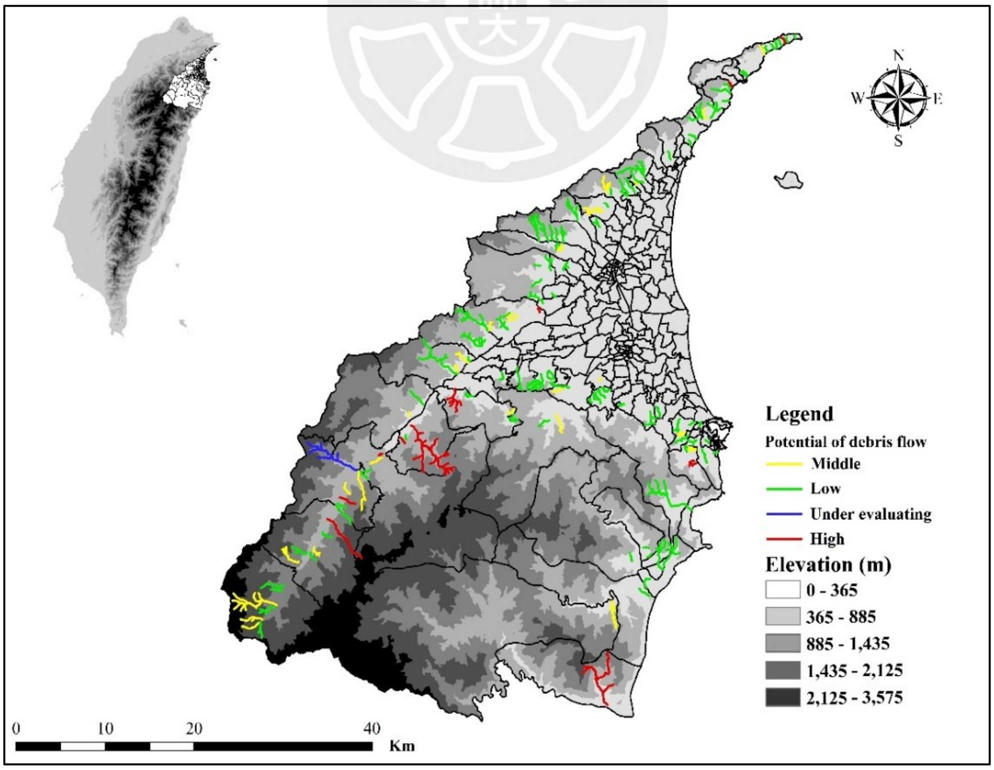

Fig. 3.8 Distribution of debris flow torrents

This study also considers debris flow. The potential for debris flow is acquired from the Soil and Water Conservation Bureau, and there are 144 potential debris flow torrents in Yilan County (Fig 3.8). The potential of debris flow includes two main elements, the probability of debris flow and the probability of harm. The following matrix illustrates how the potential for debris flow is calculated.

The probability of causing harm is calculated base on Table. 3.3. The primary component for evaluating harm is whether any buildings or transportation facilities are damaged, and the scores represent thresholds of harm. A score of 60 or over indicates a high probability of harm, between 40 and 60 indicates medium probability, and under 40 is a low probability.

The calculation for the probability of debris flow is very similar to that for the probability of causing harm, as shown in the following matrix. Evaluation for the probability of debris flows is also based on the score threshold, with high probability over 62, medium between 46 and 62. and low under 46.

Table. 3.3 Matrix for the potential of debris flow

Potential of debris flow		Probability of debris flow		
		High	Medium	Low
Probability of causing harm	High	High	High	Medium
	Medium	High	Medium	Low
	Low	Medium	Low	Low

3.4 Variable standardization

Since variables are socioeconomic characteristics, they must be transformed into a universal scale, so data standardization rescales all the indexes and variables.

$$\text{Standardization} = \frac{\bar{X} - \mathrm{X}}{\sigma_X} \tag{7}$$

where X is the value of variables, $\bar{X}$ is the mean value of a variable, and σ_X is the standard deviation of a variable.

Table. 3.4 Matrix for the probability of causing harm

Probability of causing harm		
Indicator	Classification	Score
Buildings	Public services	65
	More than five houses	60
	Between one and four houses	30
	None	0
Transportation Facilities	Bridge	35
	Road	20
	None	0

Table. 3.5 Matrix for the probability of debris flow

Probability of debris flow		
Indicator	Classification	Score
The scale of debris flow	Large area	25
	Medium area	15
	None	5
Slope	A slope greater than 50°	25
	Slope 30° to 50°	15
	Slope less than 30∘	5
Deposit	Average grain diameter larger than 30 cm	30
	Average grain diameter is 7.5 cm to 30 cm	13
	Average grain diameter is less than 7.5 cm	2
	None	2
Lithological character	Category one	15
	Category two	15
	Category three	5
Vegetation	Barren	15
	Sparse	15
	Medium-Sparse	6
	Compressed	3

3.5 Factor analysis

Due to the characteristic of the variables, the variables within the dataset are highly correlated with one another. Multicollinearity becomes a crucial issue for follow-up multiple regression analysis. In order to avoid the multicollinearity between the variable, the Factor Analysis was applied. In this study, we use SPSS to perform rotation Principal components analysis (PCA). Most studies apply the varimax orthogonal rotation with Kaiser normalization. We select the components based on the eigenvalue and scree plot.

3.6 Spatial autocorrelation

GIS technology is widely used for visualizing data, and in this study, GIS is used for both visualization and spatial statistical analysis. With the spatial statistical analysis, we can identify spatial patterns of the SoVI, BRIC, and SERV. Numerous studies (Frazier *et al.,* 2013; Frazier *et al.,* 2014; Frigerio and Amicis, 2016; Hung *et al.,* 2016; Wang and Yarnal, 2012) have used spatial autocorrelation to detect patterns of vulnerability and resilience.

This research also uses spatial autocorrelation to investigate spatial patterns. ArcGIS10.3 and R language are the platform to apply Moran's Index and local indicators of spatial association (LISA) to identify spatial patterns, as calculated by the following equation (Moran, 1950; Moran, 1948; Anselin, 1988; Anselin, 1995):

$$\text{Moran's I} = \frac{\mathrm{n}}{\sum_{\mathrm{i}=1}^{\mathrm{n}}\sum_{\mathrm{j}=1}^{\mathrm{n}} \mathrm{W_{ij}}} \times \frac{\sum_{\mathrm{i}=1}^{\mathrm{n}}\sum_{\mathrm{j}=1}^{\mathrm{n}} \mathrm{W_{ij}}(\mathrm{X_i} - \overline{\mathrm{X}})(\mathrm{X_j} - \overline{\mathrm{X}})}{\sum_{\mathrm{i}=1}^{\mathrm{n}}(\mathrm{X_i} - \overline{\mathrm{X}})^2} \tag{7}$$

$$\text{LISA} = \frac{(X_{\mathrm{i}} - \overline{\mathrm{X}})}{\sum_{\mathrm{i}=1}^{\mathrm{n}}(X_i - \overline{\mathrm{X}})^2} \sum_{\mathrm{j}=1}^{\mathrm{n}} \mathrm{W_{ij}}(X_{\mathrm{j}} - \overline{\mathrm{X}}) \tag{8}$$

where N is the number of spatial numbers, and W_{ij} is the spatial weighted matrix that is defined by the relationship of spatial units. "Contiguity_Edges_Corner" (Queen's) was used because it is a relatively well-explained definition of polygon contiguity. X_i and X_j are the spatial variables, and $\overline{X}$ is the mean of the spatial variables.

Moran's Index is a global autocorrelation analysis to determine spatial autocorrelation based on a feature's location and attribute values of the overall study area. Index values range between 1 and -1, with an index greater than 0 representing a cluster, one less than 0 indicating a dispersed pattern, and 0 indicating a random pattern.

LISA is a local autocorrelation analysis that distinguishes hot and cold spots with the four different results of H-H, L-L, H-L, and L-H. H-H means a statistically significant cluster of high values, L-L is a statistically significant cluster of low values, while H-L and L-H are features of outliers. H-L indicates a high value surrounded by low values, and L-H is a low value surrounded by high values.

3.7 Spatial multivariate regression

Validate the performance is one of the aims. To achieve this aim, we apply Spatial multivariate regression. Our research starts with the classic ordinary least squares(OLS); through the OLS, we can have the initial holistic result about the performance. However, the data we used is spatial data. As a result, spatial dependence is a critical issue to resolve. Therefore we apply the spatial lag and spatial error model to resolve the spatial dependence.

GeoDa is the platform for this article to perform the OLS, as well as the spatial lag model (SLM) and spatial error model (SEM) used to validate our model. The following equation is used to calculate OLS, SLM, and SEM:

$$Y = X\beta + \varepsilon \tag{9}$$

Y is the dependent variable, β is the coefficient matrix, X is the matrix of the independent variable matrix, and ε is the error term vector. The SLM is calculated by the following equation:

$$Y = \rho Wy + x\beta + \varepsilon \tag{10}$$

The ρWY is the spatially lagged DVs for the weights matrix W, x is the matrix of the observations on the explanatory variables, ε is the vector of the error term, and ρ is the spatial coefficient. If there is no spatial dependence and y does not depend on neighboring y values, the ρ value will be 0. SEM is calculated by the following equation:

$$y = x\beta + \varepsilon \tag{11}$$

$$\varepsilon = \lambda Ws + \xi \tag{12}$$

ε is the vector of the error term, spatially weighted using the weight matrix (W); λ is the spatial error coefficient, and ξ is the vector of uncorrelated error terms. If there is no spatial correlation between the errors, then λ will be 0.

3.8 Geographically weighted regression

Because of differences between each spatial unit, spatial non-stationarity may exist across the study area, so we use the GWR to resolve this problem. As a modification of linear regression, GWR also can characterize local circumstances (Yoon *et al.,* 2015). Traditional OLS, SLM, and SEM consider the whole study a single unit, whereas GWR separates the overall area into several groups by creating many kernels based on the bandwidth. GWR is calculated by the following equation (Fotheringham *et al.,* 1998):

$$y_i(u) = \hat{\beta}_{0i}(u) + \hat{\beta}_{1i}(u)X_{1i} + \hat{\beta}_{2i}(u)X_{2i} + \hat{\beta}_{3i}(u)X_{3i} + \cdots + \hat{\beta}_{mi}(u)X_{mi} \tag{13}$$

where $\hat{\beta}_{0i}$ is the constant term of the GWR, $\hat{\beta}_{mi}$ is the coefficients of the model, which is the vector of the estimated parameters; X_{mi} is a matrix containing the values of the independent variables; and $y_i(u)$is the observed values of the dependent variables in each spatial unit. The coefficients are estimated by the following equation:

$$\hat{\beta}_{mi}(u) = (X^T W(u) X)^{-1} X^T W(u) y \tag{14}$$

where $\hat{\beta}(u)$ are the coefficients of the GWR that is estimated by the X matrix, the $W(u)$ weighted matrix and the dependent variables among each spatial unit; X^T represents the transfer matrix of the X matrix, $(X^T W(u) X)$ is the geographically weighted variance-covariance matrix, and $(X^T W(u) X)^{-1}$ is the inverse matrix of $(X^T W(u) X)$.

$$W(u) = \begin{bmatrix} w_1(u) & 0 & 0 & 0 \\ 0 & w_2(u) & 0 & 0 \\ 0 & 0 & \ddots & 0 \\ 0 & 0 & 0 & w_n(u) \end{bmatrix} \tag{15}$$

Here, $W(u)$ is the weighted matrix in the model, which is a square matrix, and the matrix element is calculated by the following equation:

$$w_n(u) = e^{-0.5\left[\frac{d_n(u)}{h}\right]^2} \tag{16}$$

where $w_n(u)$ is the geographically weighted n^{th} observation in the study area relative to the location (u); $d_n(u)$ is the distance between the n^{th} observation and the local (u); and h is the bandwidth, also known as the radius of the kernel. The distances generally are Euclidean.

3.9 Dependence variables

One of the most important sections of this study is utilizing the real flood and debris flow event recorded by the NCDR (https://den.ncdr.nat.gov.tw/Advanced) as dependent variables to validate our social vulnerability to environmental hazards and BRIC. There are several reasons for selecting the actual events rather than the damage caused by the environmental hazard. First, according to the official website of the NCDR, we could obtain only limited data of the period for which the damage was recorded and measured in Taiwan dollars. Second, these data are estimated according to the interest-free loan provided by the government. These data are, thus, not authentic environmental hazard damage and may contain some bias. Finally, because of the feature of these data and the Personal Information Protection Act, the government only provides the data on a township scale, but this research focuses on a smaller scale—the village. Moreover, a central concept for considering the actual event as the dependent variable for spatial multivariate regression is that compared with other groups, the disadvantaged group has no choice but to live in the more vulnerable areas. Nevertheless, those who are not underprivileged seem to have more ability to select a better location to dwell; even if these groups of people somehow decided to live in the more vulnerable areas, they might still have the ability to alter the condition of the region. The actual events have been used as dependent variables in previous studies (Bakkensen *et al.,* 2016; Yoon *et al.,* 2016). Moreover, the spatial scale and the quantity seem to be able to fit this research. Taking these reasons together, we considered the actual event as the dependent variable for the regression.

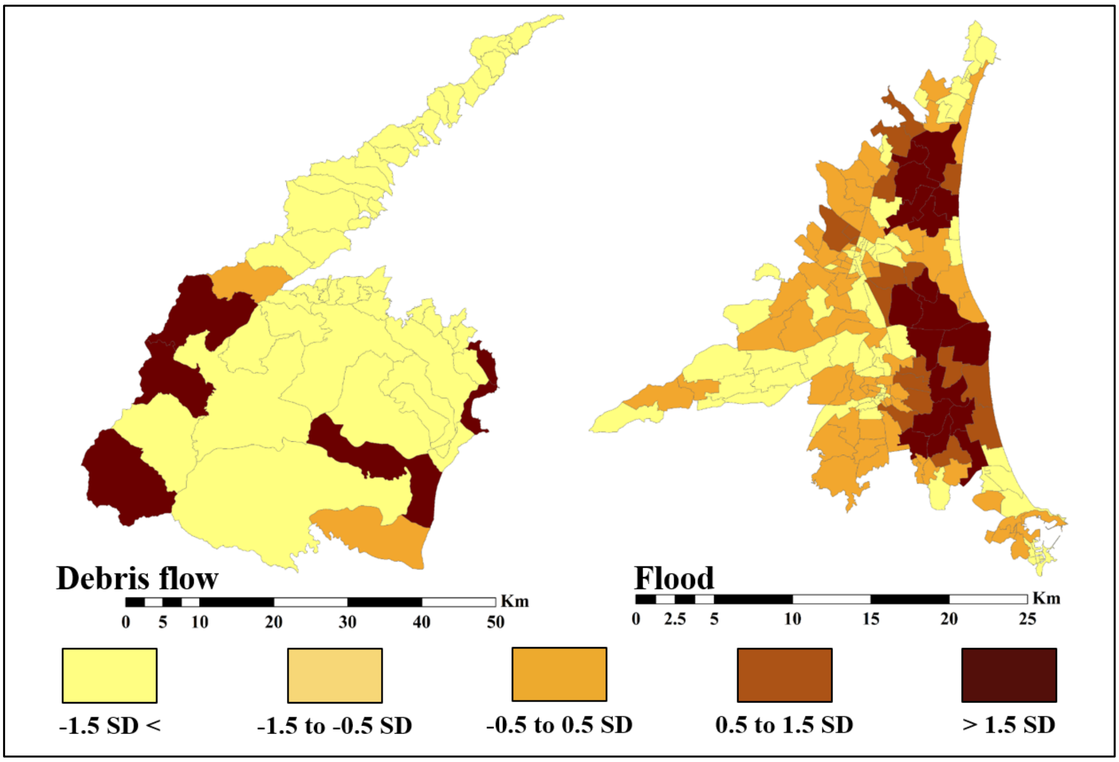

Fig. 3.9 Distribution of real flood and debris flow

CHAPTER 4
RESULTS AND DISCUSSION

This chapter presents the results of this study in four different sections. The first section includes the visualization and results of the spatial analysis of SoVI. The second section presents the visualization and spatial analysis result of BRIC. The third section shows the outcome of the matrix of risk and SERV model and its spatial analysis results. The fourth section presents the results of multivariate regression, using actual environmental hazard damage to validate the SoVI, BRIC, risk, and SERV models. Spatial autocorrelation analysis is applied to identify the spatial patterns, and spatial relationships are defined by “contiguity edges and corners.” Fig 4.1 shows how all spatial units are involved. The study area includes 234 spatial units, and the average linkage between units is 5.59. Fig 4.2 demonstrates the relationship between each spatial unit in floodplain areas. The average linkage between units is 5.21. Fig 4.3 represents the relationship between each spatial unit in mountain areas. The average linkage between units is 3.56

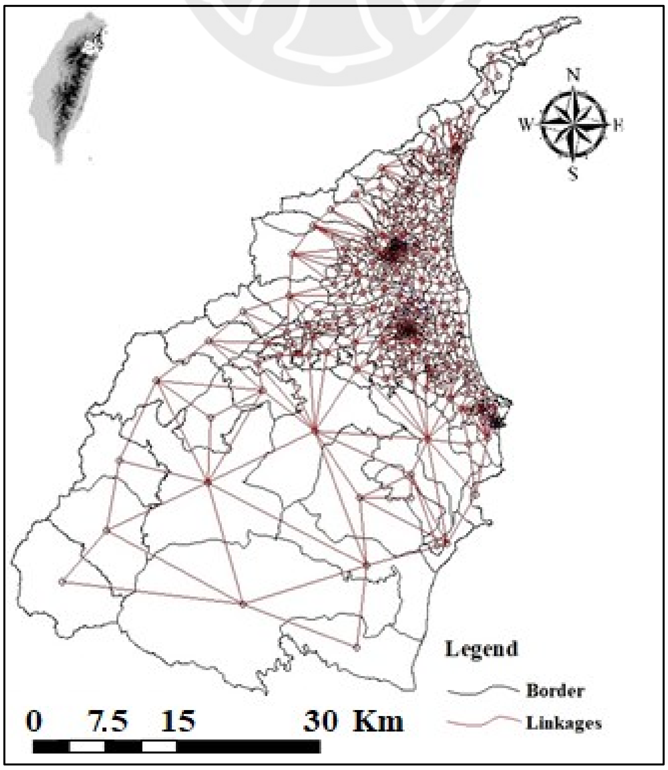

Fig. 4.1 Relationship of the spatial units in Yilan County

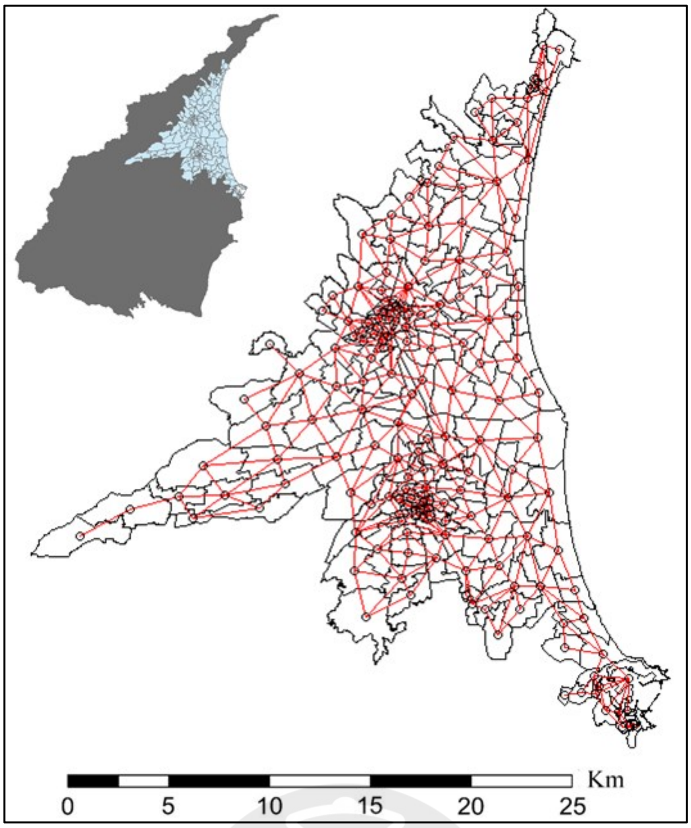

Fig. 4.2 Relationship of the spatial units in floodplain areas

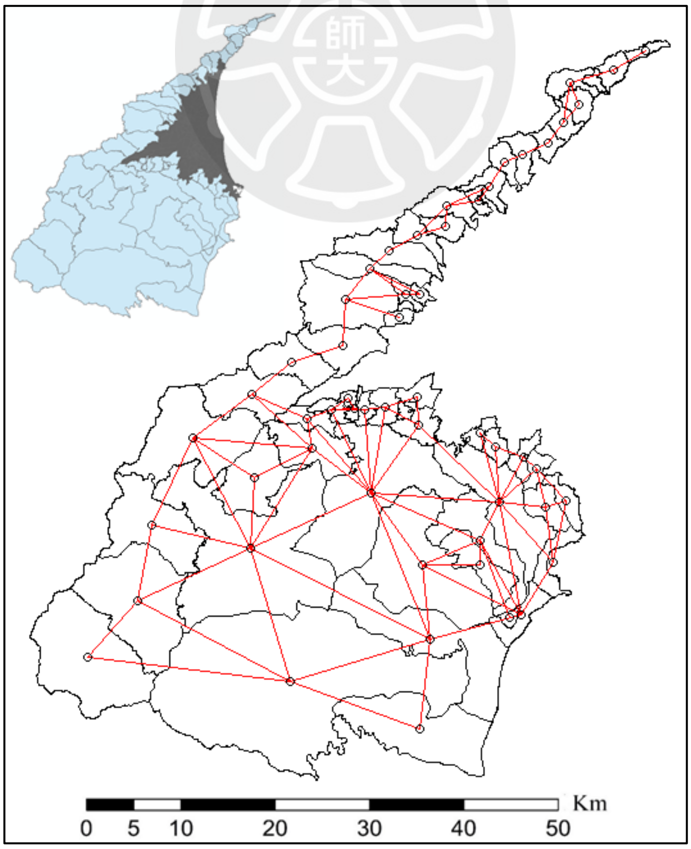

Fig. 4.3 Relationship of the spatial units in mountain areas

4.1 SoVI

4.1.1 SoVI of Yilan County

This section presents the quantification and visualization of all socioeconomic variables, SoVI, and the outcome of spatial autocorrelation analysis. The socioeconomic variables used to construct the SoVI are presented in Table 3.1. Fig 4.4 presents the spatial distribution of all socioeconomic variables, and Fig 4.4 shows that most of the socioeconomic variables seem to have a congregate appearance.

Due to the collinear relationship between the Population Density and Ratio of the Female Population, the spatial pattern of Population Density and Ratio of the Female Population are very similar. The spatial distribution of Population Density and Ratio of the Female Population present a notable congregate event, especially in urban areas, such as Yilan City and Luodong Township. This distribution suggests that environmental hazard exposure in urban areas is higher than in other areas.

The Ratio of Population Younger than 5 Years Old, Ratio of Indigenous People, Ratio of Low-Income Households, and Ratio of Population without a High School Diploma have a significant cluster in the southwestern mountain areas. The other variables, such as Dependency Ratio, Ratio of Solitary Elderly, Ratio of Handicapped, Aging Index, and Ratio of Population Older than 65 Years Old, seem to have no particular spatial pattern.

Fig 4.4 shows that some variables are clustered, so spatial autocorrelation analysis is used to determine the spatial pattern of socioeconomic variables. Fig 4.4 also presents the results of spatial autocorrelation analysis, and the Moran's *I* shows the spatial pattern of all variables; all are higher than 1, indicating that all the variables are clustered.

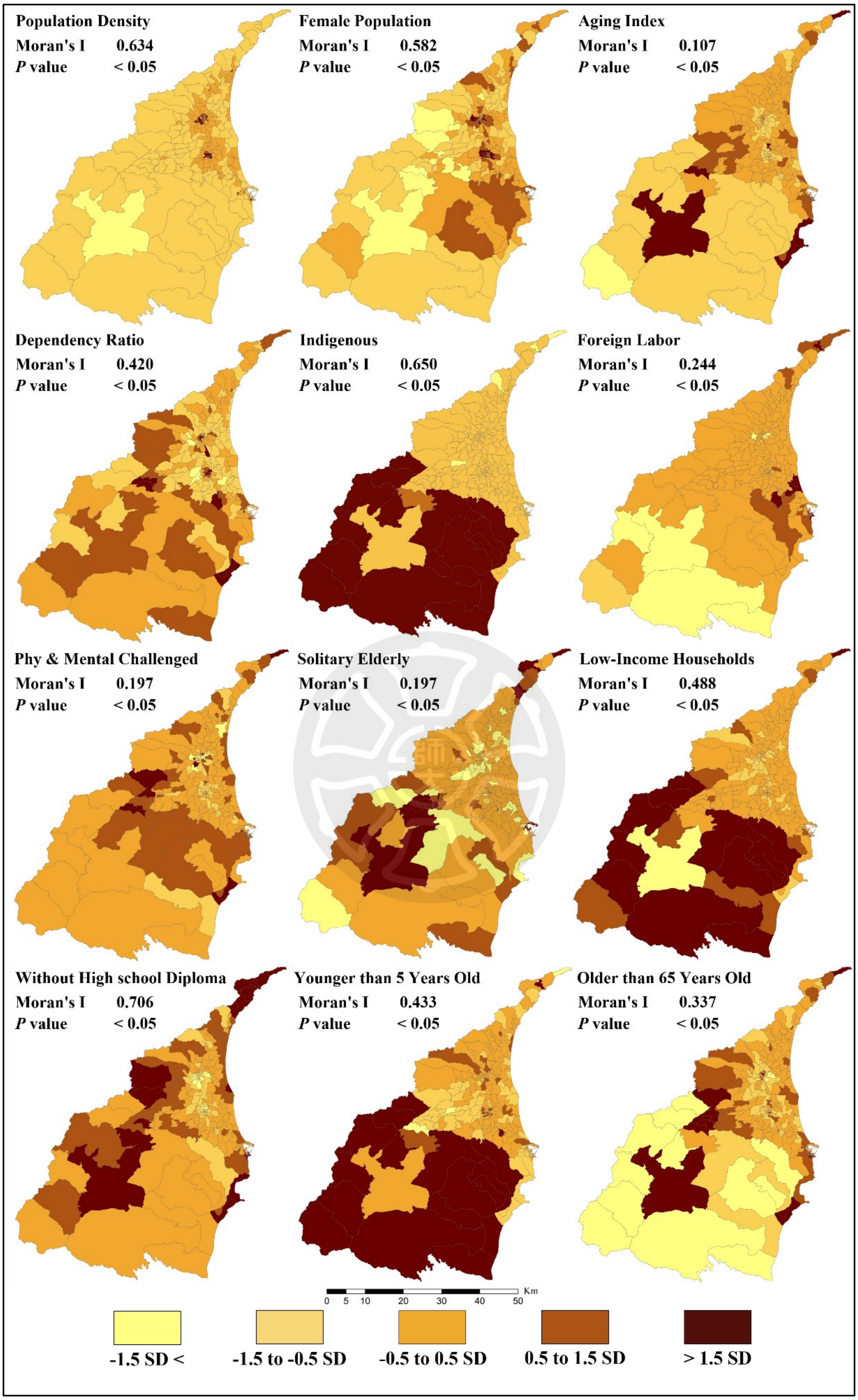

Fig. 4.4 Spatial distribution of socioeconomic variables (SoVI).

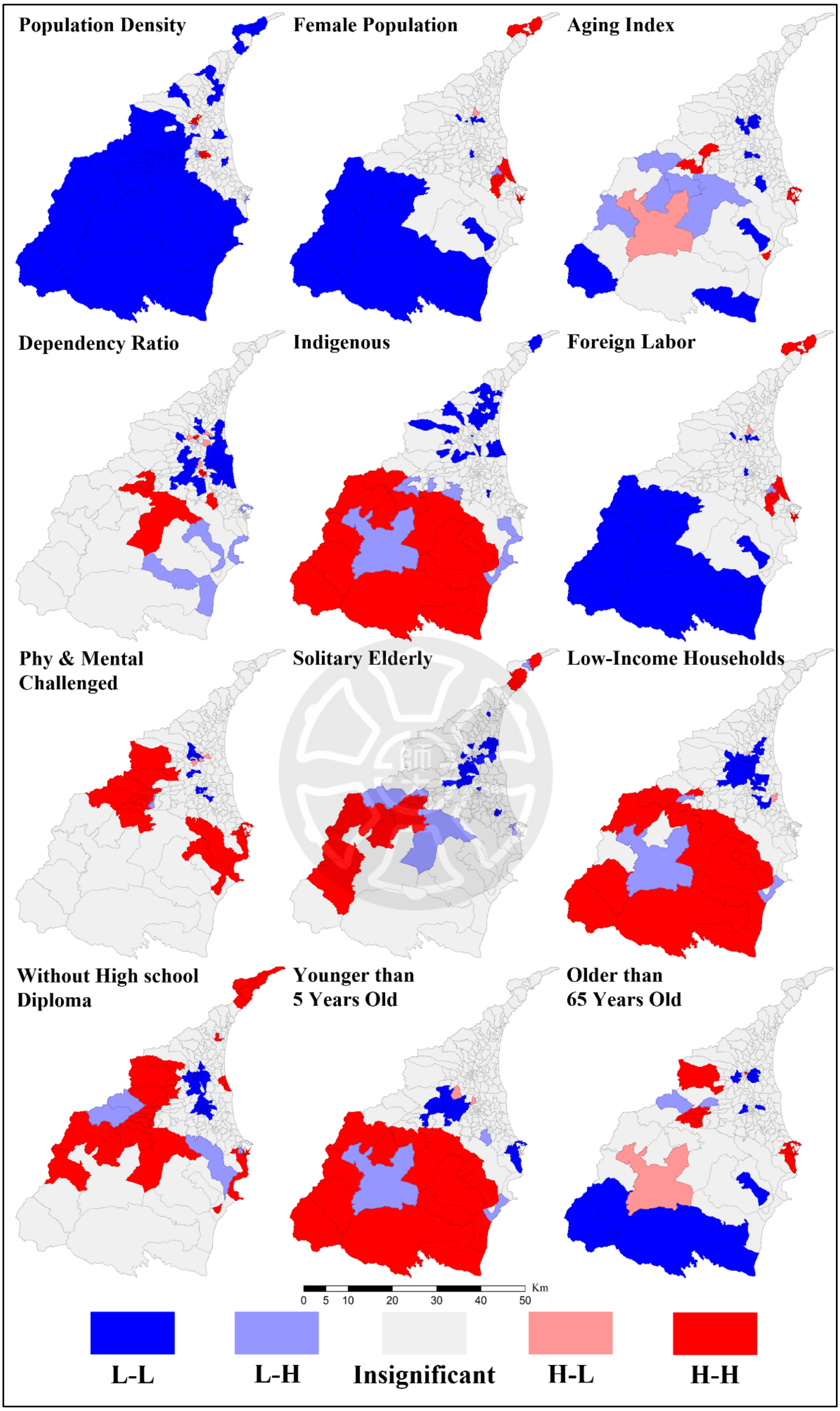

Fig. 4.5 Spatial clusters of socioeconomic variables (SoVI).

Fig 4.5 shows that the spatial pattern of most variables is reasonably consistent with the previous contents. The LISA results show that most of the Foreign Laborers and Population without a High School Diploma are significantly clustered in the coastal and harbor areas, perhaps due to the fishery and maritime transport industries. The spatial pattern of the Population without a High School Diploma also has a cluster in the mountainous areas, which might be due to the type of agriculture. Although the distribution for Population Younger than Five Years Old could be expected to coincide with the Population Density and Female Population, it is significantly clustered in the southwestern mountain areas. It is also similar to the distribution of the Ratio of the Indigenous Population and the Ratio of Low-Income Households.

Subsequently, we applied PCA to reduce the dimension of the socioeconomic variables and resolve the multicollinearity among the variables. The KMO value is 0.647, while the total variance explained is 77.024%. These indices indicate that the result of PCA is acceptable. Through the scree plot and eigenvalue, the foundation to determine the principal component, demonstrated by Fig 4.6, PCA generates four principal components. Component 1 includes the Population Without a High School Diploma, the Aging Index, the Ratio of Female Population, the Ratio of Solitary Elderly, the Ratio of Physically and Mentally Challenged, and the Ratio of Population Older than 65 Years Old. Component 2 is composed of the Ratio of the Indigenous Population, the Ratio of Low-Income Households, and the Ratio of Population Younger than 5 Years Old. Component 3 comprises the Dependency Ratio and Population Density. Component 4 is the Ratio of Foreign Laborers.

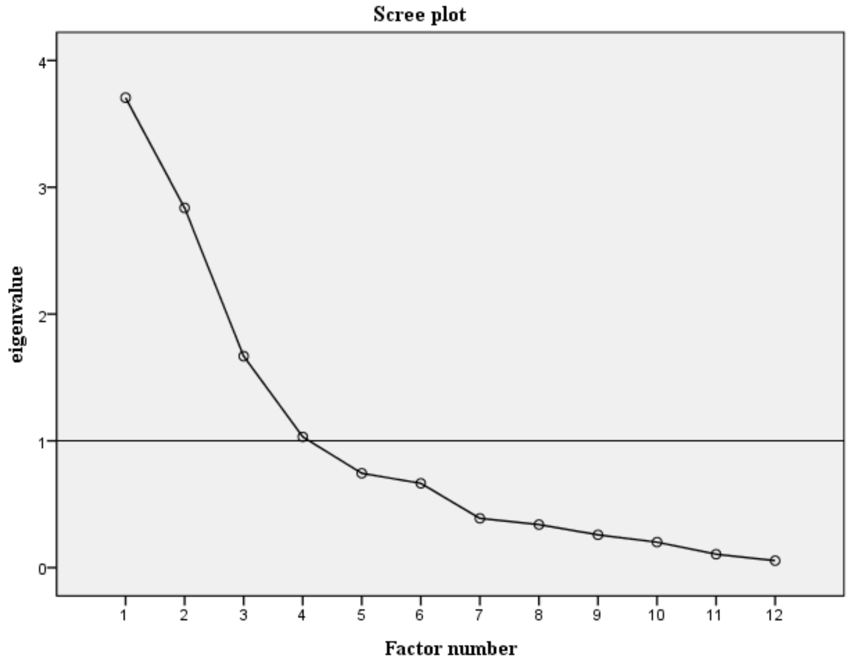

Fig. 4.6 Scree plot of PCA (SoVI).

The spatial distributions and patterns of components 1 to component 4 are illustrated in Fig 4.7 and Fig 4.8. Component 1 shows a difference between urban areas and rural areas. We can see that the colors of urban areas are relatively bright and blue, representing low values. However, in the rural areas, such as mountain areas and coastal areas, the colors are significantly darker and red, meaning the values are comparatively high. In other words, since all the variables in this section represent disadvantageous proportions in relation to environmental hazards, within the prospect of component 1, the rural areas are more vulnerable than the urban areas. The second component shows a different distribution. The higher values in mountain areas lead to dark and red colors when compared to the floodplain areas. Therefore, in this principal component, the mountain areas are also more vulnerable than the floodplain areas are.

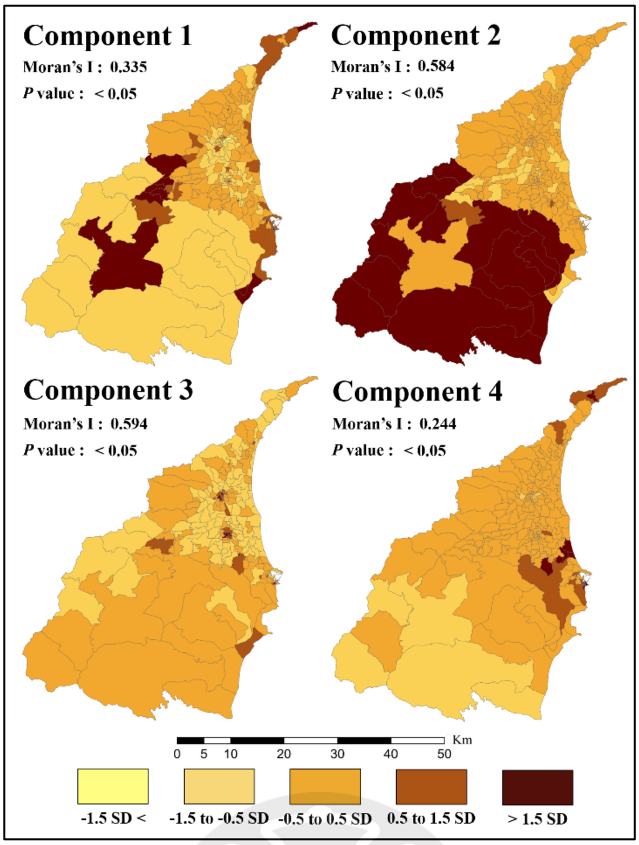

Fig. 4.7 Spatial distribution of all principal components (SoVI).

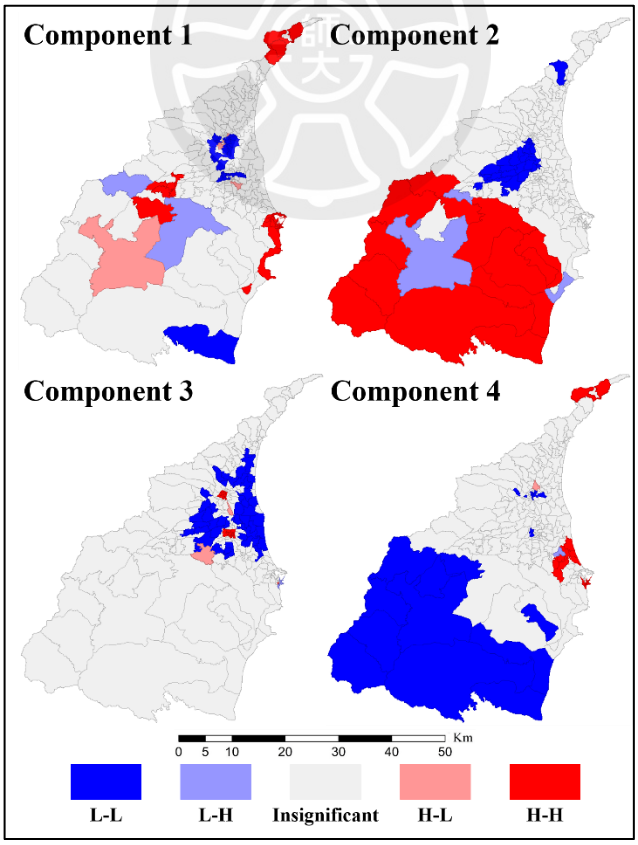

Fig. 4.8 Spatial clusters of all principal components (SoVI).

Because component 3 is built up by population density and dependence ratio, the population distribution is a key factor since most of the population congregates in urban areas. As a result, the values of urban areas are substantially higher than those of other areas, meaning the urban areas are comparatively vulnerable from the perspective of component 3. The last component includes the Ratio of Foreign Laborers, and most of them are gathered in coastal areas, especially around harbors. Therefore, undoubtedly, the coastal areas have higher values.

Table. 4.1 Moran's *I* Summary of SoVI

Moran's *I*	0.584
p-value	< 0.05

The results of the global autocorrelation analysis are presented in Table 4.1. Moran's *I* is 0.584 while the *p*-value is also less than 0.05, meaning the distribution of SoVI is statistically clustered. The linear relationship between spatial lag and SoVI demonstrates that the SoVI of Yilan County is strongly and significantly clustered. LISA analysis detects the location clusters, as shown in Fig 4.9, indicating that most H-H clusters are in mountainous areas, consistent with previous results. In addition to urban areas, some villages also are H-H clusters, such as Zhongshan Village and Renhe Village.

After we visualize and quantify all the socioeconomic variables, most of the population is in urban areas, which can lead to considerable exposure to environmental hazards. We also find that most of the underprivileged populations are clustered in mountainous areas. To verify this clustering, we analyze the spatial patterns of all socioeconomic variables by global and local spatial autocorrelation analysis. Moran's *I* and *p*-value show that all variables are statistically and significantly clustered. LISA detects the location clusters, showing significant population concentrations in urban areas, with underprivileged clusters in mountainous areas.

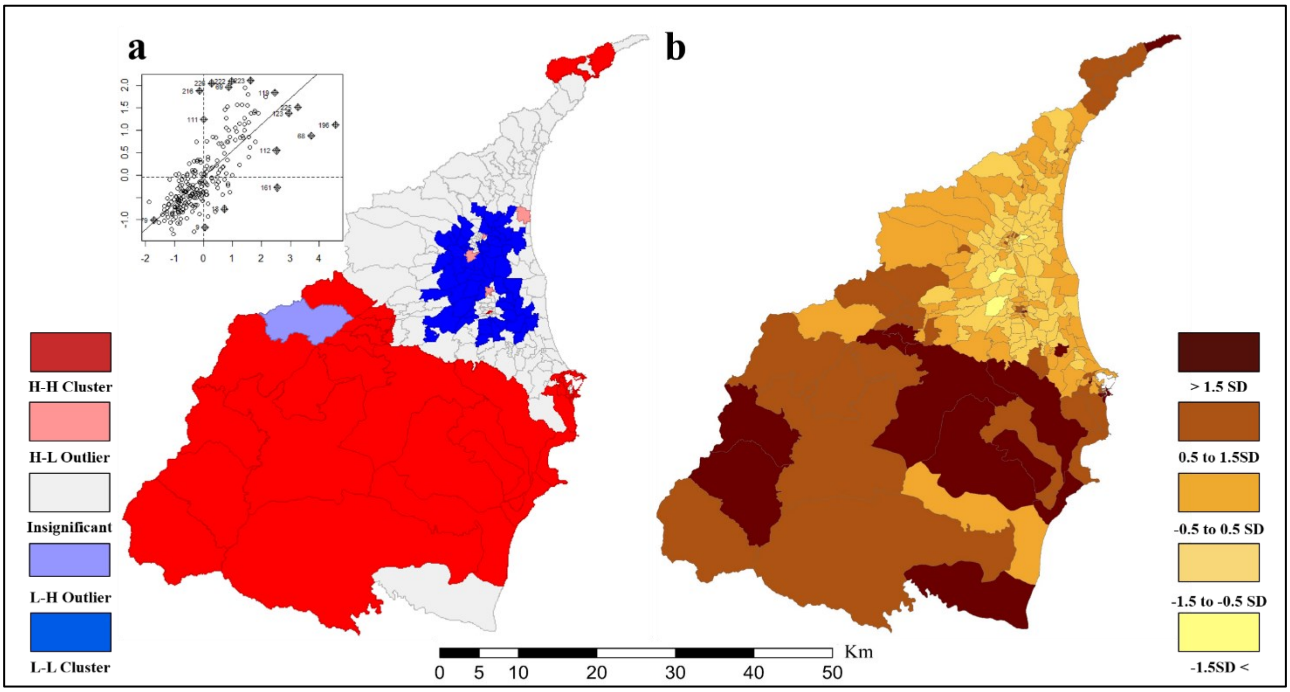

Fig. 4.9 The result of LISA (a) and spatial distribution (b) of SoVI in Yilan County.

Then all the variables are aggregated to construct the SoVI. Global autocorrelation and Lisa are applied to verify the SoVI spatial pattern. Moran's *I* and the *p*-value both show that the SoVI distribution of Yilan County is strongly and significantly clustered. The relationship between the SoVI and the spatial lag of SoVI also has a conspicuously positive relation. Finally, LISA identifies the hot spots, cold spots, and an outlier, with most of the H-H clusters located in mountainous areas, some in coastal regions, and a few in urban areas.

4.1.2 SoVI of Floodplain Areas

Due to the topographical characteristics of Yilan County, this study divided Yilan County into floodplain and mountain areas. In order to provide a further discussion of SoVI in the floodplain areas, this section demonstrates the spatial distributions and patterns of the socioeconomic variables and SoVI in the floodplain areas by quantifying all the socioeconomic variables and SoVI. Moreover, global and local spatial autocorrelation analysis is also be used to explore the distribution pattern.

Based on Fig 4.10, the distributions of all socioeconomic variables in the floodplain areas also seem to show some cluster events. The Population Density and the Ratio of Female Population undoubtedly congregate in urban areas such as Yilan City and Luodong Township. Fig 4.10 also reveals that most of the socioeconomic variables, including the Ratio of Physical and Mentally Challenged, the Population without High School Diploma, the Ratio of Low-Income Households, the Ratio of Foreign Laborer, and the Aging Index, present notable cluster events in the coastal areas. The distribution of the Ratio of Population Younger than 5 Years Old differs from the others; most of this population is gathered in the centers of the floodplain areas. The distributions of the rest of the socioeconomic variables are comparatively insignificant. Thus, further analysis is needed to determine the spatial pattern.

As a result, for further analysis, we apply spatial autocorrelation analysis. Based on Moran's *I*, we found that all the socioeconomic variables have statistically significant cluster events. In order to target the spatial patterns and clusters, we apply local spatial autocorrelation analysis. Fig 4.11 demonstrates the spatial patterns and clusters of all socioeconomic variables in the flood plain areas.

The distribution of population has a conspicuous cluster in the urban areas, for instance, Yilan City and Luodong Township. The reason for this kind of distribution is that Yilan City and Luodong Township are the most prosperous areas in northeastern Taiwan. As a result, most of the population congregates in Yilan City and Luodong Township. Moreover, we also notice that the southeastern harbor area is one of the most vulnerable areas since most of the disadvantaged socioeconomic variables such as the Population of Without High School Diploma, Ratio of Low-Income Households, Ratio of Population Older than 65 Years Old, Ratio of Physical and Mentally Challenged, Ratio of Solitary Elderly, Aging Index, Ratio of Foreign Laborer are clustered in harbor areas. The reason for this spatial distribution is caused by the fishery and maritime transport industries in these areas.

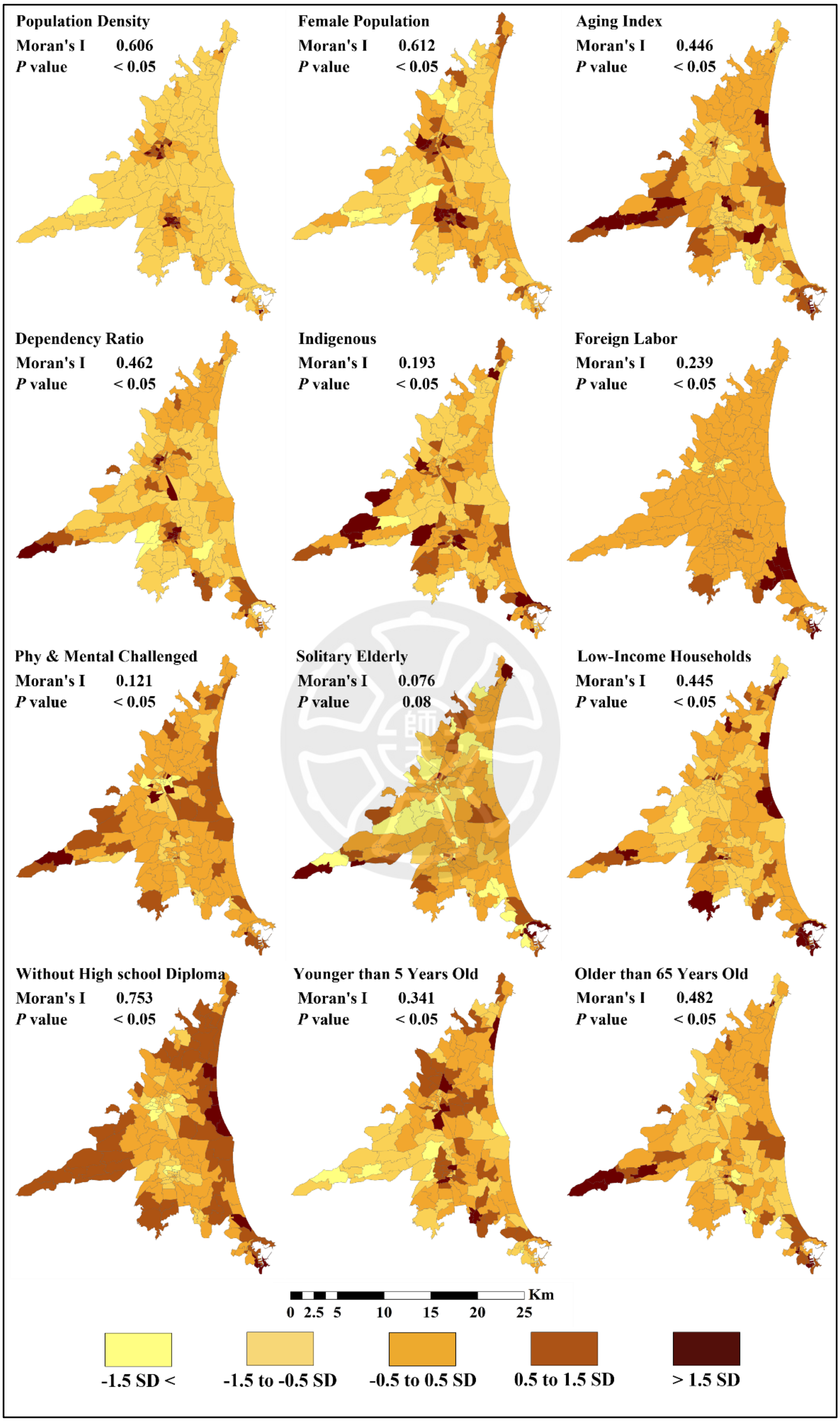

Fig. 4.10 Spatial distribution of socioeconomic variables in floodplain areas (SoVI).

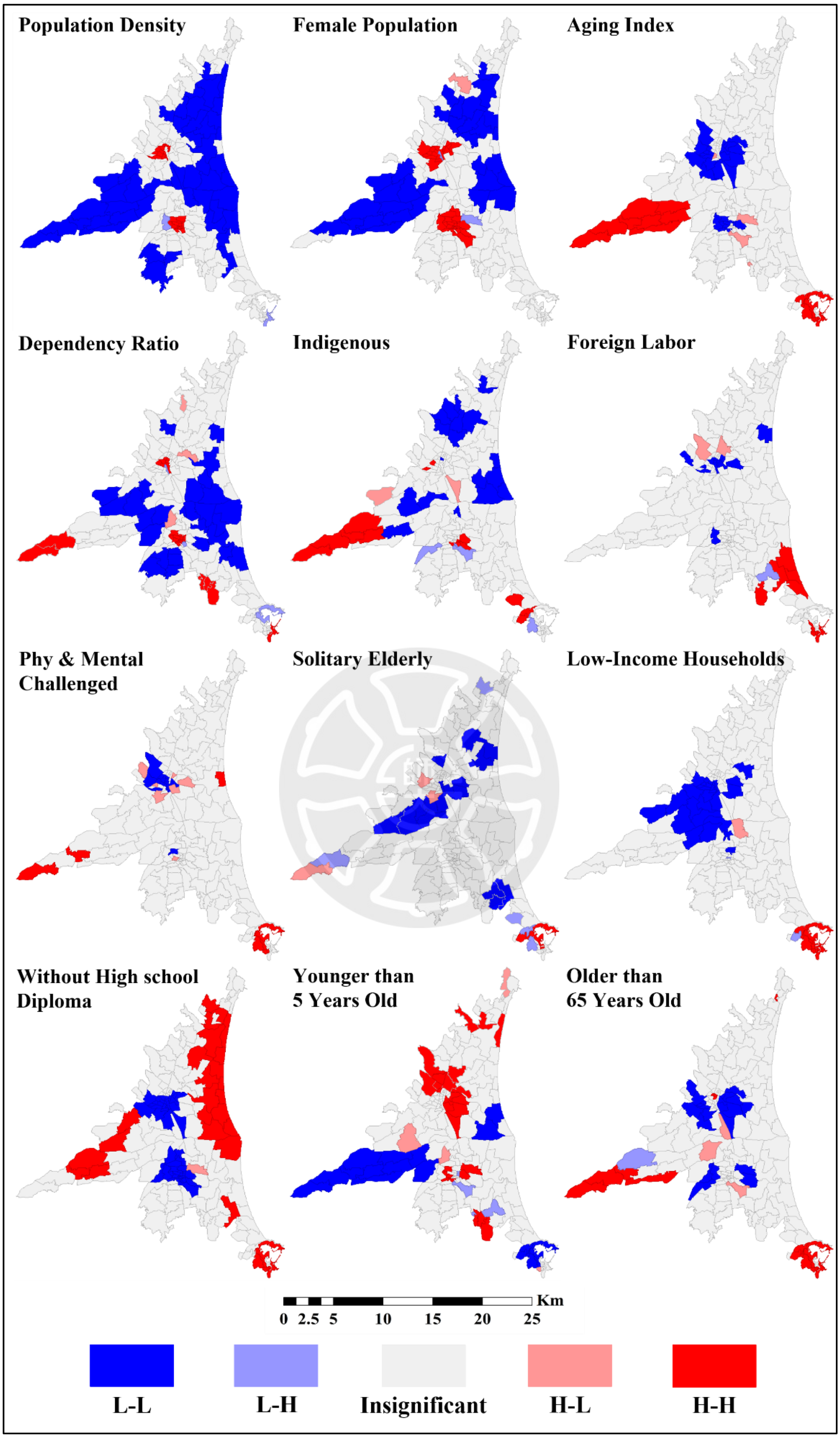

Fig. 4.11 Spatial clusters of socioeconomic variables in floodplain areas (SoVI).

Generally speaking, the results of LISA show that most of the L-L clusters are congregated in the center of the floodplain areas, while most of the H-H clusters are gathered close to the southwestern areas and coastal areas. This is because the center of the floodplain areas is relatively close to urban areas, meaning more opportunities than in the coastal and southwestern areas. As a result, most of the areas in the center of the floodplain have better socioeconomic conditions, leading to less vulnerability compared to the coastal and southwestern areas. However, the situations in the coastal and southwestern areas are different from those in the floodplain areas. Due to the industry characteristics and remoteness of urban areas, we find significantly fewer opportunities in these areas than in the center of the floodplain areas. As a result, most of the socioeconomically vulnerable conditions are focused on these areas.

Although the spatial distribution of all socioeconomic variables in the floodplain areas is slightly different from the situation of the entire Yilan County, the distribution of population and socioeconomically vulnerable areas are entirely consistent with the big picture of the spatial distribution of SoVI in Yilan County.

We also apply PCA to solve the multicollinearity issue. The total variance explained is 73.613%, and the value of KMO is 0.669. According to the scree plot and eigenvalue in Fig 4.13, we found that PCA generates four principal components in floodplain areas.

Component 1 includes the Aging Index, Population without a High School Diploma, Ratio of Population Older than 65 Years Old, and Ratio of Population Younger than 5 Years Old. Component 2 is composed of the Population Density, Dependency Ratio, and Ratio of Female Population. The contents of component 3 are the Ratio of Solitary Elderly, Ratio of the Indigenous Population, Ratio of Low-Income Households, and Ratio of Physically and Mentally Challenged. Last but not least, the fourth component includes only the Ratio of Foreign Laborers.

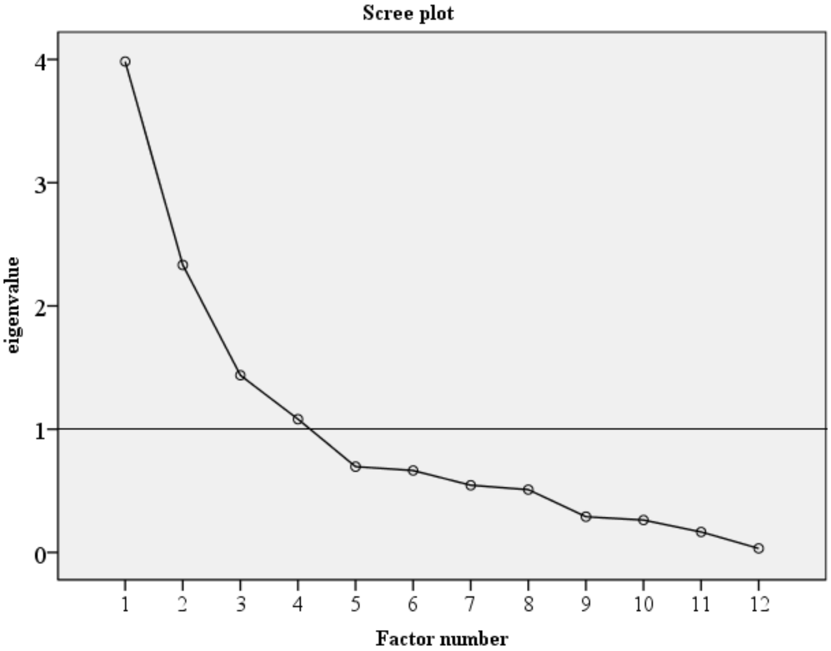

Fig. 4.12 Scree plot of PCA in floodplain areas (SoVI).

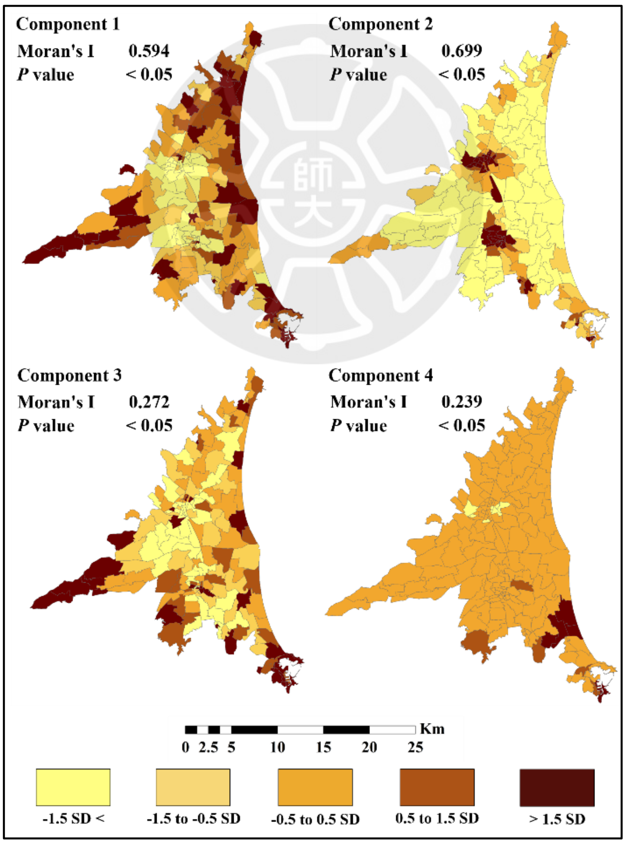

Fig. 4.13 Spatial distribution of all principal components in floodplain areas (SoVI).

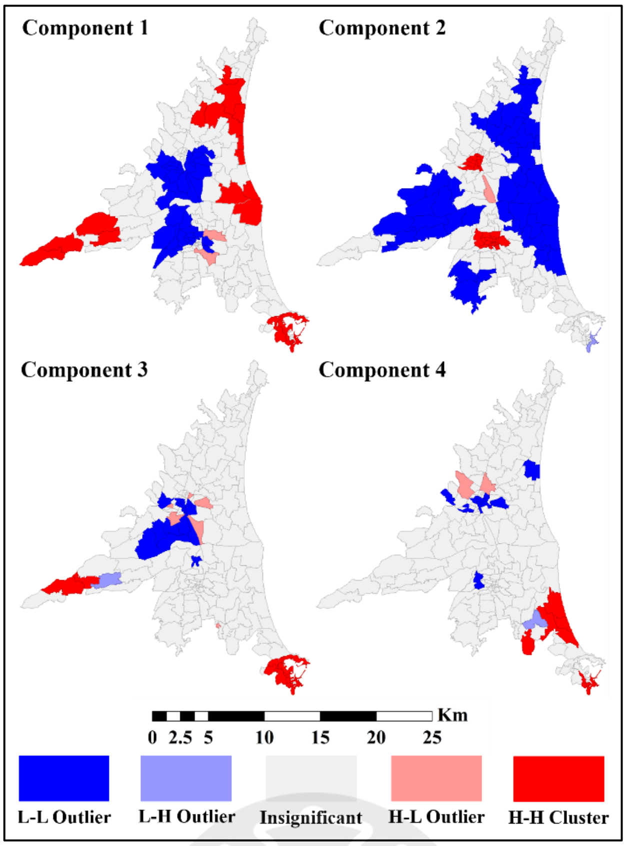

Fig. 4.14 Spatial clusters of all principal components in floodplain areas (SoVI).

Fig 4.13 and Fig 4.14 show the spatial distribution and result of LISA. Through the distribution and the pattern, we found a significant difference between component 1 and component 2. For component 1, the value in the center of the floodplain areas is relatively low, while component 2 seems to have the opposite distribution. The reason is due to the population distribution; most of the population is concentrated in urban areas such as Yilan City because of the substantially higher job opportunities compared to other areas. As a result, component 2 has a higher value in urban areas. However, most of the elderly congregate in the outlying parts of the urban areas, especially the coastal and southwestern regions. Therefore, the distribution of component 1 shows a conspicuous cluster in the coastal and southwestern areas. Component 3 also has an L-L cluster in the center of the flood plain areas. This distribution is similar to component 1. The last component is foreign laborers, most of whom work in the fishery and maritime transport industries, leading to clustering around the harbor. Some of the foreign laborers are hired as domestic workers, but the number is insignificant and has thus no influence on the spatial distribution.

Table. 4.2 Moran's *I* Summary of SoVI in floodplain areas (SoVI).

Moran's *I*	0.548
p-value	< 0.05

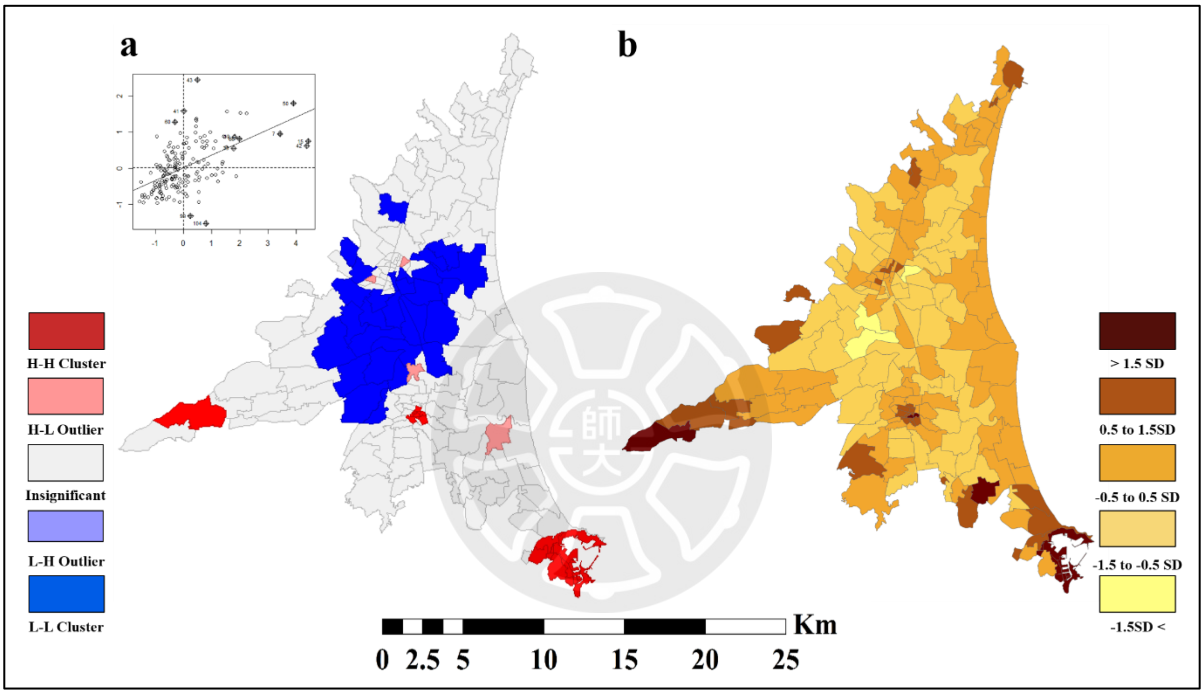

Fig. 4.15 The result of LISA (a) and spatial distribution (b) of SoVI in floodplain areas.

Table 4.2 and Fig 4.15 demonstrate the spatial distribution of SoVI in Yilan County and the result of global and local autocorrelation analysis. Although based on the result of previous analysis, we found most of the population is congregated in urban areas, which could create substantial exposure to environmental hazards, but does not have a significant influence on the distribution of SoVI. The Moran's *I* and *p*-value show the SoVI in the floodplain areas has statistically significant clusters, and Fig 4.15 demonstrates that the L-L cluster is in the center of the floodplain areas, meaning most of the central areas of the floodplain areas are relatively less vulnerable compared to other areas such as the harbor and southwestern areas. Due to the remote distance from urban areas, the socioeconomic condition in these outlying areas is comparatively uninspiring, and thus the harbor and southwestern areas are the most vulnerable areas in the floodplain areas.

4.1.3 SoVI of Mountain Areas

This section presents the SoVI in the southwestern mountain areas of Yilan County. Global and local spatial autocorrelation analyses are also used to explore the pattern of SoVI in mountain areas. Fig 4.16 and Fig 4.17 illustrate the spatial distribution, Moran's *I*, *p*-value, and spatial clusters of the SoVI in the mountain areas. Fig 4.16 shows that the spatial distribution of the socioeconomic variables is relatively random based on Moran's *I* and *p*-value. Moreover, most of Moran's *I* are also lower than the spatial autocorrelation result in floodplain areas.

Although some of the variables, for example, the Aging Index and Dependence Ratio, do not have significant clusters based on Moran's *I* and *p*-value, we still apply LISA to analyze the spatial pattern. Based on Fig 4.17, we found the Ratio of Indigenous Population, Ratio of Low-Income households, and Ratio of Population Younger than 5 Years Old are H-H clusters, while the Population Density, the Ratio of Foreign Labor, and the Ratio of the Population Older than 65 Years Old are L-L clusters. Indeed, the socioeconomic distribution in mountain areas is comparatively different from that in floodplain areas because of the distance from urban areas, characteristics of the industry, and composition of the population. Although some of the variables do not reveal conspicuous cluster occurrences, it is clear that most of the H-H clusters are located in the southwestern areas and are relatively in mountain areas.

The distribution is consistent with our expectation, i.e., social vulnerability increases as elevation increases. Reasons for this could be the social character of the vulnerable groups, resources, and opportunities in mountain areas. Compared to other areas around the urban areas, the resources and opportunities in mountain areas are lacking. Also, most of these groups do not have enough resources or the ability to move or dwell in other areas.

PCA is also applied to reduce the dimensions of socioeconomic variables. The KMO and total variance explained are 0.678 and 70.375, respectively. Fig 4.18 is the scree plot of PCA. PCA generates three principal components in mountain areas. The first component includes the Ratio of the Indigenous Population, Ratio of Low-Income Households, Population Density, Ratio of Population Older than 65 Years Old, and Ratio of Population Younger than 5 Years Old. The second component is composed of the Ratio of Physically and Mentally Challenged, Population without a High School Diploma, Aging Index, Ratio of Solitary Elderly, and Dependency Ratio. The third component comprises the Ratio of Foreign Laborers and Ratio of Female Population. The spatial distributions of each component are demonstrated in Fig 4.19.

Moran's I shows that all the components are a cluster. However, based on the p-value, only the first and the third component are significant clusters. Fig 4.20 reveals that component 1 has H-H clusters in mountain areas, while component 3 has a totally different pattern, an L-L cluster. This means the mountain areas are hot spots for the Ratio of the Indigenous Population, Ratio of Low-Income Households, Population Density, Ratio of Population Older than 65 Years Old, and Ratio of Population Younger than 5 Years Old. As for the Ratio of Foreign Laborers and Ratio of Female Population, mountain areas are cold spots.

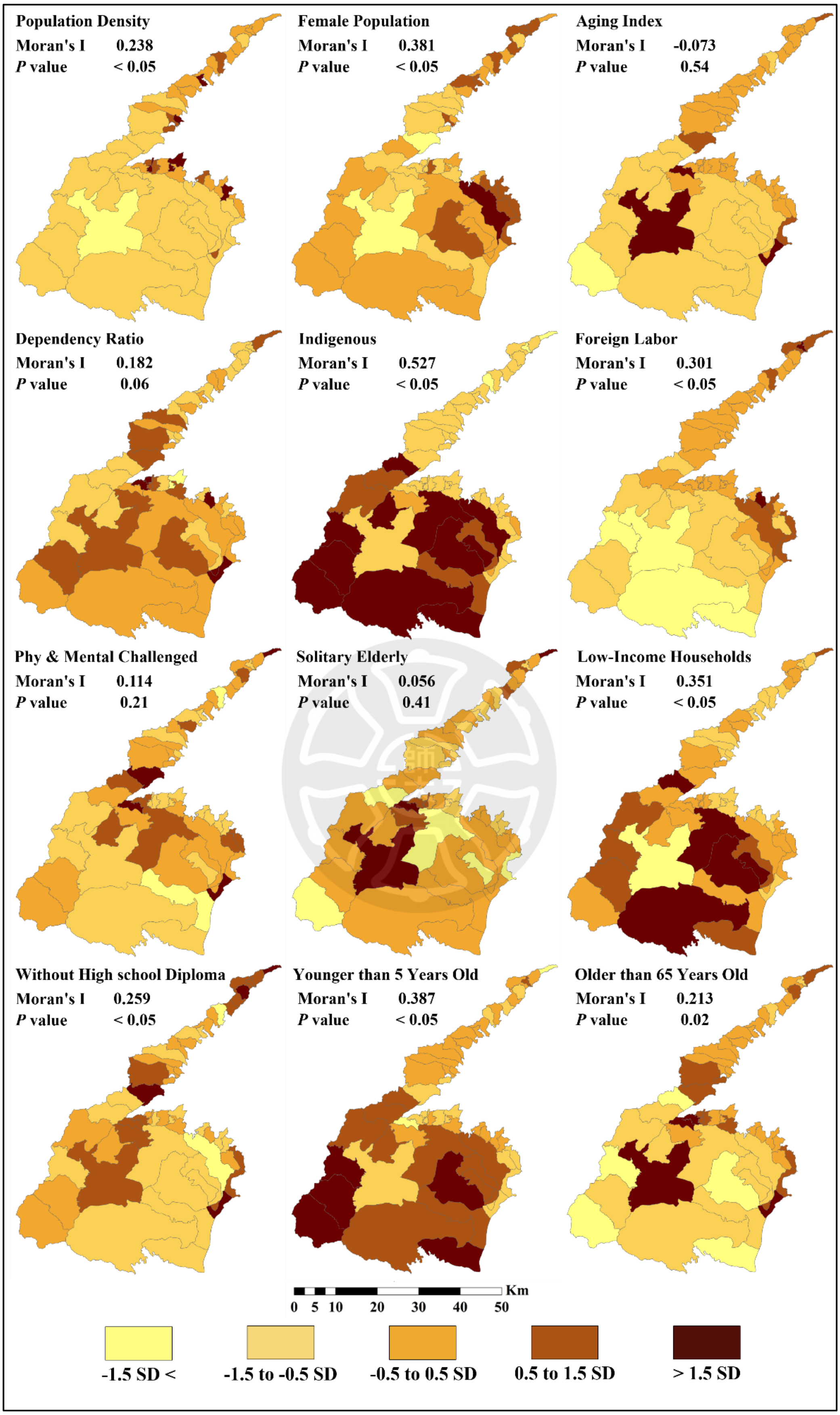

Fig. 4.16 Spatial distribution of socioeconomic variables in mountain areas (SoVI).

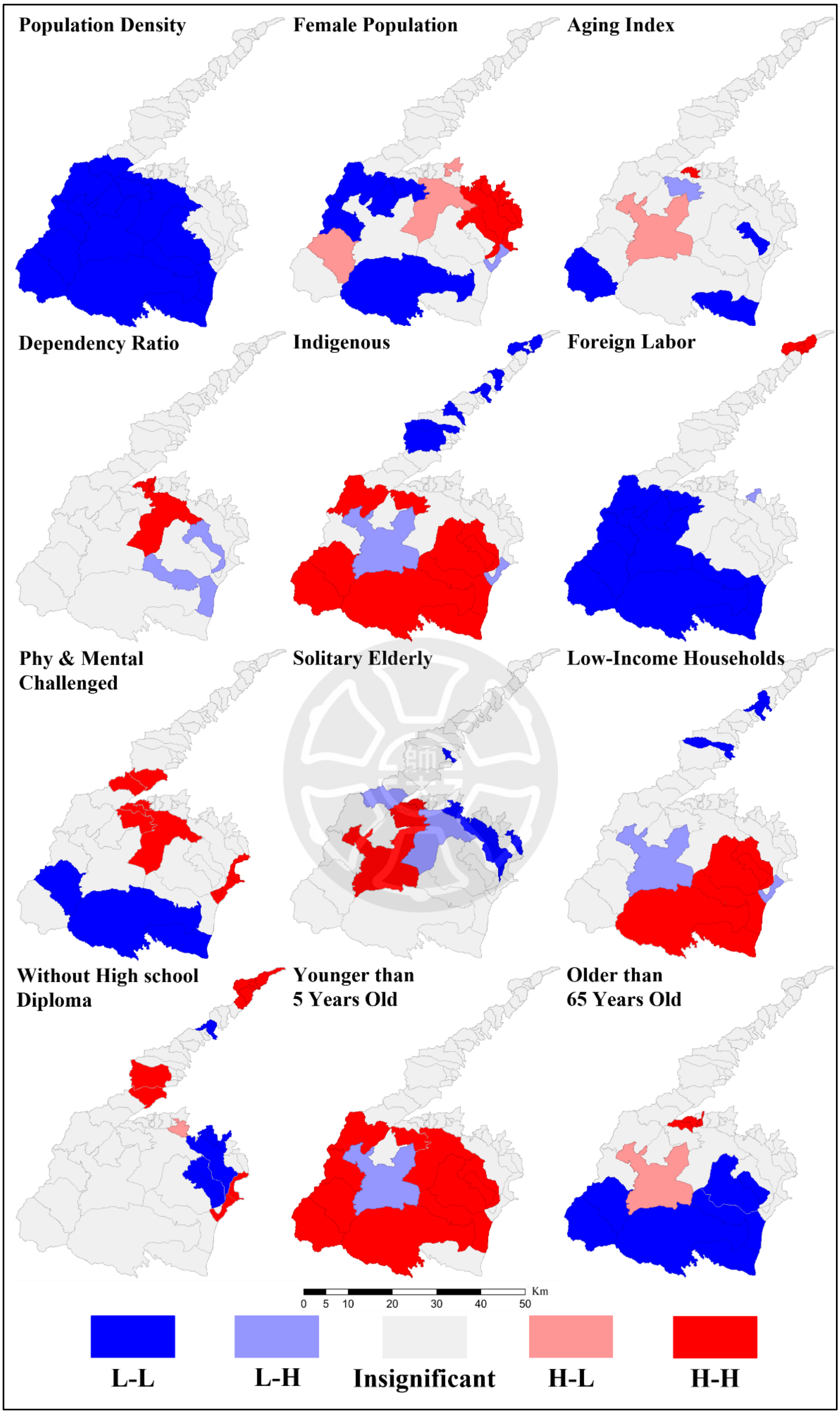

Fig. 4.17 Spatial clusters of socioeconomic variables in mountain areas (SoVI).

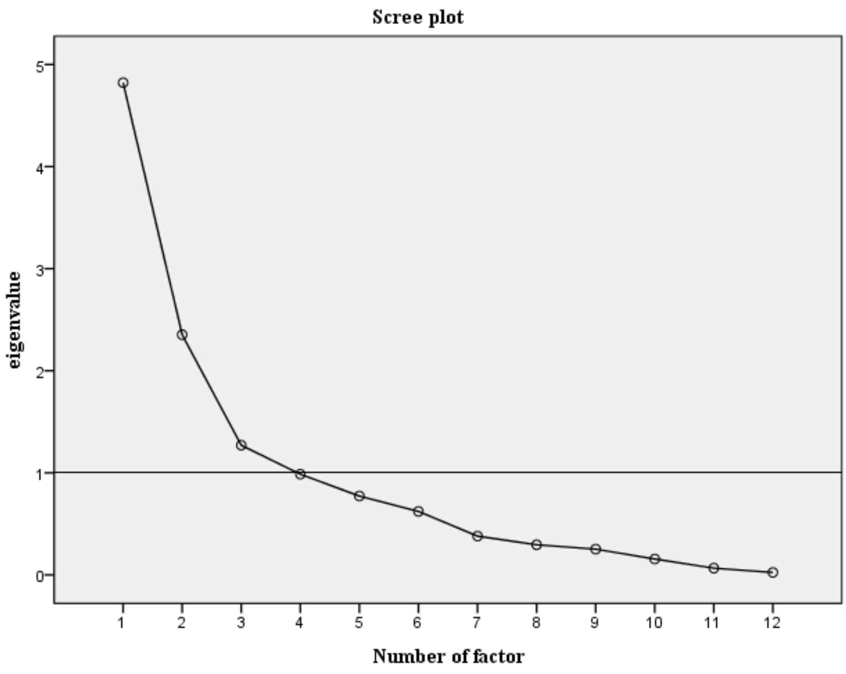

Fig. 4.18 Scree plot of PCA in mountain areas (SoVI).

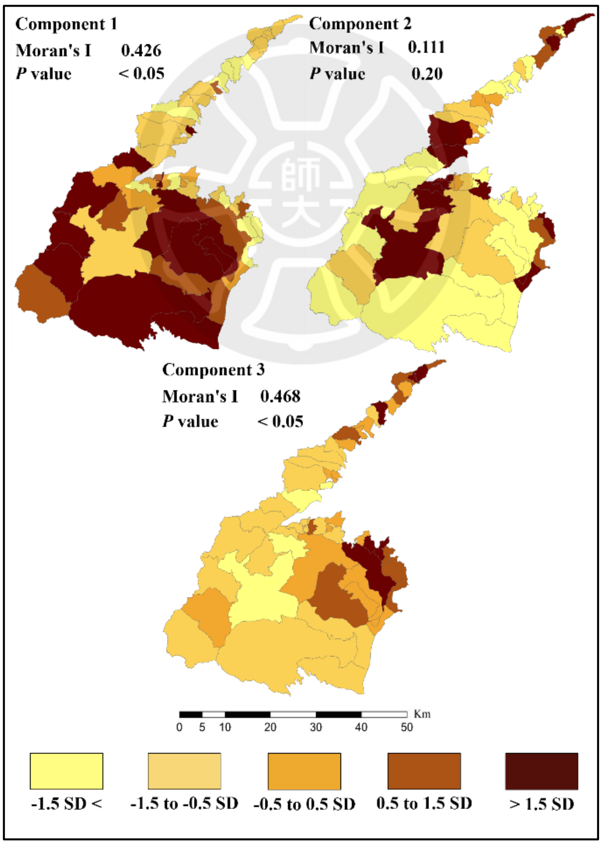

Fig. 4.19 Spatial distribution of all principal components in floodplain areas (SoVI).

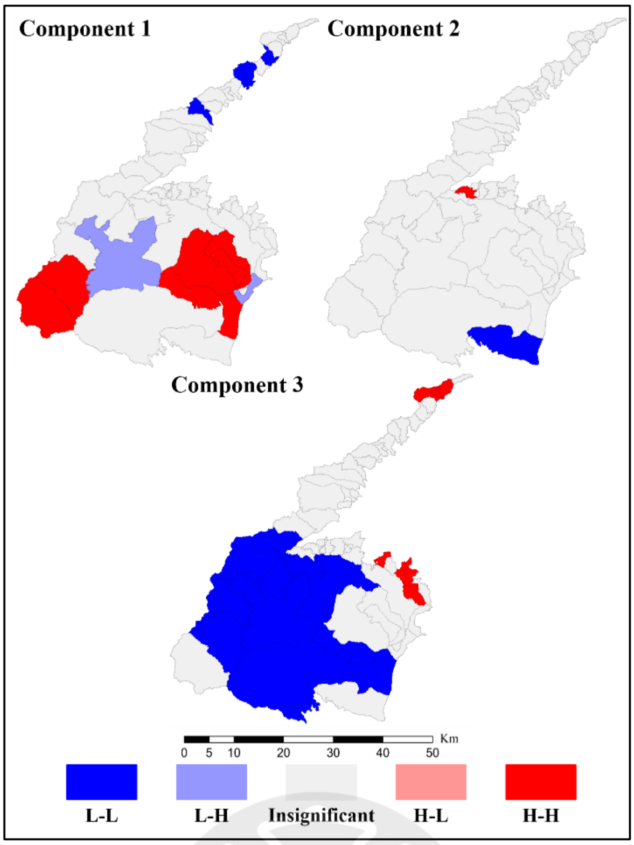

Fig. 4.20 Spatial clusters of all principal components in floodplain areas (SoVI).

Fig 4.21 and Table 4.3 demonstrate the spatial distribution and the result of global and local spatial autocorrelation. Based on Moran's *I* and *p*-value, we notice that SoVI also shows statistically significant congregation events. Compared to the flood plain areas, although Moran's *I* and the *p*-value of the SoVI represent a statistically significant cluster, the extent is relatively moderate.

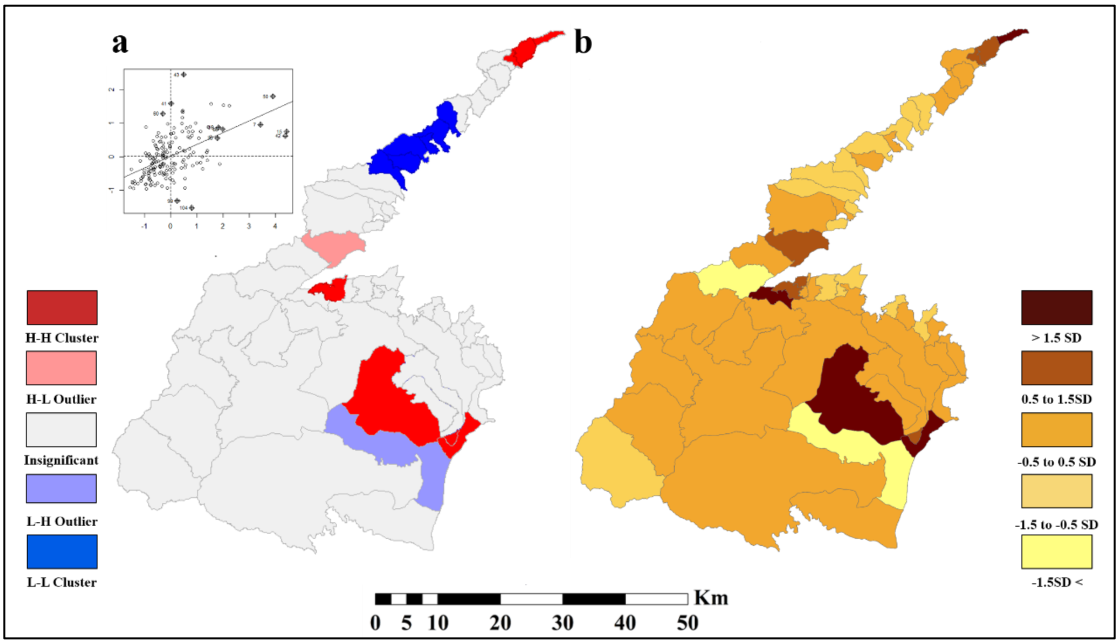

Fig. 4.21 The result of LISA (a) and spatial distribution (b) of SoVI in mountain areas

Table. 4.3 Moran's *I* summary of SoVI in mountain areas

Moran's *I*	0.251
p-value	< 0.05

4.2 BRIC

4.2.1 BRIC of Yilan County

This section demonstrates the spatial distribution of BRIC and the result of spatial autocorrelation, which are demonstrated in Fig 4.22 and Fig 4.23. The spatial distribution of the variables we use is different from the variables we use to construct SoVI. Based on Fig 4.22, most of the variables seem to gather in floodplain areas, especially the urban areas such as Yilan City and Luodong Township. However, according to the Moran's *I* and *p*-value, five of the variables, the Distribution of the Number of Hospital Beds, Number of Licensed Medical Personnel, Number of Ambulances, Number of Fire Stations, and t Number of Emergency Shelters, do not show any significant statistic pattern of either clustering or dispersing. The Number of Pharmacies is one of the most distinct variables. Through Moran's *I* and *p*-value, the spatial pattern of the Number of Pharmacies is dispersed. Also, in the upper six variables, the colors are very homogeneous. This is because the averages of these six variables are mostly less than 1, and the standard deviations are far more extensive than the average. Therefore, their averages and standard deviations lead their standardized values to be almost 0. This situation also occurs in floodplain areas and mountain areas.

LISA is applied in order to offer a more thorough exploration of the distribution. The result is mapped out in Fig 4.23. The result of the analysis shows that most of the urban areas are H-H clusters, while only a few of the H-L outliers are located in mountain areas. Also, most of the L-L clusters are in mountain areas. The reason for these distributions is that the variables used to build BRIC mostly include infrastructure, medical resources, and socioeconomic conditions. Nevertheless, most of them are gathered in the floodplain areas due to the population distribution and development, meaning floodplain areas have a better chance of obtaining more resources. As a result, the BRIC in mountain areas are environmentally inferior to those of the floodplain areas, and, based on our previous findings, we know that most of the mountain areas are already vulnerable. Moreover, the distribution of BRIC leads the mountain areas into a more vulnerable situation. When encountering environmental hazards, the mountain areas are not only extraordinarily vulnerable but lack the resources to cope.

Based on the scree plot (Fig 4.24) and eigenvalue, PCA generates four principal components. The KMO and the total variance explained are 0.622 and 65.817, respectively. Component 1 includes the Standardized Income, Presidential Election Voting Rate, Number of Social Units, Ratio of the Population with a College Diploma, and Ratio of Population between 20 to 50 Years Old. Component 2 comprises the Capacity of Emergency Shelters, Number of Clinics and Hospitals, Number of Pharmacies. Components 3 includes the Number of Licensed Medical Personnel and Number of Hospital Beds. The last component includes the Number of Ambulances and Number of Fire Stations.

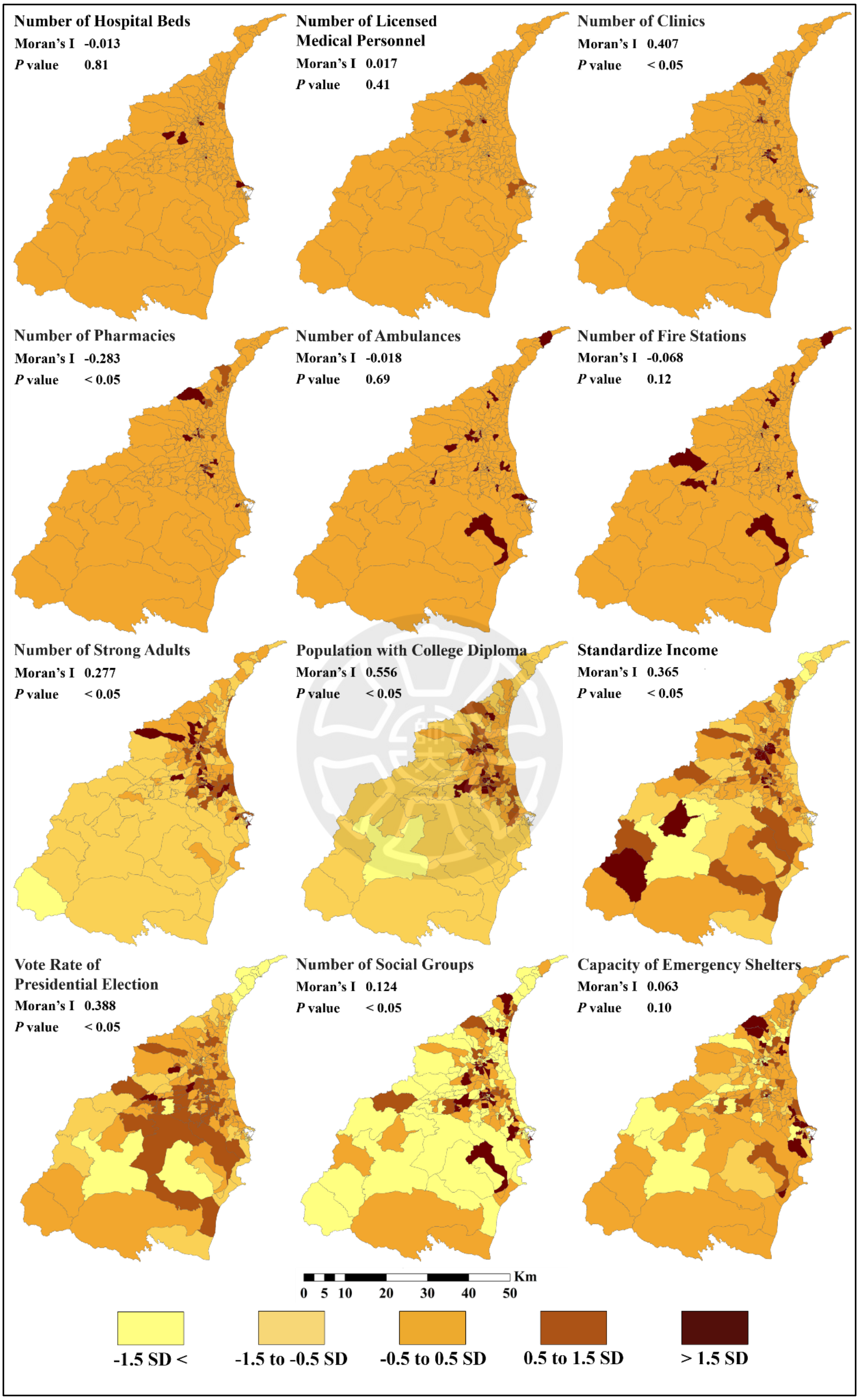

Fig. 4.22 Spatial distribution of socioeconomic variables (BRIC).

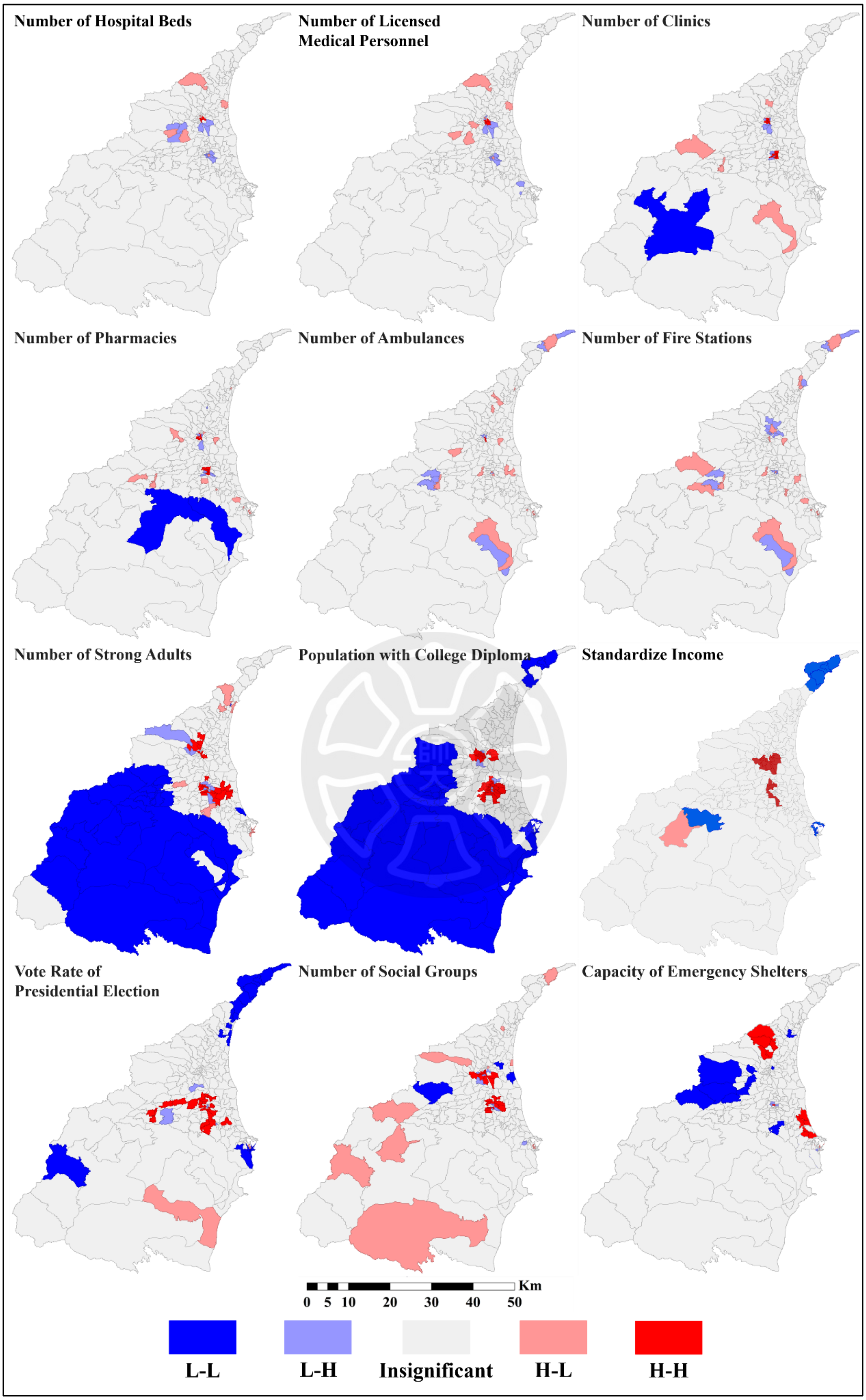

Fig. 4.23 Spatial clusters of socioeconomic variables (BRIC).

The result of the spatial distribution of these components is mapped out in Fig 4.25. Based on Moran's *I* and *p*-value, two of the components have a statistically significant cluster and seem to be in the center of the floodplain areas, while other variables show neither significant clustering nor dispersing.

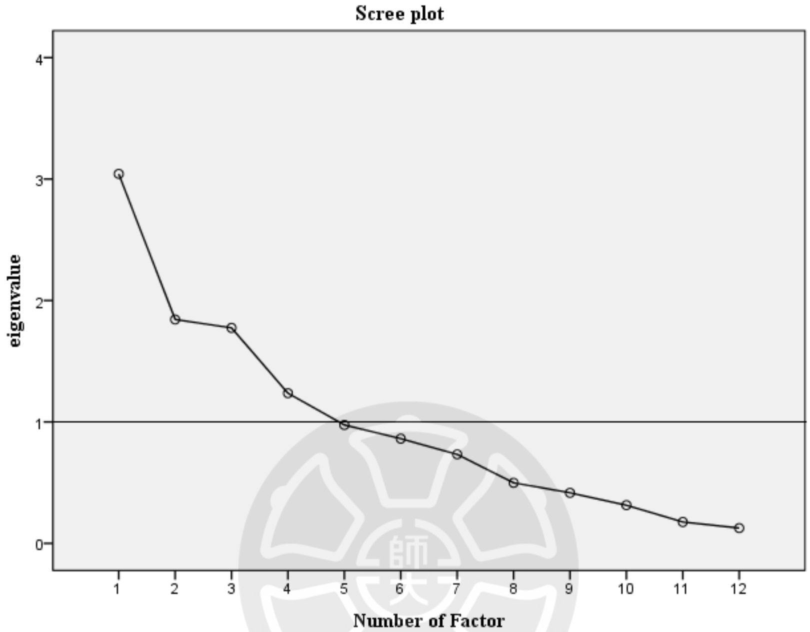

Fig. 4.24 Scree plot of PCA (BRIC).

The result of LISA is mapped out in Figure 4.26, which is remarkably similar to the distribution demonstrated in Fig 4.22 and 4.23. Most of the mountain areas are L-L clusters, while the center of the floodplain areas, the urban areas, are H-H clusters. Based on Fig 4.22 through Fig 4.26, the spatial distribution of the resources is concentrated in the floodplain areas. As a result, most of the H-H clusters are located in the floodplain areas. However, due to a lack of resources, the mountain areas are mostly L-L clusters.

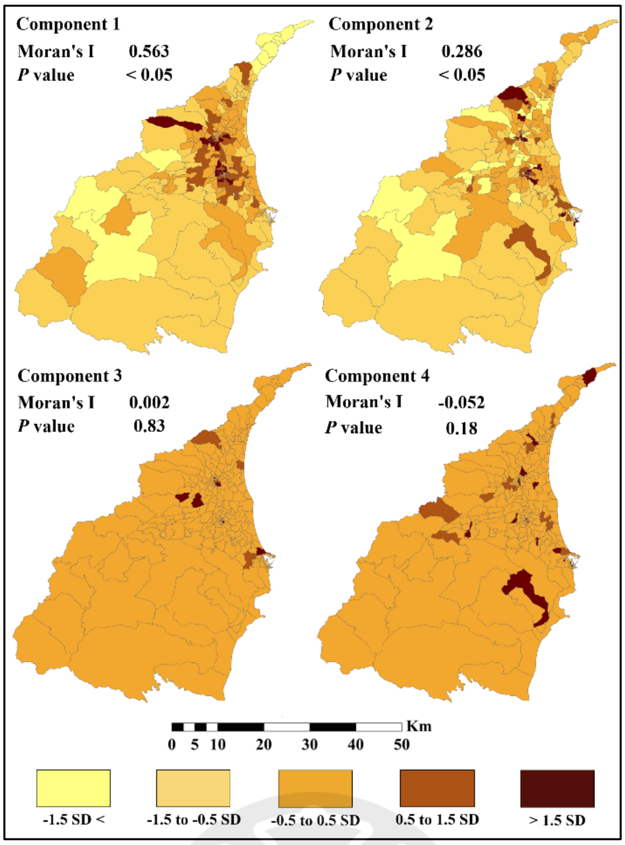

Fig. 4.25 Spatial distribution of all principal components (BRIC).

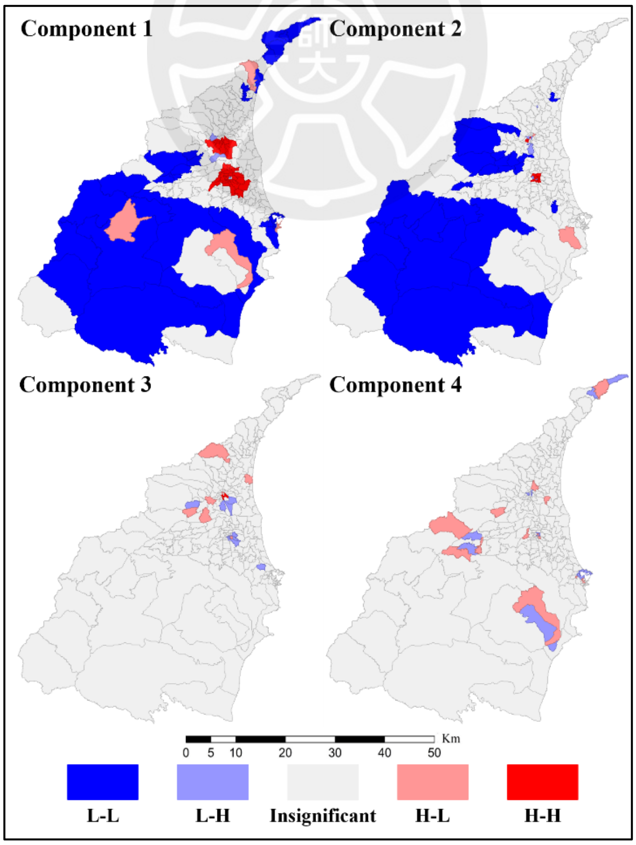

Fig. 4.26 Spatial clusters of all principal components (BRIC).

Table. 4.4 Moran's *I* Summary of BRIC

Moran's *I*	0.295
p-value	< 0.05

Table 4.4 and Fig 4.27 present the spatial distribution of BRIC and the result of global and local spatial autocorrelation analysis. According to Moran's *I* and *p*-value, the distribution of BRIC is a statistically significant cluster. Fig 4.26 shows the BRIC in the floodplain areas is conspicuously higher than in the mountain areas. Also, most of the high BRIC areas are located in urban areas such as Yilan City and Luodong Township. LISA also confirms this distribution since most of the mountain areas are L-L clusters while Yilan City and Luodong Township are H-H clusters.

The distribution of the variables causes the uneven distribution of BRIC. Although the statistical test results of some variables seem to be insignificant, based on the distribution map of the variables, the variables are either located in the floodplain areas or in the mountain areas. The inevitable difference caused by diverging socioeconomic status and infrastructure between the mountain areas and floodplain areas creates the uneven distribution of BRIC.

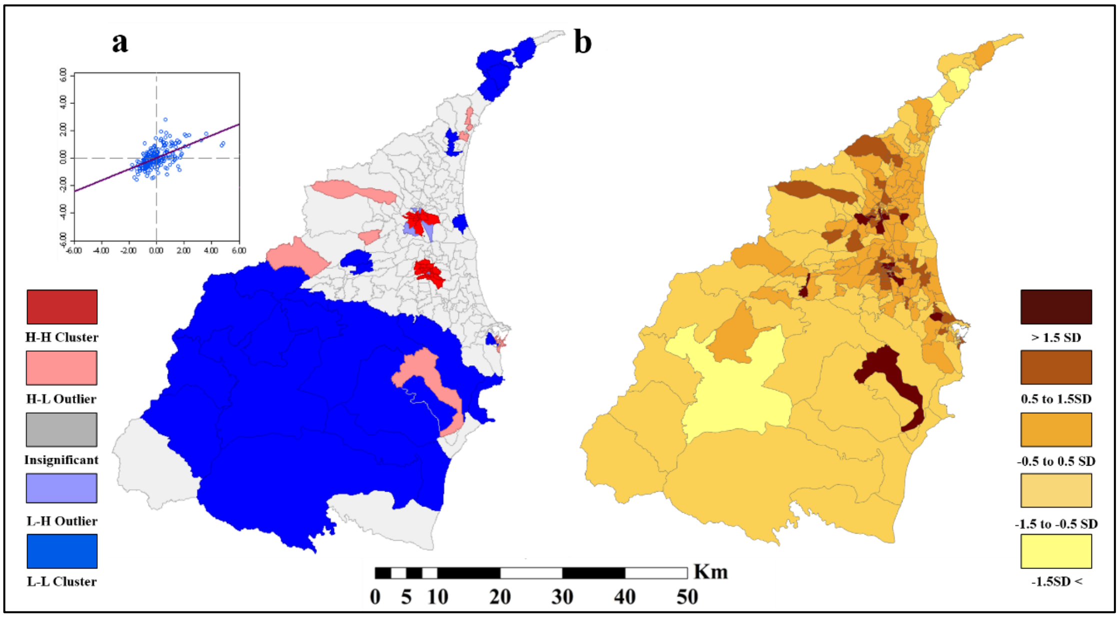

Fig. 4.27 The result of LISA (a) and spatial distribution (b) of BRIC in Yilan County.

4.2.2 BRIC of Floodplain Areas

The result of the previous section demonstrates a notable difference between the floodplain areas and mountain areas. In order to offer a specific exploration, this section aims to investigate the distribution of BRIC and variables in floodplain areas.

Fig 4.28 demonstrates the spatial distribution of the variables used to construct BRIC. The figure and the result of global autocorrelation indicate a situation similar to the previous section. Based on the Moran's *I* and *p*-value in Fig 4.28, most of the infrastructure and medical resources, for instance, the Number of Hospital Beds, the Number of Licensed Medical Personnel, the Number of Ambulances, and the Number of Fire Stations, are also distributed randomly in the floodplain areas. Furthermore, most of the urban areas have comparatively high values in the socioeconomic aspects, for example, the Ratio of Population Between 20 to 50 Years Old, Ratio of the Population with a College Diploma, Standardized Income, and Number of Social Units, while the values of the areas close to the coastal and southwestern areas are comparatively low. Dramatically uneven distribution of resources also occurred in the floodplain areas. In order to find the locations of clusters, LISA is applied.

The result of LISA is demonstrated in Fig 4.29. According to the figure, most of the infrastructure and medical resource variables such as the Number of Hospital Beds, Number of Licensed Medical Personnel, Number of Ambulances, and Number of Fire Stations do not have conspicuous clusters, while the socioeconomic variables, the Ratio of Population Between 20 to 50 Years Old, Ratio of the Population With a College Diploma, Standardized Income, and the Number of Social Units, show salient H-H clusters close to urban areas. Moreover, the areas close to the southwestern areas and the harbor areas also have conspicuous L-L clusters.

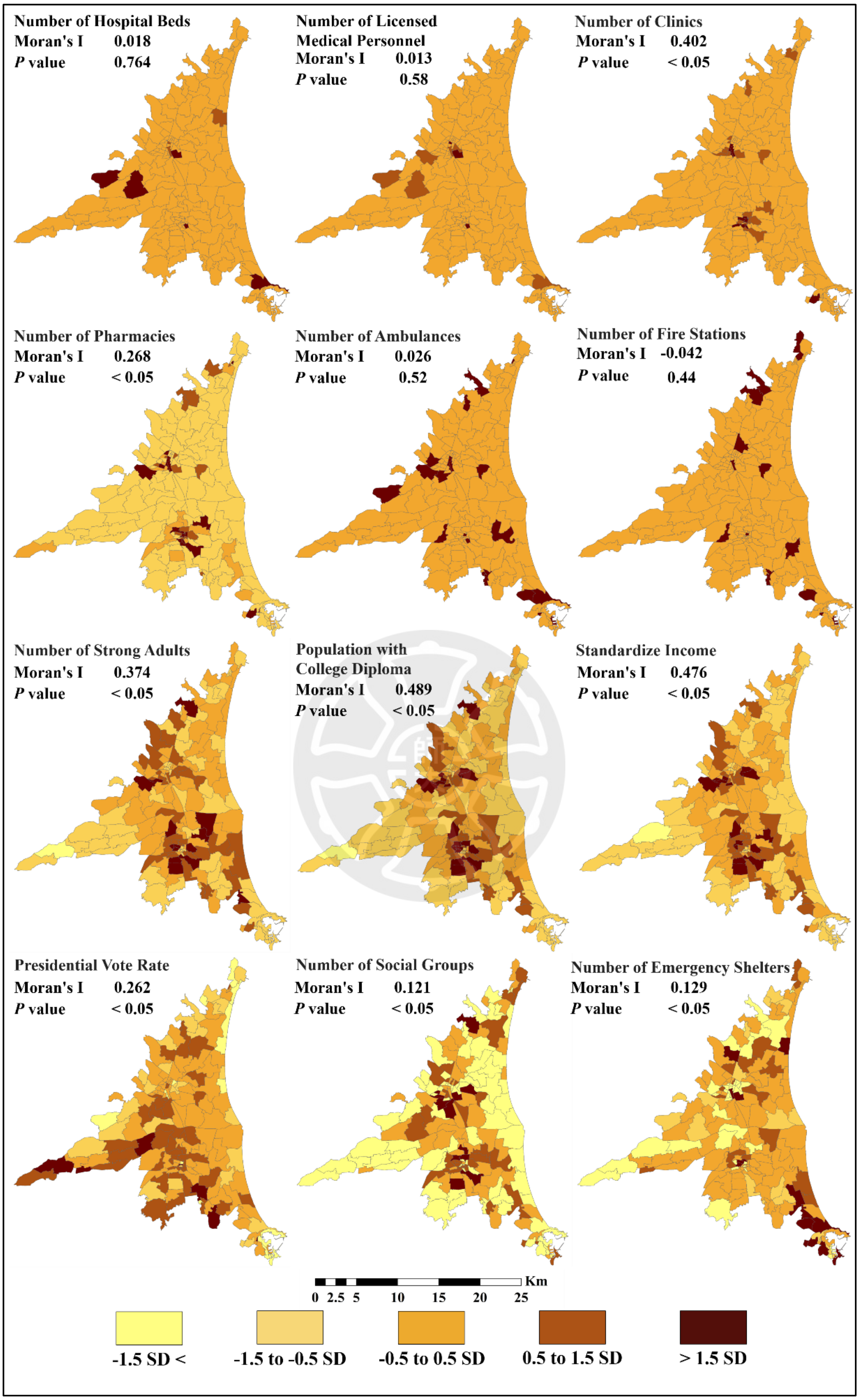

Fig. 4.28 Spatial distribution of socioeconomic variables in floodplain areas (BRIC).

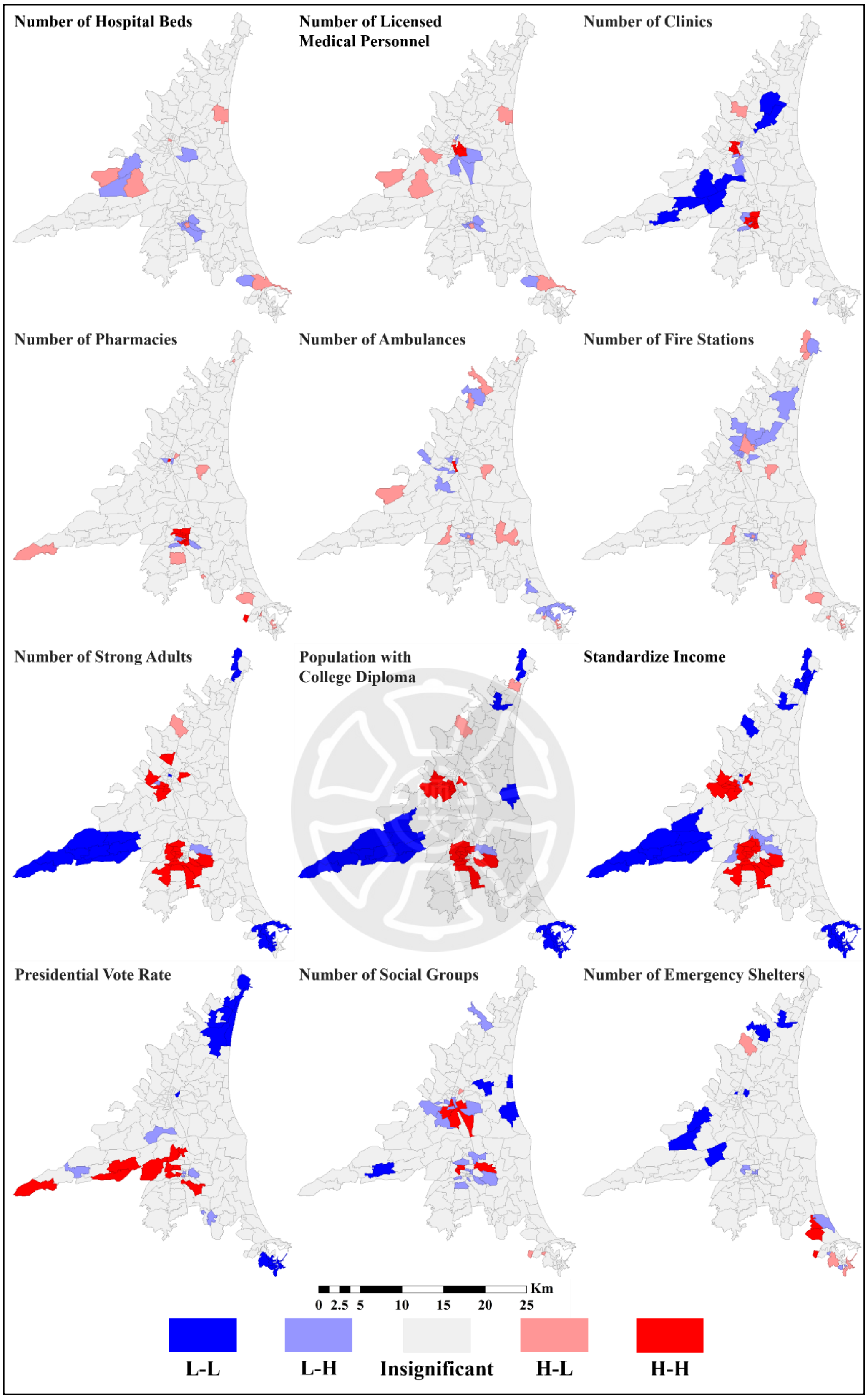

Fig. 4.29 Spatial clusters of socioeconomic variables in floodplain areas (BRIC)

Through the result of global and local spatial autocorrelation analysis, we found that the difference in the floodplain areas is also notable. Most of the resources are concentrated in urban areas, creating uneven distribution in floodplain areas.

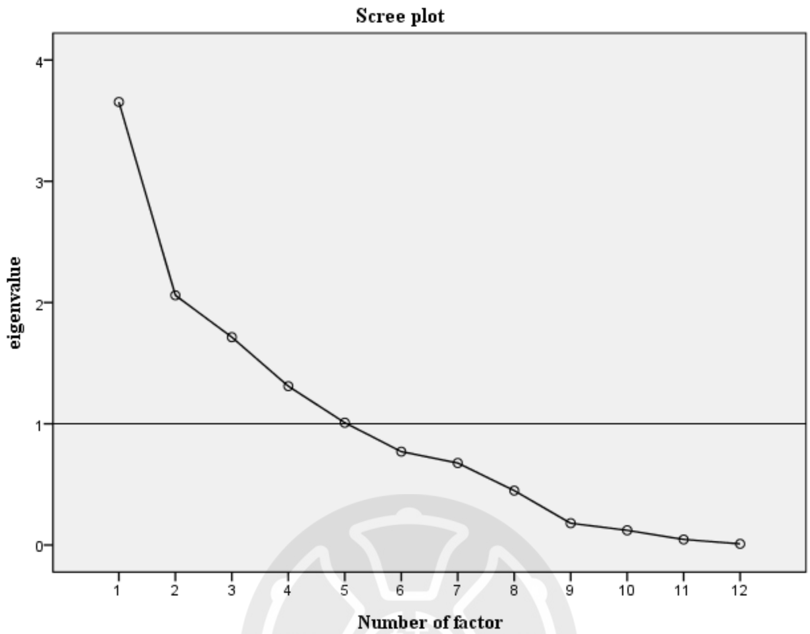

Fig. 4.30 Scree plot of PCA in floodplain areas (BRIC).

Fig 4.30 is the scree plot of PCA. Based on the PCA results, the variables can be reduced into five subcomponents. The KMO and the total variance explained are 0.646 and 81.224, respectively. The first component consists of the Ratio of the Population with a College Diploma, Standardized Income, Ratio of Population between 20 to 50 Years Old, and Number of Social Units. The second component includes the Number of Pharmacies and Number of Clinics and Hospitals. The third component is composed of the Number of Hospital Beds and Number of Licensed Medical Personnel. The fourth component is made by the Number of Ambulances and Number of Fire Stations. Last but not least, the fifth component includes the Presidential Election Voting Rate and Capacity of Emergency Shelters.

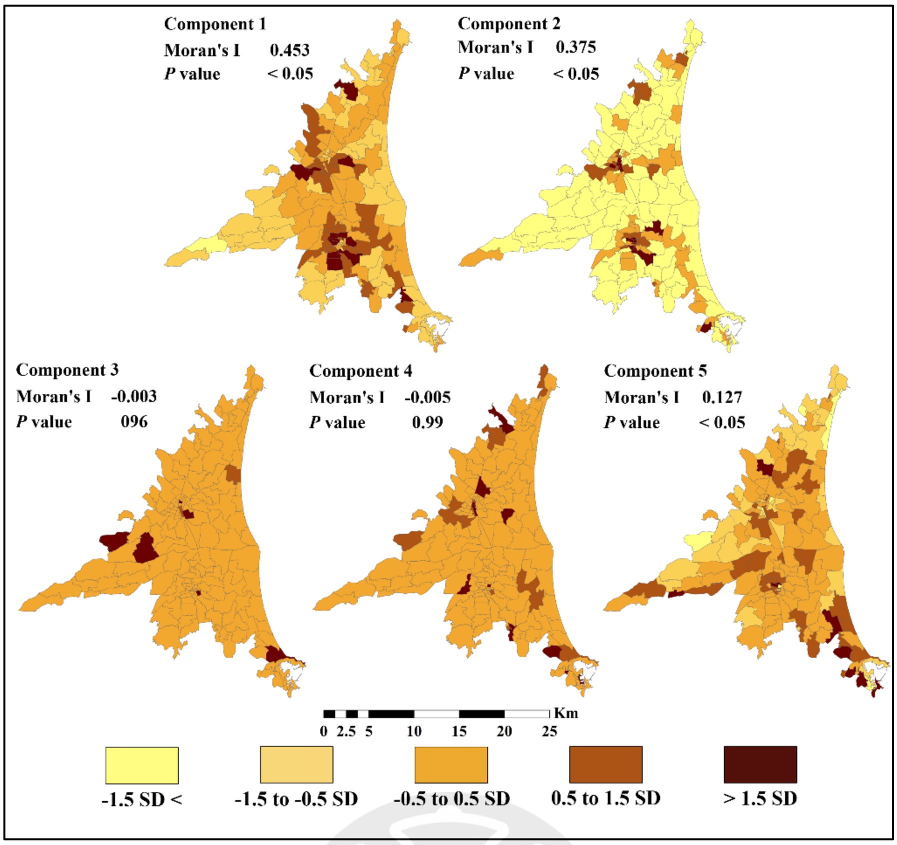

Fig. 4.31 Spatial distribution of all principal components in floodplain areas (BRIC).

According to Fig 4.31, the value of the first component is relatively higher in urban areas than in the southwestern and coastal areas. Moreover, according to Moran's *I* and *p*-value, the first component show a statistically significant cluster. The second component has a situation similar to the first component. The value in the urban areas is significantly higher than in other floodplain areas. Furthermore, the Moran's *I* and *p*-value indicate the second component is a statistically significant cluster. The third and the fourth components have totally different distributions compared to the first and second components, based on Moran's *I* and *p*-value; both of these components show comparatively random distribution. The last component is also a statistically significant cluster; however, the situation is different from the first and the second components. Moran's *I* is relatively low compared to the first and the second component. Moreover, the cluster seems to congregate in the southeastern areas and harbor areas rather than in the urban areas.

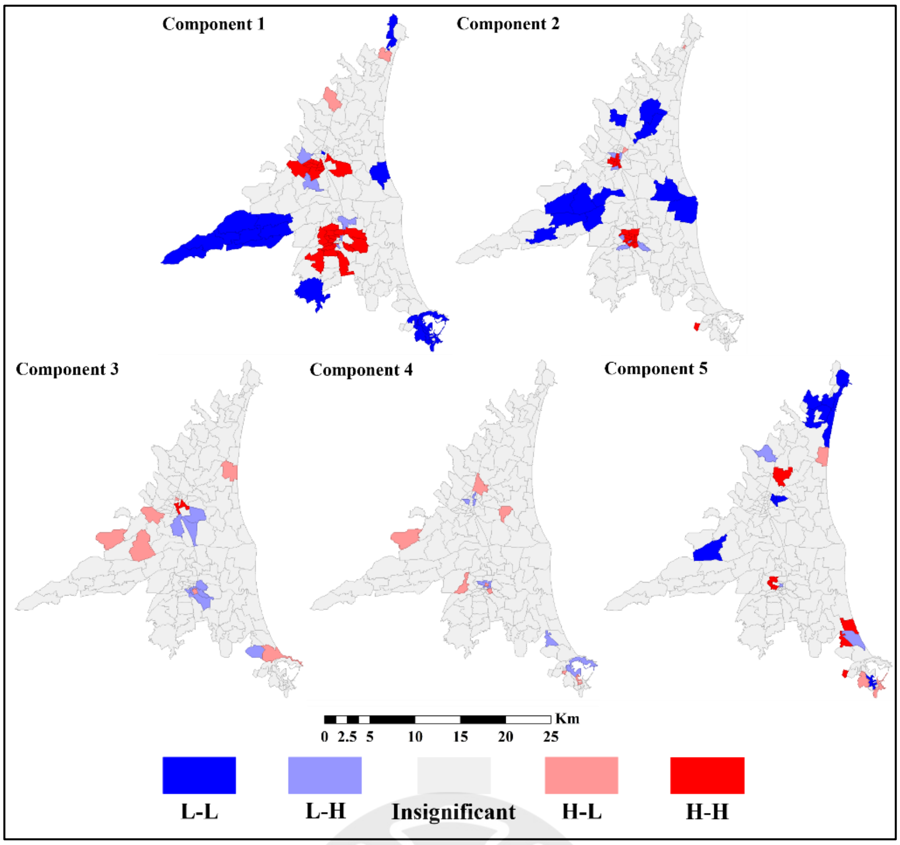

Fig. 4.32 Spatial clusters of all principal components in floodplain areas (BRIC).

The result of LISA is demonstrated in Fig 4.32. The first and the second components both have H-H clusters in the urban areas. Furthermore, the southwestern area has an L-L cluster. The third and fourth components have no salient H-H or L-L clusters, and most of the clusters are outliers. The last component has H-H clusters in the southeastern areas, while the northeastern areas are L-L clusters.

Table. 4.5 Moran's *I* summary of BRIC in floodplain areas

Moran's *I*	0.373
p-value	< 0.05

The distribution and result of spatial autocorrelation analysis of BRIC in the floodplain areas are shown in Table 4.4 and Fig 4.33. The urban areas undoubtedly have higher values of BRIC, while most of the southwestern and coastal areas have lower values. The Moran’s *I* and *p*-value also indicate that the BRIC in the floodplain areas represents statistically significant clusters. The local autocorrelation analysis also shows that the urban areas are H-H clusters, while the southwestern, northeastern, and part of the coastal areas are L-L clusters. Most of the infrastructure and medical resources in the floodplain areas are randomly distributed, while most of the socioeconomic resources are concentrated in the urban areas. As a result, we find a significant difference between the urban areas and other areas. The result of this section coincides with the results in the previous section.

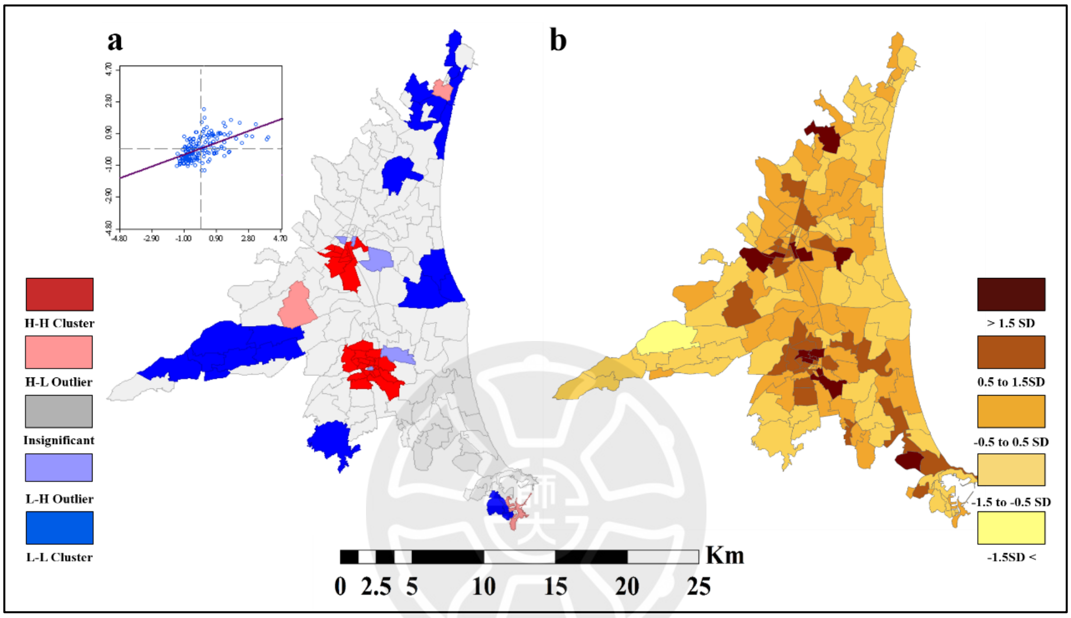

Fig. 4.33 The result of LISA (a) and spatial distribution (b) of BRIC in floodplain areas

4.2.3 BRIC of Mountain Areas

The distribution of the variables for building BRIC and the result of global spatial autocorrelation in mountain areas are demonstrated in Fig 4.34. The spatial distribution of all variables shows that the values of infrastructure and medical resources are significantly low. For example, the Number of Hospital Beds, Number of Licensed Medical Personnel, Number of Ambulances, and Number of Fire Stations are all significantly low. Moreover, the Number of Clinics and Number of Pharmacies in mountain areas is also low. It seems the situation is similar to the floodplain; nevertheless, the situation in mountain areas is more dramatic, where the scarcity of resources is quite severe. Moreover, the socioeconomic conditions in mountain areas are also deplorable. The values of the variables such as the Ratio of Population Between 20 to 50 Years Old, Ratio of the Population with a College Diploma, Standardized Income, and Number of Social Units in mountain areas are also low. Fig 4.34 presents the severe circumstance in mountain areas. Not only do we find a lack of infrastructure but also poor socioeconomic conditions in the mountains. Though nearly half of the variables seem to show no specific spatial clustering, a thorough investigation of spatial distribution and spatial autocorrelation analysis are conducted to determine cluster locations.

The Moran's *I* and *p*-value show the Ratio of Population Between 20 to 50 Years Old, Ratio of Population with a College Diploma, Standardizes Income, Presidential Election Voting Rate, and Capacity of Emergency Shelters are statistically significant. In other words, over half of the variables have no statistically significant clusters. Though the Ratio of Population Between 20 to 50 Years Old, Ratio of the Population with a College Diploma, Standardized Income, Presidential Election Voting Rate, and Capacity of Emergency Shelters are statistically significant clusters, the Moran's *I* values are relatively low, meaning the clusters of these variables are quite moderate.

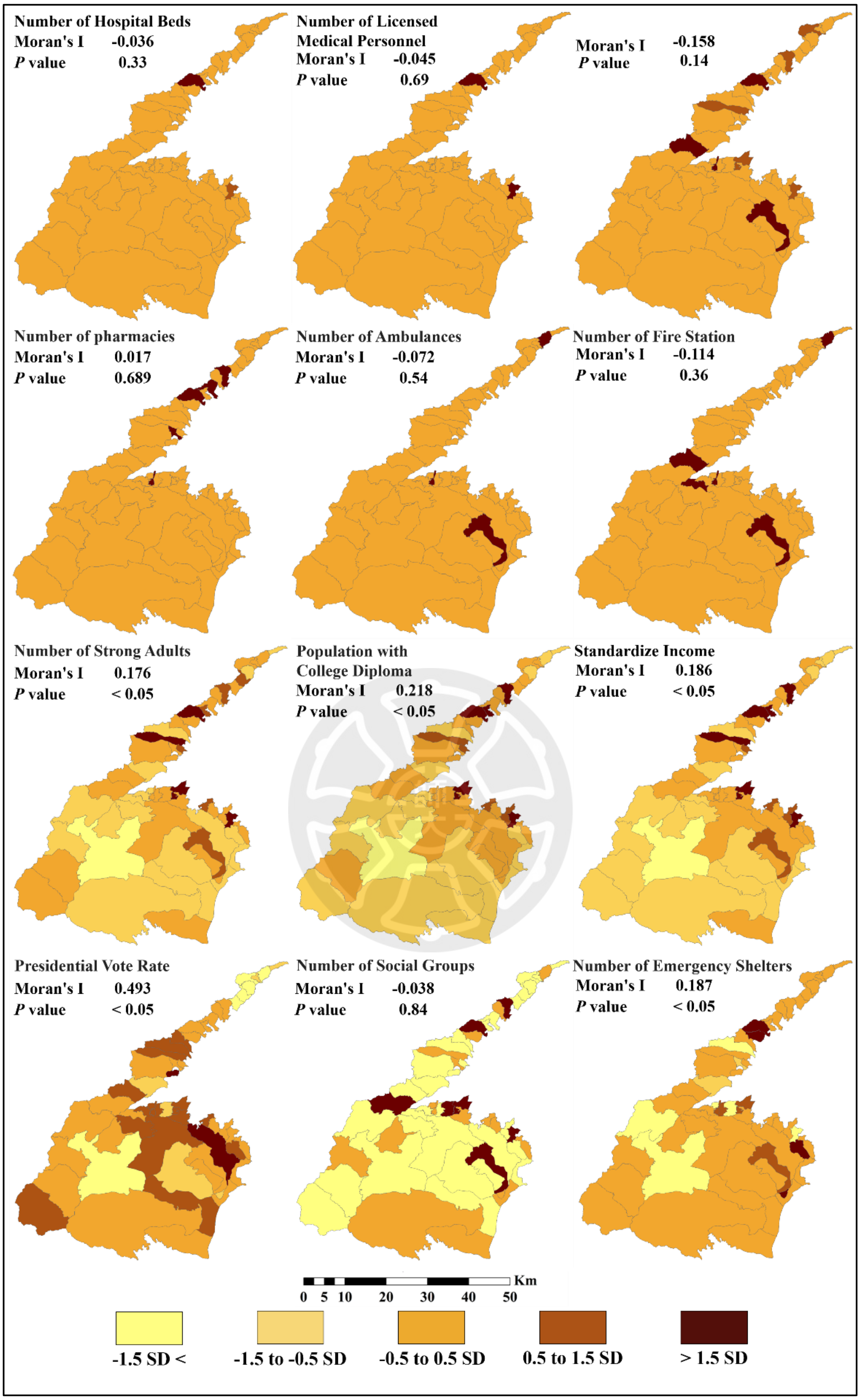

Fig. 4.34 Spatial distribution of socioeconomic variables in mountain areas (BRIC).

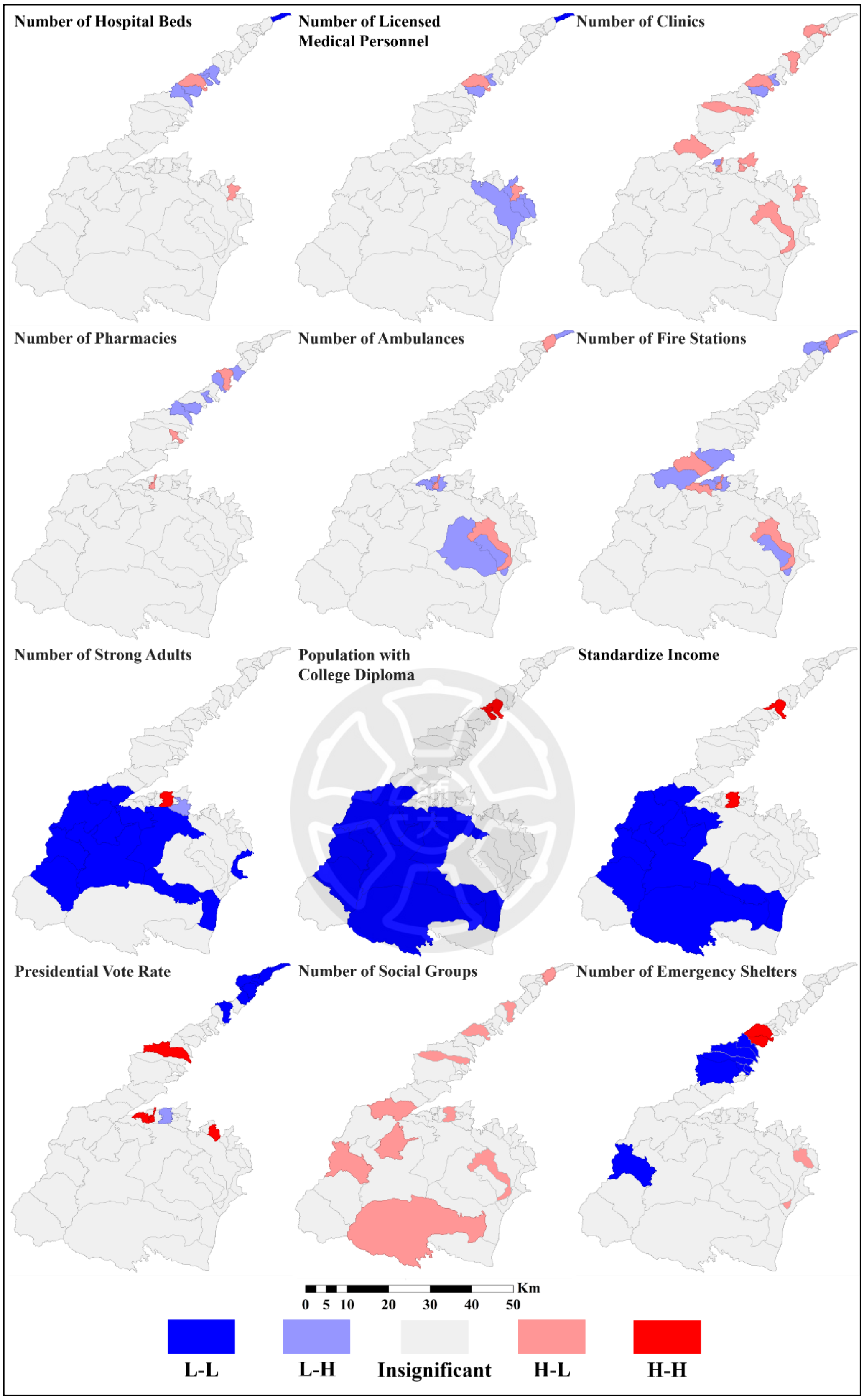

Fig. 4.35 Spatial cluster of socioeconomic variables in mountain areas (BRIC).

In order to have a thorough investigation, LISA analysis is conducted for all variables, even though some of the variables' *p*-values are insignificant. Fig 4.35 shows that most of the infrastructure and medical resources do not have a significant pattern, for instance, the Number of Hospital Beds, Number of Licensed Medical Personnel, Number of Clinics, Number of Pharmacies, Number of Ambulances, and Number of Fire Stations. Nonetheless, the Ratio of Population between 20 to 50 Years Old, Ratio of the Population with a College Diploma, and Standardized Income have salient L-L clusters in the mountain areas. Also, the Capacity of Emergency Shelters shows L-L clusters, though the locations are different from the other variables. The noticeable variables are the Presidential Election Voting Rate and the Capacity of Emergency Shelters, which have H-H clusters in the mountain areas. Although two of the variables have H-H clusters, the scopes are comparatively insignificant.

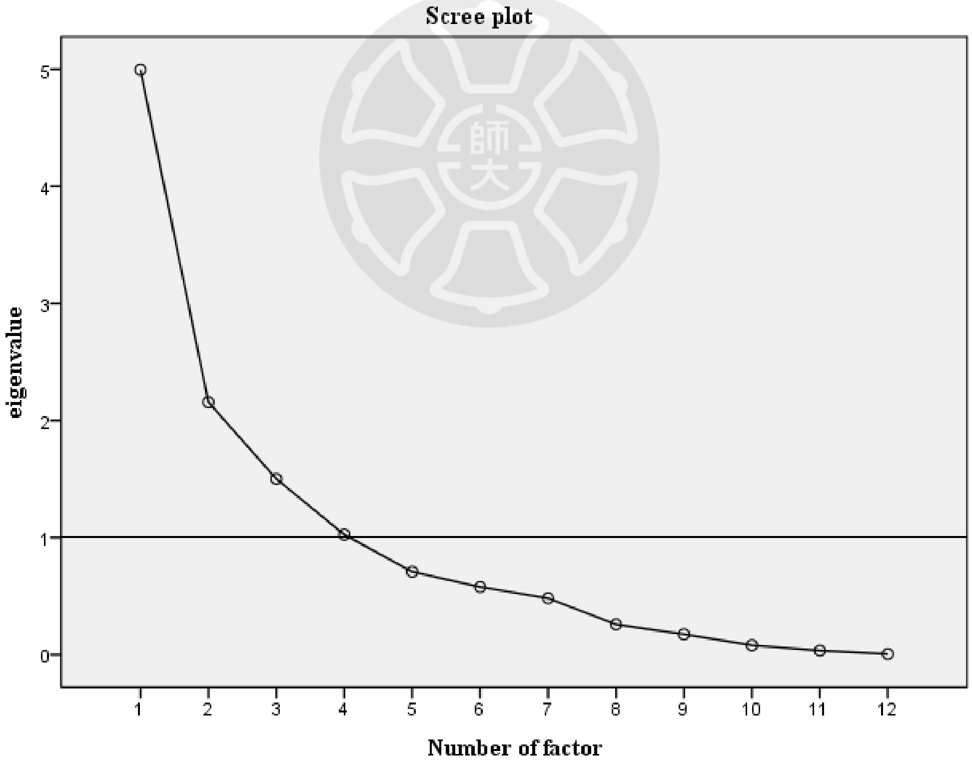

Fig. 4.36 Scree plot of PCA in mountain areas (BRIC).

Based on Fig 4.36, the PCA generates four principal components in mountain areas. The KMO and total variance explained are 0.75 and 80.654, respectively. The first component includes Standardized Income, Ratio of Population between 20 to 50 Years

Old, Ratio of the Population with a College Diploma, and Number of Social Units. The second component includes the Number of Hospital Beds, Number of Pharmacies, Capacity of Emergency Shelters, and Number of Licensed Medical Personnel. The third component includes the Number of Ambulances, Number of Fire Stations, and Number of Clinics and Hospitals. The last component includes the Presidential Election Voting Rate. The values of most of the variables in mountain areas are quite moderate. The *p*-values in Fig 4.37 show that the distributions of the first and third components are insignificant, while those of the second and fourth components are significant.

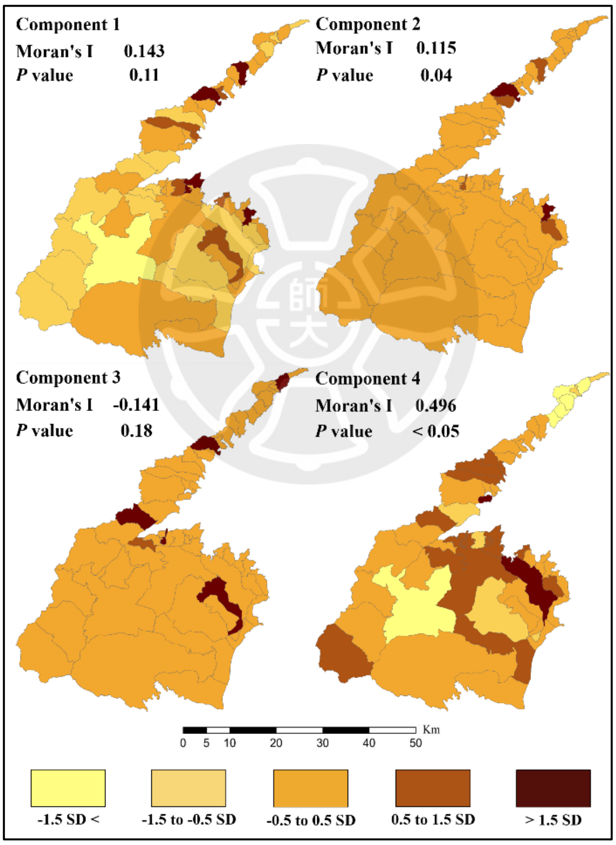

Fig. 4.37 Spatial distribution of all principal components in mountain areas (BRIC).

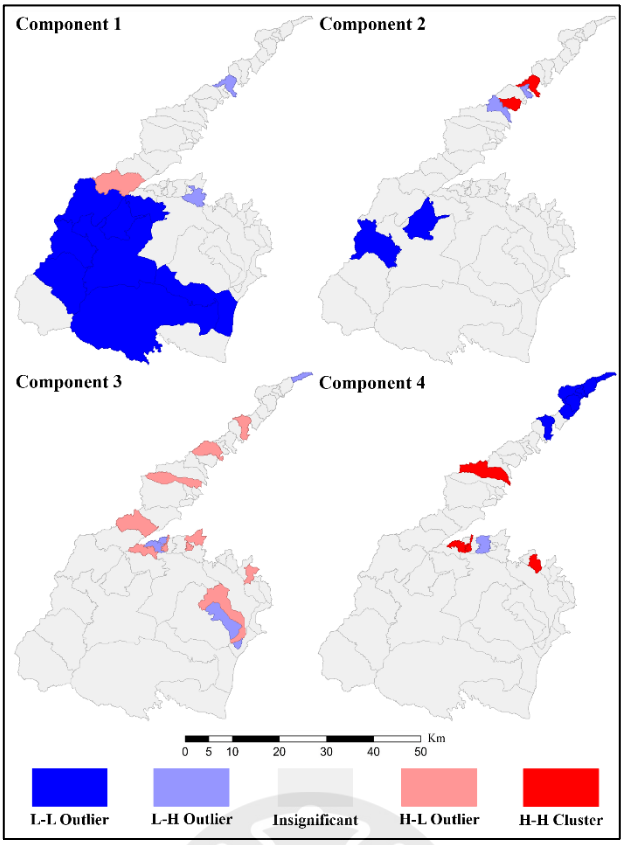

Fig. 4.38 Spatial clusters of all principal components in floodplain areas (BRIC).

The results of LISA show that only the first component has a salient L-L cluster in the majority of mountain areas. The clusters of the rest of the components are either insignificant or relatively scattered on the edge of the mountain areas. The third component has multiple H-L and L-H outliers, but these are still dispersed.

Fig 4.39 demonstrates the BRIC in the mountain areas. The value of BRIC seems to be relatively low in the center of the mountain areas, while the edge areas close to the floodplain seem to have higher values. However, according to Table 4.6, the distribution pattern of BRIC is not statistically significant, meaning the distribution is comparatively random. However, the LISA result demonstrates that the center of the mountain areas has L-L clusters, meaning the central mountain areas have many communities with low BRIC values, which coincides with the result of section 4.2.1.

Table. 4.6 Moran's *I* summary of BRIC in mountain areas

Moran's *I*	0.038
p-value	0.57

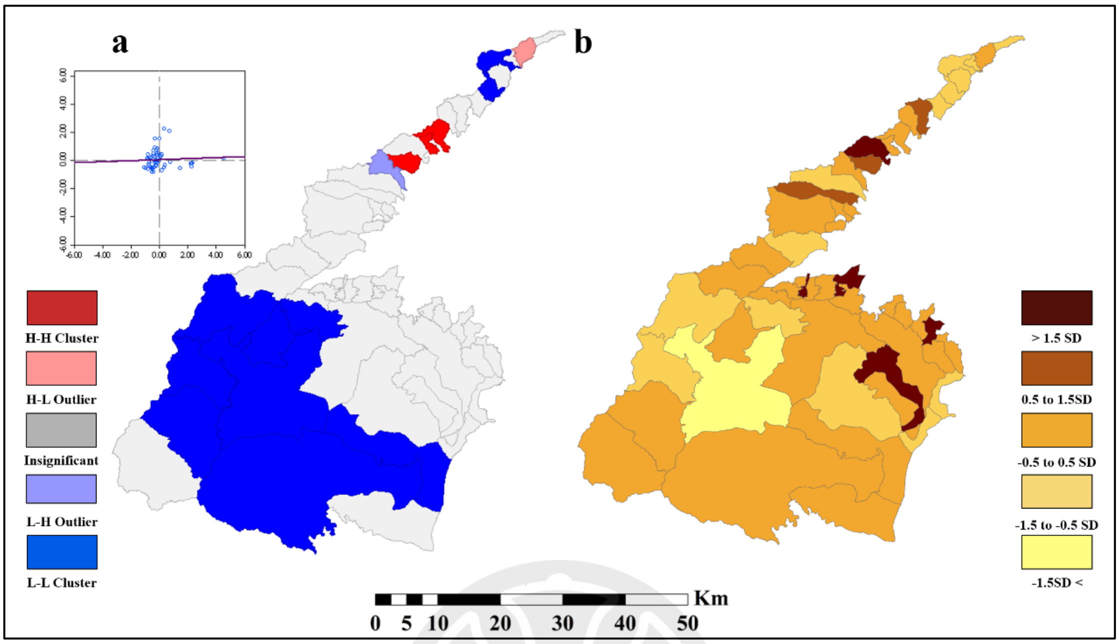

Fig. 4.39 The result of LISA (a) and spatial distribution (b) of BRIC in mountain areas

4.3 Risk and SERV

4.3.1 Risk

The results of previous sections represent the socioeconomic vulnerability to environmental hazards and the baseline resilience of the community. Both these indicators represent the social fabric of a place's vulnerability and resilience. In order to integrate the social fabric with the biophysical aspects, the concept of risk and the SERV model is applied. The biophysical aspects used in this research are the potential of environmental hazards, including the potential of floods and debris flow. Both of these potential hazards often occur in different areas. Debris flows usually occur in the mountain areas, while floods usually occur in the floodplain areas. Due to the characteristics of these two kinds of environmental hazards, this research separates the study areas into mountain and floodplain areas based on the elevation threshold. However, this research also focuses on the macro aspect of the assessment. As a result, the potential of flood and debris flow is combined after the potentials are standardized and then referred to using a general term, i.e., environmental hazard potential.

This section focus on the entire scope of Yilan County. Environmental hazard potential, the general term mentioned above, is used in this section. The flood potential includes the possibility of 200 mm, 350 mm, 450 mm, and 600 mm. The general environmental hazard potential is generated by combining the standardized potential of debris flow with each standardized flood potential. Therefore, this section presents four different results based on the potential for different environmental hazards.

Fig 4.40 includes the results of the different scenarios. The risks of most communities in Yilan County are at a medium-high level. The Zhaoyang and Shicheng Villages are the only two villages that exceed the high. The risk of southwestern areas shows no change because the potentials for debris flow of the four results are the same.

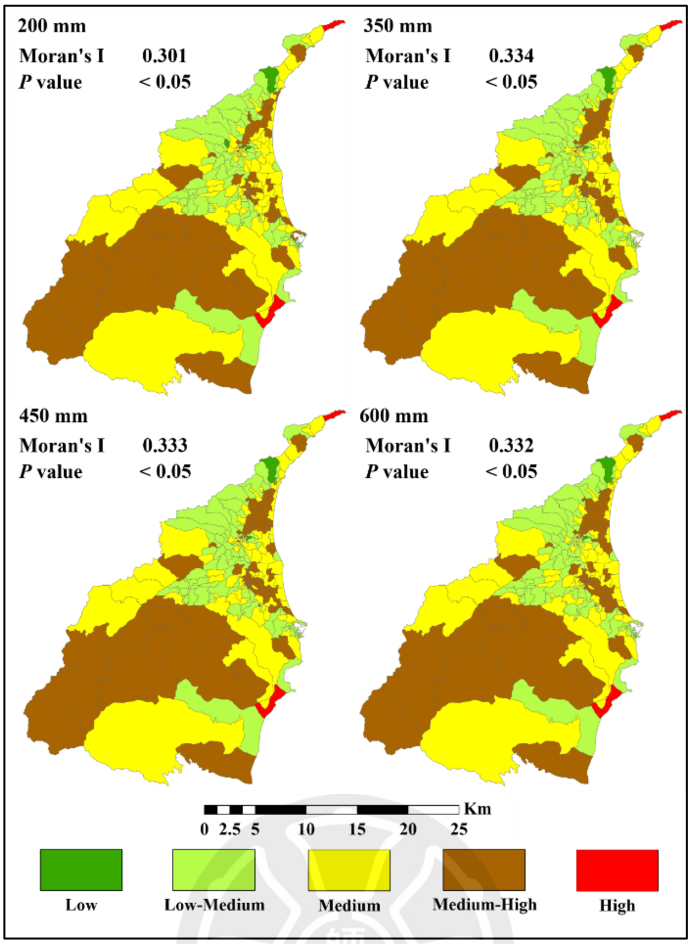

Fig. 4.40 The spatial distribution of risk in all scenarios.

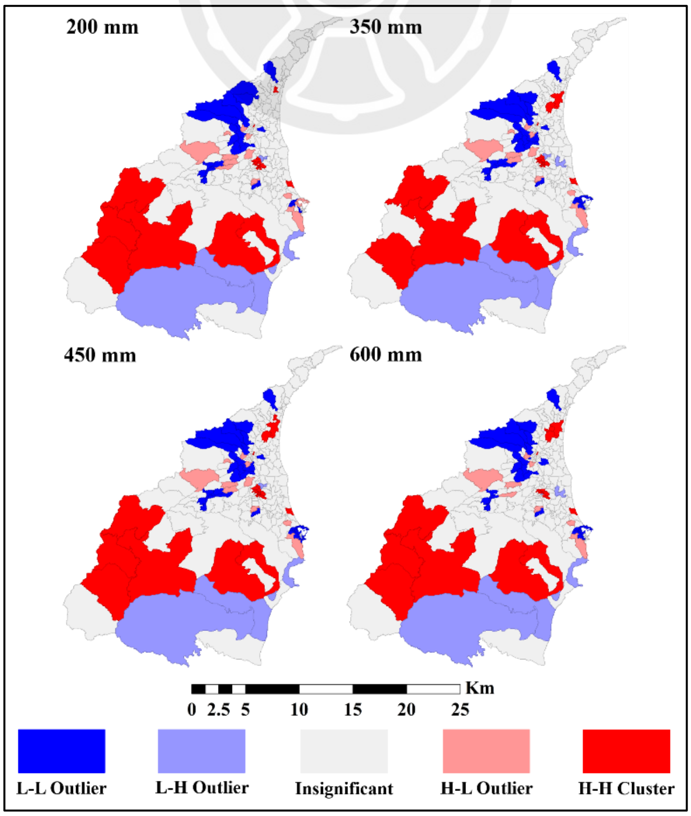

Fig. 4.41 Fig. 4.40 The spatial clusters of risk in all scenarios.

However, the conditions in the floodplain areas are quite different. The medium-high risk levels in the floodplain areas increase with flood potential. Moreover, Moran's *I* and *p*-value show statistically significant clusters of risk in Yilan County. Fig 4.41 demonstrates the result of LISA. The southwestern areas are undoubtedly an H-H cluster since the majority of these areas are medium-high risk. Although the scope of the H-H cluster in the floodplain areas also increases with flood potential, the degree of increase is relatively insignificant.

In order to specify the risk distribution of floodplain areas, this study separates the floodplain areas from the rest of Yilan County. Fig 4.42 represents the distribution of risk in floodplain areas. The highest degree of risk in floodplain areas is also a medium-high level. The medium-high risk areas are concentrated in the northern and southern areas of the floodplain area. Based on Fig 4.43, we found that the H-H cluster areas also increase with flood potential.

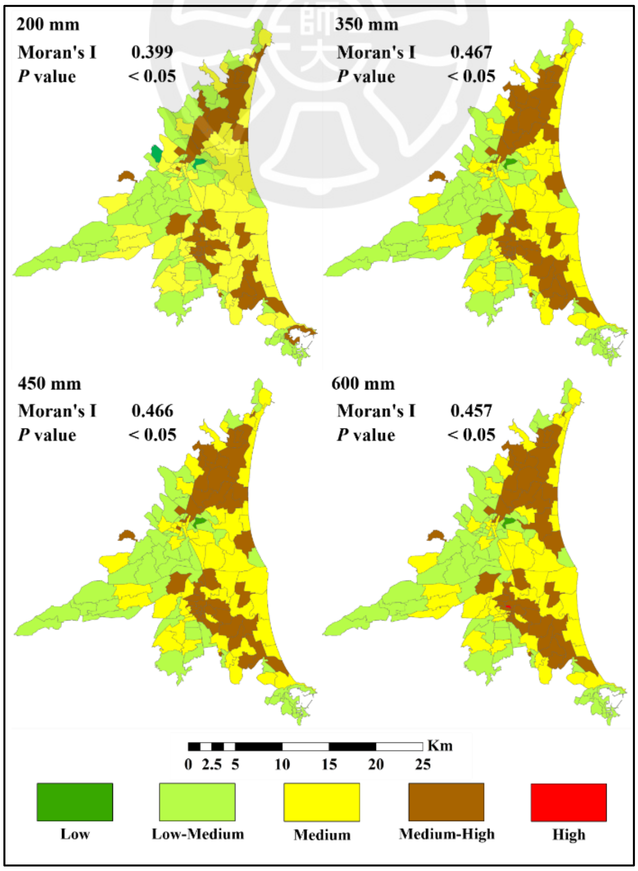

Fig. 4.42 The spatial distribution of risk in floodplain areas.

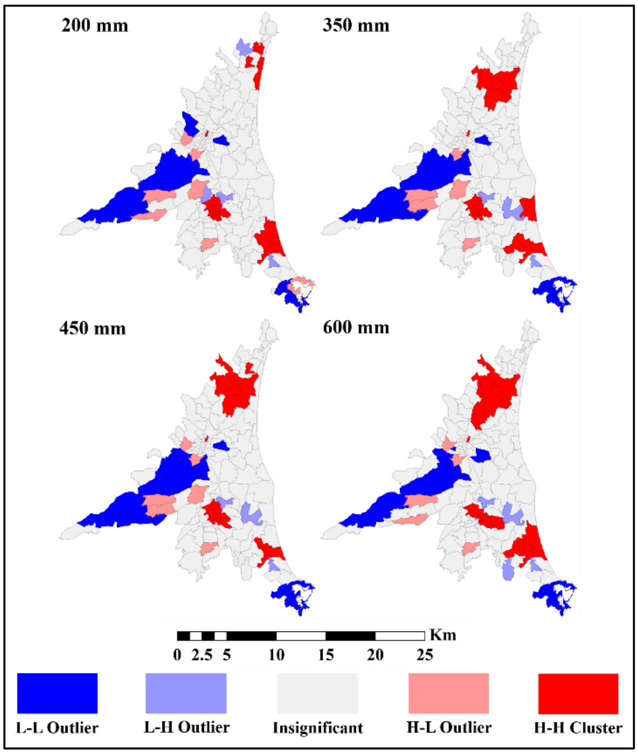

Fig. 4.43 The spatial clusters of risk in floodplain areas.

Fig 4.44 and Fig 4.45 demonstrate the distribution of risk and the result of global and local spatial autocorrelation analysis in mountain areas. Although the risk level in mountain areas does reach a high level, the results are insignificant. In the mountain areas, the distribution coincides with the distribution in Fig 4.38 and 4.39. Medium-high level risk areas are clustered in the center of the mountain areas. The Moran's *I* and *p*-value also show the risk in the mountain areas is statistically and significantly clustered. One noticeable area is Luodong Township. Although the risk is relatively high, as seen in Fig 4.31 and 32, the baseline resilience of the community is also higher than in other areas.

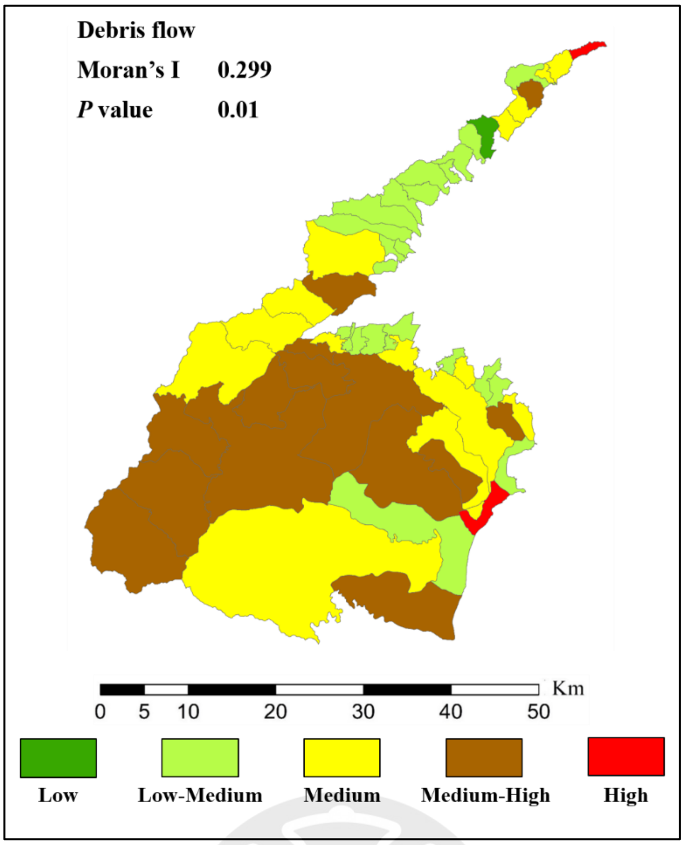

Fig. 4.44 The spatial distribution of risk in mountain areas.

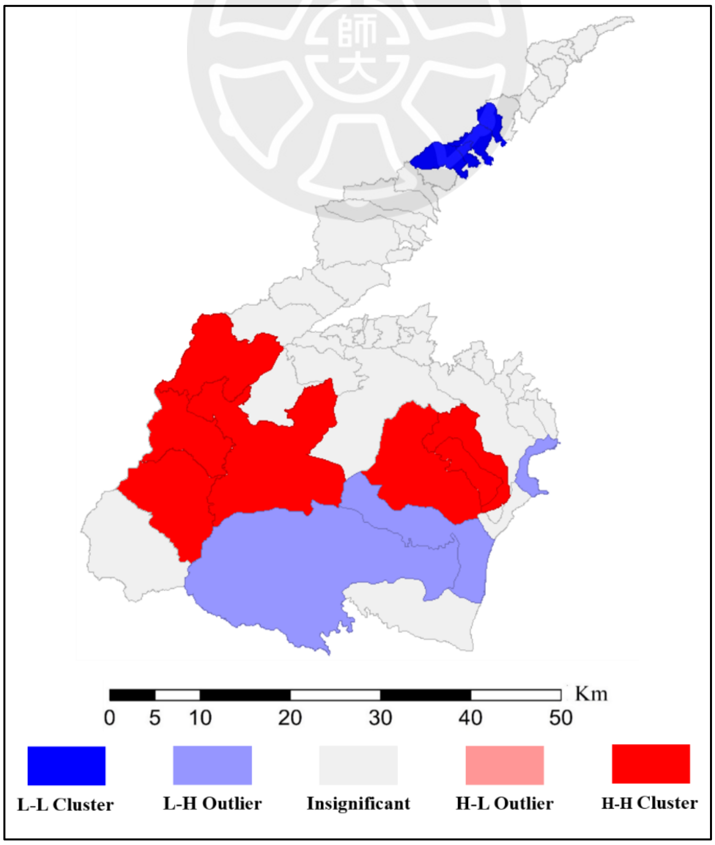

Fig. 4.45 The spatial clusters of risk in mountain areas.

4.3.2 SERV

One of the aims of this research is to combine the concepts of the social vulnerability to environmental hazards, baseline resilience of communities, and biophysical aspects of environmental hazards. Despite the fact that the previous risk concept can integrate the social vulnerability to environmental hazards and biophysical aspects of environmental hazards, it fails to take into account the baseline resilience of communities. In order to achieve this goal and provide holistic analysis, the SERV model is applied. Through SERV, all three elements mentioned above are integrated.

In Yilan County, the variables of the biophysical aspects of environmental hazards adopted here include the potential for the general environmental hazards mentioned in section 4.3.1. The environmental hazard potential is combined with the social vulnerability to environmental hazards, the SoVI. Upon the summation of the environmental hazard potential and SoVI, we then subtract BRIC value. As a result, in this section, a lower value represents higher resilience and lower vulnerability to environmental hazards.

Fig 4.46 and Fig 4.47 illustrate the distribution and the spatial clusters of SERV. In all circumstances, the majority of mountain areas have significantly higher values, while the floodplain areas are comparatively low. This condition means the mountain areas not only have higher vulnerability to environmental hazards but lower baseline resilience as well, compared to the floodplain areas. This circumstance can also be seen in Fig 4.9 and 4.26. Due to the remote distance, inferior socioeconomic status, shortage of infrastructure, inadequate medical resources, and lack of development chances, the mountain areas reveal the agglomeration of all the disadvantages, thus creating this extremely vulnerable situation. However, the floodplain areas include two major urban areas with abundant infrastructure, medical resources, and development chances. Almost all resources are concentrated in the floodplain areas, leading to less vulnerability and more resilience to any kind of flood scenario.

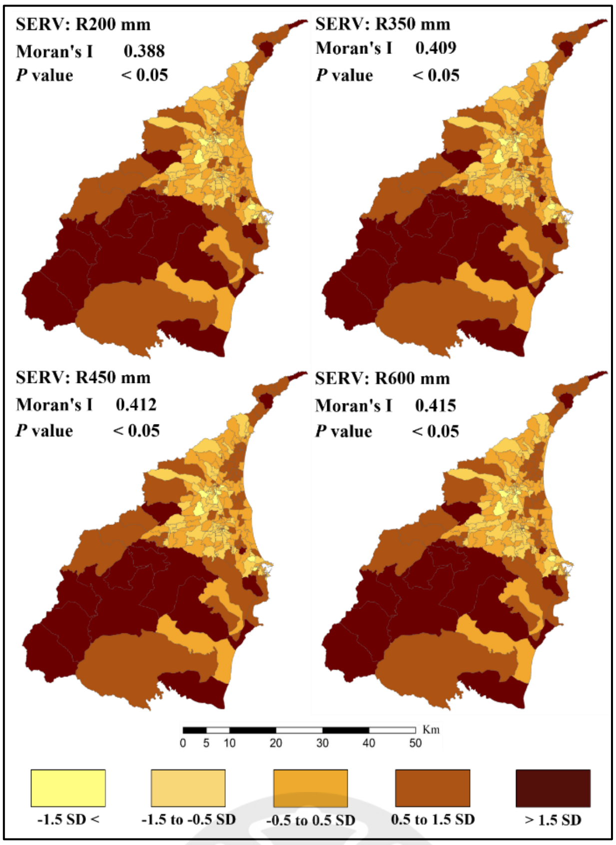

Fig. 4.46 Spatial distribution of SERV.

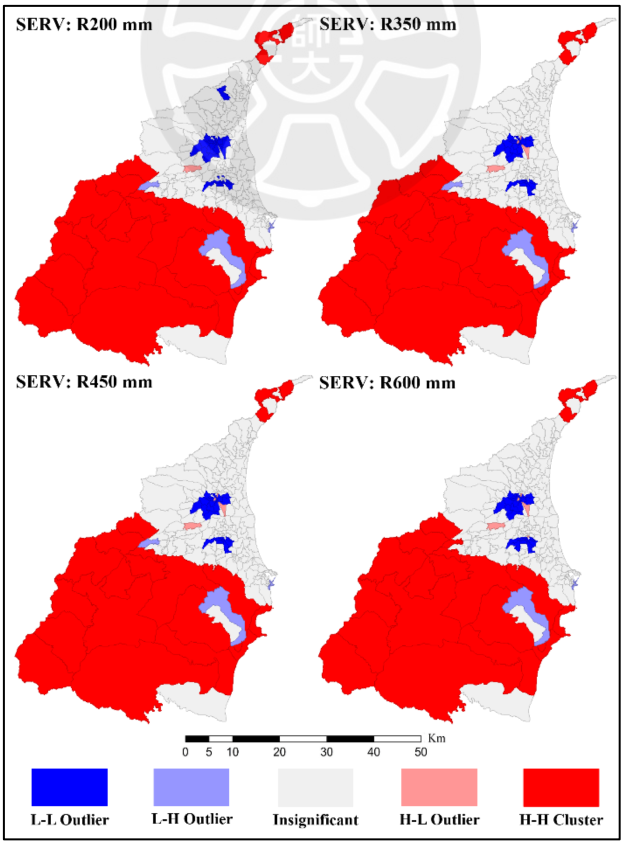

Fig. 4.47 Spatial clusters of SERV.

Through Moran's I and p-value in Fig 4.46, the spatial cluster is confirmed. The results of LISA show an H-H cluster of SERV located in almost all the mountain areas, while the regions surrounding Yilan City and Luodong Township form an L-L cluster. The distribution of H-H and L-L clusters also suggests that mountain areas represent the agglomeration of all disadvantages, while almost all resources are concentrated in floodplain areas.

Fig 4.48 and 4.49 point out the distribution of SERV in floodplain areas and the result of the spatial autocorrelation. Although SERV also combines SoVI and the potential for flooding, the distribution of SERV is different from that of risk since SERV also takes account of the baseline resilience of the community. The northern floodplain areas have lower BRIC, and after subtracting BRIC, the northern part of floodplain areas still has a higher vulnerability in all flood scenarios.

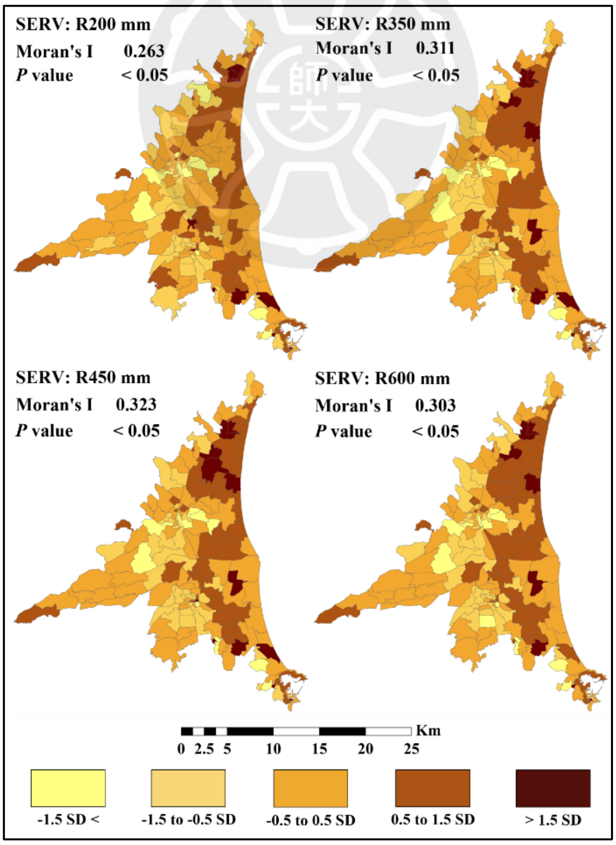

Fig. 4.48 Spatial distribution of SERV in floodplain areas.

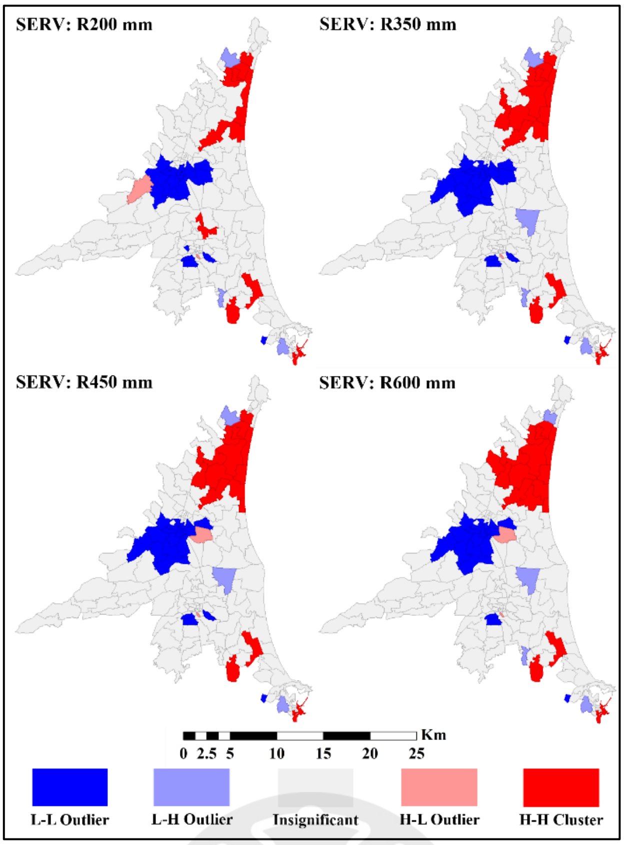

Fig. 4.49 Spatial clusters of SERV in floodplain areas.

The Moran's *I* and *p*-value show that the distribution of SERV in floodplain areas also forms a statistically significant cluster. Fig 4.49 not only demonstrates the location of the cluster but also confirms that the northern part of the floodplain area has a higher vulnerability and a lower baseline resilience for the community since SERV shows an H-H cluster. Although the regions surrounding Yilan City and Luodong Township seem to have a lower vulnerability and a higher baseline resilience of the community, based on Fig 4.49, the area of the L-L cluster encompassing Yilan City is larger than that of Luodong Township. Both Yilan City and Luodong Township have higher BRIC values, but the latter overlaps with flood potential and has higher SoVI. Thus, comparatively, the vulnerability of Luodong Township is directly increased by the potential for flooding, thus creating this difference. This difference, yet, cannot refute the fact that Luodong Township has a higher baseline community resilience based on Fig 4.31.

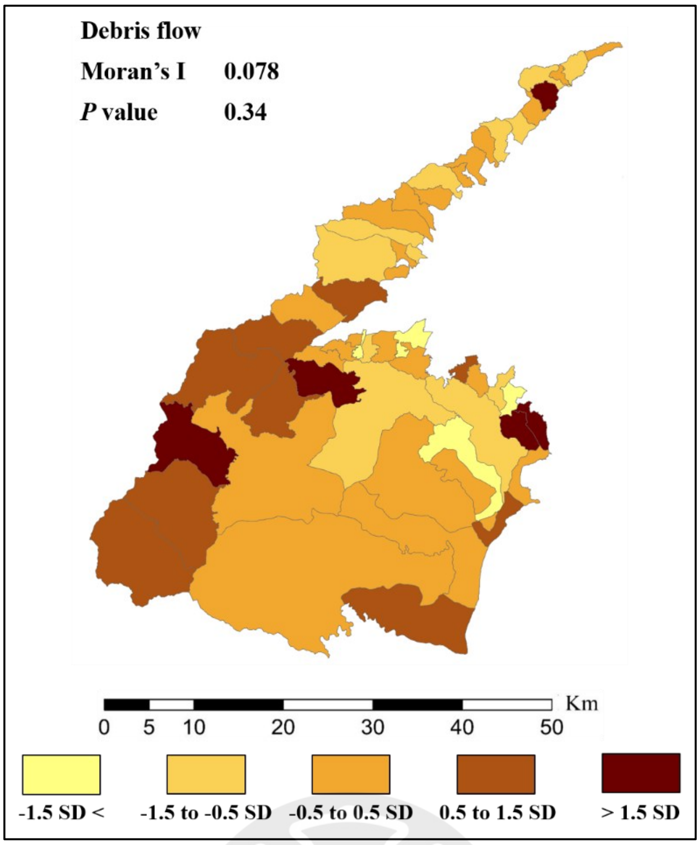

Fig. 4.50 Spatial distribution of SERV in mountain areas.

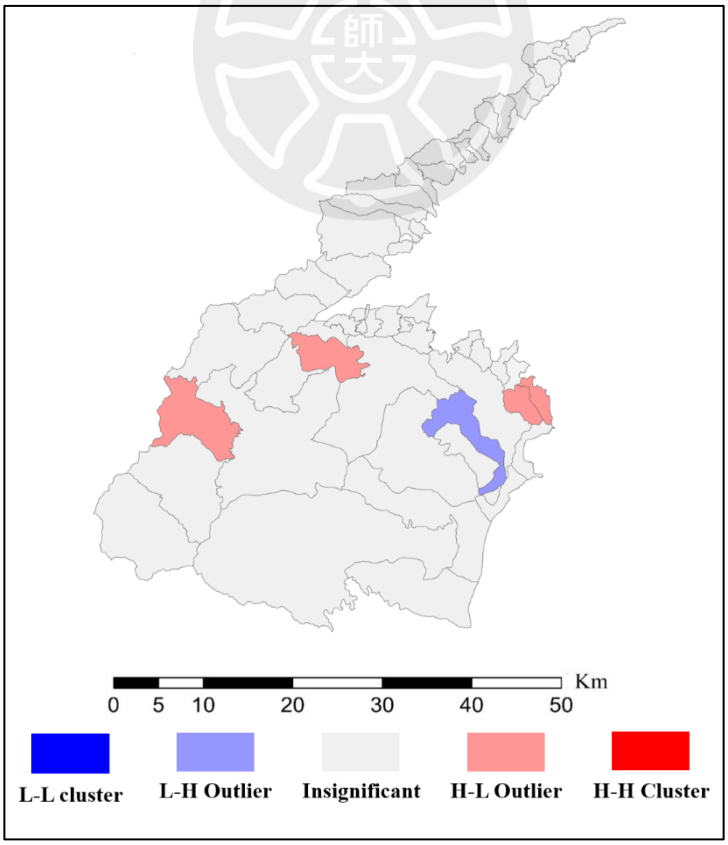

Fig. 4.51 Spatial clusters of SERV in mountain areas.

Last but not least, Fig 4.50 and Fig 4.51 demonstrate the spatial distribution of SERV in mountain areas and the result of the spatial autocorrelation analysis. Fig 4.50 shows higher SERV values congregated in the west of the mountain areas. The SERV value in the remaining west and north areas is significantly close to the mean value of SERV in mountain areas. Although The villages of Yongchun and Yongle have higher SERV values, most of the remaining south and east areas are also very close to the mean value of SERV in mountain areas. In other words, though some of the communities have higher SERV values, most have relatively homogenous SERV values. The Moran's *I* and *p*-value show the distribution of SERV in mountain areas does not reveal any statistically significant pattern, neither clustering nor dispersing. According to Fig 4.51, the SERV in mountain areas does show any H-H or L-L clusters, only a few H-L and L-H outliers

4.4 Multivariate Regression

One of the purposes of this research is to validate the effectiveness of the indices. As a result, we applied multivariate regression to validate the indices through multivariate regression and authentic environmental hazard events, including floods and debris flows. The multivariate regression is conducted on two scales: (1) county-wide and (2) flood plain and mountain areas. In the floodplain areas, the dependent variable is flooding, while the dependent variable in mountain areas is debris flow. Additionally, on a county-wide scale, we applied the combination (NH) of authentic floods and debris flows as the dependent variable to validate the indices. In order to resolve the multicollinearity issue, the independent variables used in the regression are the components generated by PCA. The first regression to validate the indices is OLS.

Further analysis (SLM and SEM) determines the statistical significance of LM-Lag, and LM-Error. If both LM-Lag and LM-Error are insignificant, it means that neither SLM nor SEM is required. However, if either LM-Lag or LM-Error is significant, it means that SLM or SEM is needed. Moreover, if both LM-Lag and LM-Error are significant, both the SLM and SEM are needed. In the last scenario, the statistical significance of Robust LM-Error and Robust LM-Lag determine which model to use. The procedure of the regression decision process is presented in Fig 4.52. Nevertheless, both SLM and SEM are still conducted in all scenarios and indices in order to achieve a holistic result.

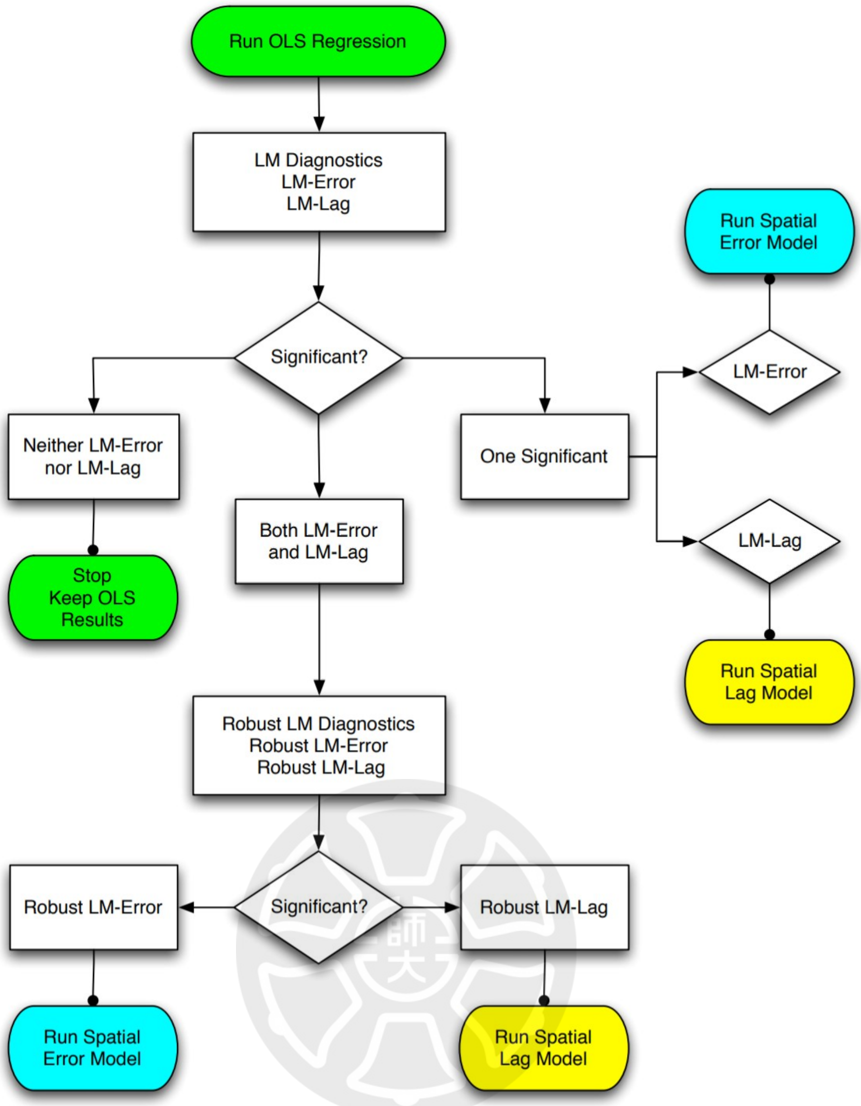

Fig. 4.52 Spatial regression decision process (Anselin, 2005: 199).

Spatial nonstationarity is one of the most critical issues in this research since the difference between each spatial unit is important. In order to solve the spatial nonstationarity, GWR is applied.

4.4.1 Multivariate Regression of SoVI

SoVI represents the social vulnerability to environmental hazards, also meaning the potential losses dues to environmental hazards. The variables used to build the SoVI generally represent the disadvantageous aspects of the society, meaning the individual or groups with higher SoVI represent poor socioeconomic status. In other words, they might have less ability or resources. As a result, the individuals or groups with higher SoVI have no choice but to dwell in these areas with high exposure to environmental hazards.

Table 4.7 demonstrates the result of OLS on a county-wide scale, floodplain areas, and mountain areas. All the R^2 and R^2-ADJ in these three areas are relatively deficient, meaning that the goodness of fit of SoVI is inadequate in all of these areas. Also, the hypothesis we have mentioned, i.e., the relationship between high exposure to environmental hazards and poor socioeconomic status, does not seem to exist. Also, the majority of coefficients show a negative correlation with authentic environmental hazard events. However, this outcome might be triggered by spatial dependence and spatial nonstationarity. Therefore, further analysis is needed.

On the scale of all of Yilan County, the second component shows a positive correlation, but it is insignificant. This component includes the Ratio of the Indigenous Population, Ratio of Low-Income Households, and Ratio of Population Younger than 5 Years Old.

In the floodplain areas, only the first component presents a positive correlation, but it is still insignificant. This component includes the Aging Index, Population without a High School Diploma, Ratio of Population Older than 65 Years Old, and Ratio of Population Younger than 5 Years Old.

Table. 4.7 Summary of OLS (SoVI).

County-wide scale		
R^2	R^2-ADJ	AIC
0.107	0.091	643.872
Variable	Coefficient	*p*-value
CONSTANT	0.000	1.000
Component 1	-0.050	0.453
Component 2	0.060	0.359
Component 3	-0.306	0.000**
Component 4	-0.033	0.605
TEST	VALUE	*p*-value
Robust LM (lag)	1.662	0.197
Robust LM (error)	0.500	0.479
Floodplain areas		
R^2	R^2-ADJ	AIC
0.150	0.131	485.169
Variable	Coefficient	*p*-value
CONSTANT	0.000	1.000
Component 1	0.017	0.647
Component 2	-0.146	0.000**
Component 3	-0.051	0.073*
Component 4	-0.043	0.552
TEST	VALUE	*p*-value
Robust LM (lag)	0.622	0.430
Robust LM (error)	3.231	0.072*
Mountain areas		
R^2	R^2-ADJ	AIC
0.035	-0.021	162.910
Variable	Coefficient	*p*-value
CONSTANT	0.000	1.000
Component 1	0.033	0.698
Component 2	-0.044	0.293
Component 3	-0.034	0.701
TEST	VALUE	*p*-value
Robust LM (lag)	0.005	0.947
Robust LM (error)	0.000	0.985

$0.05 \leq P < 0.1$ = *; $P < 0.05$ = **

In mountain areas, the first component also shows a positive correlation, but it is still insignificant. Component 1 also includes the Ratio of the Indigenous Population, Ratio of Low-Income Households, Population Density, Ratio of Population Older than 65 Years Old, and Ratio of Population Younger than 5 Years Old. These three components all include the Ratio of the Indigenous Population and Ratio of Population Younger than 5 Years Old, representing that the environmental hazard might have a positive correlation with the Ratio of the Indigenous Population, and Ratio of Population Younger than 5 Years Old.

Component 2 from the county-wide scale and floodplain areas have a statistically significant negative correlation with environmental hazards. On the other hand, component 3 in the floodplain areas also shows a significant negative correlation with environmental hazards. These components all include the Dependency Ratio and Population Density, meaning these two variables might have a significant negative correlation with environmental hazards. Based on the content of these components, the Ratio of the Indigenous Population, Ratio of Low-Income Households, and the Ratio of Population Younger than 5 Years Old all seem to have a positive relationship with environmental hazards.

Table 4.8 demonstrates the results of SLM and SEM, through R^2 and R^2-ADJ. The goodness of fit improved since the spatial dependence in the dependent variables has been solved. However, the majority of coefficients still show a negative correlation with environmental hazards, which is similar to the result of OLS. Due to the characteristics of OLS, SLM, and SEM, the spatial non-stationarity cannot be resolved because these regression models neglect the differences between the spatial units; therefore, GWR is applied. Table 4.8 demonstrates the result of GWR. Based on the R^2, R^2-ADJ, and AIC, the goodness of fit is improved. The R^2, and R^2-ADJ from the county-wide scale and floodplain areas are above 0.5. The R^2 (0.786) of GWR of SoVI in the floodplain areas is the highest in this study. Moreover, the AIC on a county-wide scale and floodplain areas also show significant drops. This means that by creating many kernels and regressions based on the differences of spatial units, the goodness of fit increases. However, the R^2 and R^2-ADJ in mountain areas are still not ideal; also, the AIC of GWR is remarkably similar to the previous regression.

Table. 4.8 Summary of SLM, SEM, and GWR (SoVI).

County-wide scale								
SLM			SEM			GWR		
R^2	R^2-ADJ	AIC	R^2	R^2-ADJ	AIC	R^2	R^2-ADJ	AIC
0.359	0.342	587.284	0.364	0.347	585.081	0.665	0.508	568.236
Variable	Coefficient	*p*-value	Variable	Coefficient	*p*-value	Variable	Coeff_MAX	Coeff_MIN
SL_EnvironmentalHaz	0.595	0.000**	CONSTANT	-0.029	0.832	Component 1	0.697	-0.758
CONSTANT	-0.019	0.718	Component 1	-0.076	0.280	Component 2	1.481	-4.524
Component 1	-0.042	0.443	Component 2	-0.045	0.594	Component 3	0.034	-1.094
Component 2	0.033	0.549	Component 3	-0.250	0.001**	Component 4	6.925	-1.413
Component 3	-0.171	0.002**	Component 4	-0.036	0.543			
Component 4	-0.035	0.514	LAMBDA	0.617	0.000			
Floodplain areas								
SLM			SEM			GWR		
R^2	R^2-ADJ	AIC	R^2	R^2-ADJ	AIC	R^2	R^2-ADJ	AIC
0.510	0.492	412.000	0.517	0.500	409.096	0.786	0.654	394.646
Variable	Coefficient	*p*-value	Variable	Coefficient	*p*-value	Variable	Coeff_MAX	Coeff_MIN
SL_Flood	0.692	0.000**	CONSTANT	-0.125	0.488	Component 1	0.408	-0.161
CONSTANT	-0.043	0.417	Component 1	0.041	0.274	Component 2	0.042	-1.018
Component 1	0.020	0.476	Component 2	-0.104	0.005**	Component 3	0.256	-0.712
Component 2	-0.058	0.012**	Component 3	-0.035	0.106	Component 4	7.731	-2.504
Component 3	-0.034	0.106	Component 4	-0.081	0.171			
Component 4	-0.062	0.252	LAMBDA	0.710	0.000			
Mountain areas								
SLM			SEM			GWR		
R^2	R^2-ADJ	AIC	R^2	R^2-ADJ	AIC	R^2	R^2-ADJ	AIC
0.056	-0.039	164.120	0.064	-0.030	161.916	0.326	0.159	160.201
Variable	Coefficient	*p*-value	Variable	Coefficient	*p*-value	Variable	Coeff_MAX	Coeff_MIN
SL_DebrisFlow	0.162	0.304	CONSTANT	0.016	0.918	Component 1	0.408	-0.161
CONSTANT	0.010	0.940	Component 1	-0.013	0.886	Component 2	0.042	-1.018
Component 1	0.017	0.833	Component 2	-0.057	0.156	Component 3	0.256	-0.712
Component 2	-0.047	0.231	Component 3	-0.036	0.685	Component 4	7.731	-2.504
Component 3	-0.031	0.706	LAMBDA	0.206	0.184			

$0.05 \le P < 0.1$ = *; $P < 0.05$ = **

4.4.2 Multivariate Regression of BRIC

BRIC represents the community's inherent resilience to environmental hazards, including the inherent ability and capacity to adapt and recover from environmental hazard events. A higher BRIC value stands for a higher inherent ability and capacity. In other words, the individuals or groups with higher BRIC have more resources and better socioeconomic status. Therefore, those individuals or groups with higher BRIC have more chances to select areas to dwell in. Moreover, they might be able to avoid exposure to environmental hazards or even move to areas with less exposure to environmental hazards. In this section, the multivariate regression and authentic environmental hazard events are also applied to validate the effectiveness of BRIC and explore the relationship between environmental hazard events and the positive aspects of the socioeconomic variables. Table 4.9 demonstrates the result of OLS. The values of R^2 and R^2-ADJ in three different areas show that the goodness of fit is comparatively low.

On the county-wide scale, the majority of the component coefficients show a negative correlation with environmental hazard events, which is in accord with our speculation. However, only component 2 is significant. Component 2 includes the Capacity of Emergency Shelters, Number of Clinics and Hospitals, and Number of Pharmacies. The Robust LM (lag) is also significant, meaning the diagnosis of OLD suggests using the SLM to conduct further exploration.

The results of OLS in the floodplain areas are also similar to the county-wide scale. Component 2 also shows a significant negative correlation with environmental hazards. In floodplain areas, the second component includes the Number of Pharmacies and Number Clinics and Hospitals, which is almost the same as component 2 on the county-wide scale. The OLS result in mountain areas shows that the first and third components negatively correlate with environmental hazard events. However, both of them are significant.

Table. 4.9 Summary of OLS (BRIC)

County-wide scale		
R^2	R^2-ADJ	AIC
0.023	0.006	664.794
Variable	Coefficient	*p*-value
CONSTANT	0.000	1.000
Component 1	0.031	0.660
Component 2	-0.141	0.047**
Component 3	-0.040	0.549
Component 4	-0.028	0.675
TEST	VALUE	*p*-value
Robust LM (lag)	5.713	0.017**
Robust LM (error)	1.450	0.228
Floodplain areas		
R^2	R^2-ADJ	AIC
0.035	0.007	509.736
Variable	Coefficient	*p*-value
CONSTANT	0.000	1.000
Component 1	0.033	0.683
Component 2	-0.189	0.022**
Component 3	-0.051	0.498
Component 4	0.008	0.915
Component 5	0.057	0.480
TEST	VALUE	*p*-value
Robust LM (lag)	4.605	0.032**
Robust LM (error)	0.303	0.582
Mountain areas		
R^2	R^2-ADJ	AIC
0.063	-0.011	163.252
Variable	Coefficient	*p*-value
CONSTANT	0.000	1.000
Component 1	-0.230	0.158
Component 2	0.025	0.876
Component 3	-0.083	0.561
Component 4	0.081	0.559
TEST	VALUE	*p*-value
Robust LM (lag)	0.005	0.947
Robust LM (error)	0.000	0.985

$0.05 \leq P < 0.1$ = *; $P < 0.05$ = **

Table. 4.10 Summary of SLM, SEM, and GWR (BRIC)

County-wide scale								
SLM			SEM			GWR		
R^2	R^2-ADJ	AIC	R^2	R^2-ADJ	AIC	R^2	R^2-ADJ	AIC
0.343	0.325	596.424	0.339	0.321	596.069	0.388	0.222	645.001
Variable	Coefficient	*p*-value	Variable	Coefficient	*p*-value	Variable	Coeff_MAX	Coeff_MIN
SL_Environmental Haz	0.637	0.000**	CONSTANT	-0.058	0.696	Component 1	0.697	-0.758
CONSTANT	-0.020	0.703	Component 1	0.015	0.841	Component 2	1.481	-4.524
Component 1	0.024	0.668	Component 2	-0.064	0.301	Component 3	0.034	-1.094
Component 2	-0.087	0.130	Component 3	-0.012	0.814	Component 4	6.925	-1.413
Component 3	-0.024	0.657	Component 4	-0.009	0.857			
Component 4	-0.012	0.824	LAMBDA	0.639	0.000**			
Floodplain areas								
SLM			SEM			GWR		
R^2	R^2-ADJ	AIC	R^2	R^2-ADJ	AIC	R^2	R^2-ADJ	AIC
0.496	0.475	422.371	0.497	0.476	420.976	0.611	0.433	465.117
Variable	Coefficient	*p*-value	Variable	Coefficient	*p*-value	Variable	Coeff_MAX	Coeff_MIN
SL_Flood	0.731	0.000**	CONSTANT	-0.173	0.397	Component 1	0.818	-1.203
CONSTANT	-0.045	0.401	Component 1	0.040	0.581	Component 2	0.110	-1.384
Component 1	0.032	0.577	Component 2	-0.059	0.372	Component 3	3.406	-0.288
Component 2	-0.073	0.207	Component 3	-0.016	0.752	Component 4	0.455	-0.321
Component 3	-0.025	0.645	Component 4	-0.013	0.798			
Component 4	-0.009	0.878	Component 5	0.048	0.393			
Component 5	0.045	0.431	LAMBDA	0.739	0.000**			
Mountain areas								
SLM			SEM			GWR		
R^2	R^2-ADJ	AIC	R^2	R^2-ADJ	AIC	R^2	R^2-ADJ	AIC
0.073	-0.019	164.845	0.064	-0.030	163.211	0.178	0.047	163.784
Variable	Coefficient	*p*-value	Variable	Coefficient	*p*-value	Variable	Coeff_MAX	Coeff_MIN
SL_DebrisFlow	0.115	0.471	CONSTANT	0.003	0.985	Component 1	0.408	-0.161
CONSTANT	0.007	0.957	Component 1	-0.220	0.152	Component 2	0.042	-1.018
Component 1	-0.216	0.157	Component 2	0.022	0.889	Component 3	0.256	-0.712
Component 2	0.021	0.894	Component 3	-0.072	0.595	Component 4	7.731	-2.504
Component 3	-0.076	0.576	Component 4	0.082	0.540			
Component 4	0.080	0.540	LAMBDA	0.044	0.792			

$0.05 \le P < 0.1$ = *; $P < 0.05$ = **

The results of SLM, SEM, and GWR are presented in Table 4.10. Although the goodness of fit has some improvement, the values of R^2 and R^2-ADJ are still relatively inferior. The AIC has also been improved, yet, the improvement is quite insignificant. Based on Table 4.10, BRIC in floodplain areas seems to have a better outcome compared to the other two areas. Although R^2 and R^2-ADJ only reach 0.4, the value is higher than in the other two areas.

Moreover, most of the coefficients show a negative correlation with environmental hazards, meaning the positive aspects of socioeconomic variables have a negative correlation with environmental hazards, coinciding with our hypothesis mentioned in the previous section. The individuals or groups with a higher value of BRIC or positive socioeconomic variables seem to have less chance of encountering an environmental hazard. However, only the spatially lagged dependent variable (SL_EnvironmentalHazard and SL_Flood) and the spatially correlated errors (LAMBDA) are statistically significant.

4.4.3 Multivariate Regression of Risk

In the previous result of multivariate regression, we found that SoVI and part of the BRIC do not agree with our hypothesis. However, in the hazard-of-place model, the geographic context and biophysical vulnerability are also crucial components. Through the risk matrix, we combine the social vulnerability to environmental hazards, geographic context, and biophysical vulnerability. In this section, the SoVI and environmental hazards potential (county-wide scale: the combination of flood and debris flow; floodplain areas: floods; mountain areas: debris flow) are regarded as the independent variables to conduct the multivariate regression. Since the potential of flooding includes four different daily precipitation scenarios, both the county-wide scale and floodplain areas have four different regressions based on varying flood potential.

Table 4.11 and 4.12 demonstrate the results of OLS, SLM, SEM, and GWR on a county-wide scale. The dependent variable on the county-wide scale is the combination of authentic floods and debris flows. Through Table 4.11 and 4.12, we found the result of OLS is still similar to the result in the previous section. The R^2 and R^2-ADJ fail to reach 0.2, meaning the goodness of fit of OLS is substandard. Although the potential for environmental hazards in all scenarios shows a significant positive correlation with authentic environmental hazards, SoVI shows a significant negative correlation with authentic environmental hazards as well. Still, SoVI contradicts our expectations.

According to Table 4.11 and 4.12, neither the Robust LM (lag) nor the Robust LM (error) is statistically significant. However, SLM and SEM are still conducted to offer a thorough exploration of the relationship between authentic environmental hazards and the risk of environmental hazards. The R^2 and R^2-ADJ show the SLM and SEM also lack goodness of fit. The R^2 and R^2-ADJ of these regressions can only reach 0.3. Furthermore, the coefficient of SoVI and the potential for environmental hazards are also similar to the result of OLS. The coefficient of SoVI shows a significant negative correlation with authentic environmental hazards, while the potential for environmental hazards correlates with authentic environmental hazards positively. The R^2 and R^2-ADJ show that the goodness of fit of GWR on the county-wide scale is better than the other regressions. R^2 in all scenarios exceeds 0.5, and R^2-ADJ is also above 0.4. The result of GWR is acceptable.

In floodplain areas, one of the independent variables is the potential of flooding under four different daily precipitation rates, including 200 mm, 350 mm, 450 mm, and 600 mm. As a result, floodplain areas have four different regressions. Table 4.13 and 4.14 present the results of all the regressions of floodplain areas. The R^2 and R^2-ADJ of OLS are still similar to the previous result. The highest R^2 in all scenarios is approximately 0.2. Also, the majority of coefficients of SoVI still show a significant negative correlation with authentic environmental hazards. In other words, the relation between SoVI and authentic environmental hazards still does not agree with our expectations.

Table. 4.11 Summary of OLS, SLM, SEM, and GWR on the county-wide scale (risk)-1.

County-wide scale					
OLS (200 mm + Debris flow)			OLS (350 mm + Debris flow)		
R^2	R^2-ADJ	AIC	R^2	R^2-ADJ	AIC
0.102	0.094	641.262	0.152	0.144	627.879
Variable	Coefficient	*p*-value	Variable	Coefficient	*p*-value
CONSTANT	-0.133	0.682	CONSTANT	-0.532	0.096*
SoVI	-0.182	0.010**	SoVI	-0.146	0.034**
Environmental Hazard	0.223	0.001**	Environmental Hazard	0.318	0.000**
TEST	VALUE	*p*-value	TEST	VALUE	*p*-value
Robust LM (lag)	1.752	0.186	Robust LM (lag)	2.158	0.142
Robust LM (error)	0.919	0.338	Robust LM (error)	1.008	0.315
SLM (200 mm + Debris flow)			SLM (350 mm + Debris flow)		
R^2	R^2-ADJ	AIC	R^2	R^2-ADJ	AIC
0.339	0.327	588.897	0.351	0.339	582.471
Variable	Coefficient	*p*-value	Variable	Coefficient	*p*-value
SL_EnvironmentalHaz	0.572	0.000**	SL_EnvironmentalHaz	0.541	0.000**
CONSTANT	-0.061	0.826	CONSTANT	-0.298	0.283
SoVI	-0.126	0.035**	SoVI	-0.108	0.071**
Environmental Hazard	0.142	0.011**	Environmental Hazard	0.201	0.000**
SEM (200 mm + Debris flow)			SEM (350 mm + Debris flow)		
R^2	R^2-ADJ	AIC	R^2	R^2-ADJ	AIC
0.339	0.327	587.174	0.352	0.341	581.390
Variable	Coefficient	*p*-value	Variable	Coefficient	*p*-value
CONSTANT	-0.027	0.934	CONSTANT	-0.298	0.371
SoVI	-0.168	0.013**	SoVI	-0.156	0.020**
Environmental Hazard	0.173	0.009**	Environmental Hazard	0.248	0.000**
LAMBDA	0.590	0.000**	LAMBDA	0.561	0.000**
GWR (200 mm + Debris flow)			GWR (350 mm + Debris flow)		
R^2	R^2-ADJ	AIC	R^2	R^2-ADJ	AIC
0.555	0.401	591.687	0.503	0.382	583.469
Variable	Coeff_MAX	Coeff_MIN	Variable	Coeff_MAX	Coeff_MIN
SoVI	0.318	-1.132	SoVI	0.237	-0.826
Environmental Hazard	1.217	-1.579	Environmental Hazard	0.981	0.667

$0.05 \le P < 0.1$ = *; $P < 0.05$ = **

Table. 4.12 Summary of OLS, SLM, SEM, and GWR on the county-wide scale (risk)-2.

County-wide scale					
OLS (450 mm + Debris flow)			OLS (600 mm + Debris flow)		
R^2	R^2-ADJ	AIC	R^2	R^2-ADJ	AIC
0.155	0.148	626.926	0.183	0.176	619.239
Variable	Coefficient	*p*-value	Variable	Coefficient	*p*-value
CONSTANT	-0.557	0.081*	CONSTANT	-0.694	0.026**
SoVI	-0.143	0.038**	SoVI	-0.121	0.073*
*Environmental Hazard	0.323	0.000**	Environmental Hazard	0.356	0.000**
TEST	VALUE	*p*-value	TEST	VALUE	*p*-value
Robust LM (lag)	1.223	0.269	Robust LM (lag)	1.975	0.160
Robust LM (error)	2.033	0.154	Robust LM (error)	1.523	0.217
SLM (450 mm + Debris flow)			SLM (600 mm + Debris flow)		
R^2	R^2-ADJ	AIC	R^2	R^2-ADJ	AIC
0.354	0.343	581.275	0.364	0.353	576.685
Variable	Coefficient	*p*-value	Variable	Coefficient	*p*-value
SL_EnvironmentalHaz	0.540	0.000**	SL_EnvironmentalHaz	0.524	0.000*
CONSTANT	-0.334	0.229	CONSTANT	-0.438	0.108
SoVI	-0.105	0.080*	SoVI	-0.091	0.126
Environmental Hazard	0.209	0.000**	Environmental Hazard	0.237	0.000**
SEM (450 mm + Debris flow)			SEM (600 mm + Debris flow)		
R^2	R^2-ADJ	AIC	R^2	R^2-ADJ	AIC
0.359	0.348	578.962	0.369	0.358	574.647
Variable	Coefficient	*p*-value	Variable	Coefficient	*p*-value
CONSTANT	-0.367	0.268	CONSTANT	-0.471	0.146
SoVI	-0.154	0.022**	SoVI	-0.139	0.037**
Environmental Hazard	0.269	0.000**	Environmental Hazard	0.298	0.000**
LAMBDA	0.565	0.000**	LAMBDA	0.554	0.000**
GWR (450 mm + Debris flow)			GWR (600 mm + Debris flow)		
R^2	R^2-ADJ	AIC	R^2	R^2-ADJ	AIC
0.548	0.417	576.264	0.544	0.413	577.691
Variable	Coeff_MAX	Coeff_MIN	Variable	Coeff_MAX	Coeff_MIN
SoVI	0.271	-0.756	SoVI	0.272	-0.677
Environmental Hazard	1.063	-0.970	Environmental Hazard	1.069	-0.791

$0.05 \leq P < 0.1$ = *; $P < 0.05$ = **

Based on Tables 4.13 and 4.14, the R^2 and R^2-ADJ of SLM and SEM are roughly 0.5, meaning the goodness of fit is acceptable. The AIC of SLM and SEM also dramatically decreased, meaning that compared to OLS, the SLM and SEM have higher regression and goodness of fit. However, the coefficients of SoVI have a result similar to that of OLS, i.e., a negative correlation with authentic environmental hazards. In floodplain areas, SoVI is still not in accord with our expectations. Despite the improvement of R^2 and R^2-ADJ, the relationship between SoVI still show a significant negative correlation with authentic environmental hazards. The SOBEK ver2.13 model generates the potential for floods. As a result, undoubtedly, the relationship between flood potential and authentic floods surely has a positive correlation. The R^2 and R^2-ADJ of GWR can exceed 0.6, meaning that the goodness of fit is improved, surpassing both SLM and SEM.

Table 4.15 demonstrates the result of multivariate regression of mountain areas. The dependent variables used in the regression are authentic debris flow events. Compared to the situation on the county-wide scale and in floodplains, the result in mountain areas is totally different. In county-wide scale and floodplain areas, even though the goodness of fit of OLS is very low, after solving the spatial dependence and spatial nonstationarity through SLM, SEM, and GWR, the goodness of fit increased. However, in mountain areas, no matter which regression we apply, the goodness of fit is still remarkably low. The R^2 and R^2-ADJ of all regressions in mountain areas are extremely low. AIC also shows the same outcome. Based on the coefficients of SoVI, the result of OLS and SLM seem to fit our hypothesis, but the *p*-value shows that the results are insignificant.

Table. 4.13 Summary of OLS, SLM, SEM, and GWR of floodplain areas (risk)-1.

Floodplain areas					
OLS (200 mm)			OLS (350 mm)		
R^2	R^2-ADJ	AIC	R^2	R^2-ADJ	AIC
0.120	0.094	487.357	0.184	0.175	473.960
Variable	Coefficient	*p*-value	Variable	Coefficient	*p*-value
CONSTANT	0.071	0.863	CONSTANT	-0.574	0.156
SoVI	-0.222	0.009**	SoVI	-0.146	0.078*
Potential of Flood	0.197	0.010**	Potential of Flood	0.332	0.000**
TEST	VALUE	*p*-value	TEST	VALUE	*p*-value
Robust LM (lag)	1.270	0.260	Robust LM (lag)	1.018	0.313
Robust LM (error)	2.322	0.128	Robust LM (error)	3.478	0.062*
SLM (200 mm)			SLM (350 mm)		
R^2	R^2-ADJ	AIC	R^2	R^2-ADJ	AIC
0.509	0.497	409.026	0.515	0.504	404.393
Variable	Coefficient	*p*-value	Variable	Coefficient	*p*-value
SL_Flood	0.699	0.000	SL_Flood	0.672	0.000
CONSTANT	0.087	0.775	CONSTANT	-0.215	0.488
SoVI	-0.127	0.048**	SoVI	-0.095	0.137
Potential of Flood	0.082	0.150	Potential of Flood	0.150	0.010**
SEM (200 mm)			SEM (350 mm)		
R^2	R^2-ADJ	AIC	R^2	R^2-ADJ	AIC
0.513	0.502	407.010	0.523	0.512	401.361
Variable	Coefficient	*p*-value	Variable	Coefficient	*p*-value
CONSTANT	0.027	0.944	CONSTANT	-0.343	0.390
SoVI	-0.184	0.020**	SoVI	-0.168	0.030**
Potential of Flood	0.133	0.063*	Potential of Flood	0.242	0.002**
LAMBDA	0.716	0.000**	LAMBDA	0.696	0.000**
GWR (200 mm)			GWR (350 mm)		
R^2	R^2-ADJ	AIC	R^2	R^2-ADJ	AIC
0.608	0.485	423.606	0.586	0.481	418.802
Variable	Coeff_MAX	Coeff_MIN	Variable	Coeff_MAX	Coeff_MIN
SoVI	0.241	-1.188	SoVI	0.042	-0.701
Potential of Flood	1.213	-1.157	Potential of Flood	1.035	-0.968

$0.05 \leq P < 0.1$ = *; $P < 0.05$ = **

Table. 4.14 Summary of OLS, SLM, SEM, and GWR of floodplain areas (risk)-2.

Floodplain areas					
OLS (450 mm)			OLS (600 mm)		
R^2	R^2-ADJ	AIC	R^2	R^2-ADJ	AIC
0.189	0.179	472.931	0.227	0.218	464.393
Variable	Coefficient	*p*-value	Variable	Coefficient	*p*-value
CONSTANT	-0.616	0.128	CONSTANT	-0.838	0.032**
SoVI	-0.141	0.090*	SoVI	-0.102	0.210
Potential of Flood	0.339	0.000**	Potential of Flood	0.387	0.000**
TEST	VALUE	*p*-value	TEST	VALUE	*p*-value
Robust LM (lag)	0.304	0.582	Robust LM (lag)	0.791	0.374
Robust LM (error)	5.772	0.016**	Robust LM (error)	5.699	0.017 **
SLM (450 mm)			SLM (600 mm)		
R^2	R^2-ADJ	AIC	R^2	R^2-ADJ	AIC
0.519	0.507	403.039	0.528	0.517	398.310
Variable	Coefficient	*p*-value	Variable	Coefficient	*p*-value
SL_Flood	0.670	0.000**	SL_Flood	0.653	0.000**
CONSTANT	-0.279	0.368	CONSTANT	-0.443	0.143
SoVI	-0.088	0.170	SoVI	-0.064	0.311
Potential of Flood	0.163	0.005**	Potential of Flood	0.201	0.000**
SEM (450 mm)			SEM (600 mm)		
R^2	R^2-ADJ	AIC	R^2	R^2-ADJ	AIC
0.534	0.524	397.659	0.550	0.540	391.627
Variable	Coefficient	*p*-value	Variable	Coefficient	*p*-value
CONSTANT	-0.479	0.223	CONSTANT	-0.641	0.093
SoVI	-0.164	0.032**	SoVI	-0.137	0.072*
Potential of Flood	0.282	0.000**	Potential of Flood	0.325	0.000**
LAMBDA	0.701	0.000**	LAMBDA	0.702	0.000**
GWR (450 mm)			GWR (600 mm)		
R^2	R^2-ADJ	AIC	R^2	R^2-ADJ	AIC
0.606	0.506	410.129	0.641	0.526	408.931
Variable	Coeff_MAX	Coeff_MIN	Variable	Coeff_MAX	Coeff_MIN
SoVI	0.084	-0.755	SoVI	0.062	-0.697
Potential of Flood	1.061	-0.969	Potential of Flood	1.206	-1.058

$0.05 \leq P < 0.1$ = *; $P < 0.05$ = **

Table. 4.15 Summary of OLS, SLM, SEM, and GWR in mountain areas (risk).

Mountain areas					
OLS			SEM		
R^2	R^2-ADJ	AIC	R^2	R^2-ADJ	AIC
0.003	-0.035	162.716	0.026	-0.050	161.991
Variable	Coefficient	*p*-value	Variable	Coefficient	*p*-value
CONSTANT	-0.184	0.706	CONSTANT	0.117	0.810
Potential of DE	0.023	0.870	Potential of DE	-0.013	0.924
SoVI	0.040	0.778	SoVI	-0.023	0.871
TEST	VALUE	*p*-value	LAMBDA	0.189	0.227
Robust LM (lag)	10.413	0.001			
Robust LM (error)	10.254	0.001			
SLM			GWR		
R^2	R^2-ADJ	AIC	R^2	R^2-ADJ	AIC
0.023	-0.054	164.001	0.151	0.047	161.049
Variable	Coefficient	*p*-value	Variable	Coeff_MAX	Coeff_MIN
SL_Debris	0.158	0.320	SoVI	0.135	-0.191
CONSTANT	-0.057	0.903	Potential of DE	0.069	-0.052
Potential of DE	0.005	0.969			
SoVI	0.018	0.898			

$0.05 \leq P < 0.1$ = *; $P < 0.05$ = **

4.4.4 Multivariate Regression of SERV

In this research, we try to apply SERV to integrate not only the SoVI and potential for environmental hazards but also BRIC. As we mentioned before, SoVI represents the social vulnerability to environmental hazards, while the potential of environmental hazards stands for the geographic context and biophysical vulnerability. BRIC in this research indicates the community's inherent resilience to environmental hazards. In order to validate the effectiveness of SERV and explore the relationships within these elements, multivariate regression is applied. This section demonstrates the result of the multivariate regression. The dependent variables are authentic environmental hazards, including floods and debris flows.

The results of all regressions applied on a county-wide scale are presented in Table

4.16 and 4.17. The coefficient shows that SoVI negatively correlates to authentic environmental hazards on a county-wide scale. Also, based on the *p*-value, the majority of the negative correlations between SoVI and authentic environmental hazards are statistically significant. In other words, the relationship between SoVI and authentic environmental hazards still does not fall into accord with our presupposition. The relationship between BRIC and authentic environmental hazards entirely coincides with our hypothesis. Based on the coefficient and *p*-value, the relationship between BRIC and authentic environmental hazards is significantly positively correlated. However, the goodness of fit in all regressions is comparatively mediocre, with the exception of GWR. The R^2 and R^2-ADJ of OLS in all scenarios fall approximately between 0.1 and 0.2. Despite all the Robust LM (lag), we suggest applying SLM for further investigation. Based on AIC, the goodness of fit of SLM seems to have increased. However, the R^2 and R^2-ADJ of four SLM result only rise to between 0.35 and 0.37, meaning even though the goodness of fit has increased, it is still insignificant. The AIC, R^2, and R^2-ADJ show the goodness of fit of GWR is the highest among all regressions on the county-wide scale. The R^2 and R^2-ADJ in all scenarios are between 0.4 and 0.5, which is better than OLS, SLM, and SEM. The AIC of GWR is also lower than the other regressions

Table. 4.16 Summary of OLS, SLM, SEM, and GWR on the county-wide scale (SERV)-1.

County-wide scale					
OLS (200 mm + Debris flow)			OLS (350 mm + Debris flow)		
R^2	R^2-ADJ	AIC	R^2	R^2-ADJ	AIC
0.083	0.071	648.087	0.151	0.140	629.986
Variable	Coefficient	*p*-value	Variable	Coefficient	*p*-value
CONSTANT	0.000	1.000	CONSTANT	0.000	1.000
SoVI	-0.153	0.024**	SoVI	-0.122	0.061*
BRIC	-0.164	0.014**	BRIC	-0.155	0.015**
Environmental Hazard	0.199	0.002	Environmental Hazard	0.334	0.000
TEST	VALUE	*p*-value	TEST	VALUE	*p*-value
Robust LM (lag)	8.789	0.003**	Robust LM (lag)	13.517	0.000**
Robust LM (error)	0.791	0.374	Robust LM (error)	1.511	0.219
SLM (200 mm + Debris flow)			SLM (350 mm + Debris flow)		
R^2	R^2-ADJ	AIC	R^2	R^2-ADJ	AIC
0.351	0.337	589.032	0.367	0.353	580.305
Variable	Coefficient	*p*-value	Variable	Coefficient	*p*-value
SL_EnvironmentalHaz	0.607	0.000**	SL_EnvironmentalHaz	0.567	0.000 **
CONSTANT	-0.019	0.714	CONSTANT	-0.018	0.729
SoVI	-0.106	0.061*	SoVI	-0.088	0.116
BRIC	-0.097	0.078*	BRIC	-0.097	0.074*
Environmental Hazard	0.086	0.112	Environmental Hazard	0.187	0.001**
SEM (200 mm + Debris flow)			SEM (350 mm + Debris flow)		
R^2	R^2-ADJ	AIC	R^2	R^2-ADJ	AIC
0.357	0.343	587.402	0.361	0.347	582.775
Variable	Coefficient	*p*-value	Variable	Coefficient	*p*-value
CONSTANT	-0.046	0.750	CONSTANT	-0.038	0.768
SoVI	-0.205	0.007**	SoVI	-0.195	0.009**
BRIC	-0.079	0.220	BRIC	-0.079	0.219
Environmental Hazard	0.027	0.667	Environmental Hazard	0.154	0.020**
LAMBDA	0.638	0.000**	LAMBDA	0.596	0.000**
GWR (200 mm + Debris flow)			GWR (350 mm + Debris flow)		
R^2	R^2-ADJ	AIC	R^2	R^2-ADJ	AIC
0.566	0.401	598.351	0.565	0.433	573.057
Variable	Coeff_MAX	Coeff_MIN	Variable	Coeff_MAX	Coeff_MIN
SoVI	0.843	-1.031	SoVI	0.910	-0.878
BRIC	0.527	-0.731	BRIC	0.384	-0.673
Environmental Hazard	1.185	-1.001	Environmental Hazard	1.276	-0.352

$0.05 \leq P < 0.1$ = *; $P < 0.05$ = **

Table. 4.17 Summary of OLS, SLM, SEM, and GWR on the county-wide scale (SERV)-2.

County-wide scale					
OLS (450 mm + Debris flow)			OLS (600 mm + Debris flow)		
R^2	R^2-ADJ	AIC	R^2	R^2-ADJ	AIC
0.158	0.147	628.044	0.180	0.169	622.052
Variable	Coefficient	*p*-value	Variable	Coefficient	*p*-value
CONSTANT	0.000	1.000	CONSTANT	0.000	1.000
SoVI	-0.118	0.069*	SoVI	-0.112	0.079*
BRIC	-0.151	0.018**	BRIC	-0.152	0.016**
Environmental Hazard	0.345	0.000 **	Environmental Hazard	0.376	0.000**
TEST	VALUE	*p*-value	TEST	VALUE	*p*-value
Robust LM (lag)	13.684	0.000**	Robust LM (lag)	15.828	0.000**
Robust LM (error)	1.475	0.225	Robust LM (error)	2.040	0.153
SLM (450 mm + Debris flow)			SLM (600 mm + Debris flow)		
R^2	R^2-ADJ	AIC	R^2	R^2-ADJ	AIC
0.369	0.355	579.329	0.375	0.361	576.102
Variable	Coefficient	*p*-value	Variable	Coefficient	*p*-value
SL_EnvironmentalHaz	0.562	0.000**	SL_EnvironmentalHaz	0.548	0.000**
CONSTANT	-0.018	0.731	CONSTANT	-0.017	0.736
SoVI	-0.086	0.125	SoVI	-0.083	0.138
BRIC	-0.095	0.081**	BRIC	-0.097	0.073*
Environmental Hazard	0.196	0.000**	Environmental Hazard	0.221	0.000**
SEM (450 mm + Debris flow)			SEM (600 mm + Debris flow)		
R^2	R^2-ADJ	AIC	R^2	R^2-ADJ	AIC
0.362	0.348	582.117	0.364	0.350	580.124
Variable	Coefficient	*p*-value	Variable	Coefficient	*p*-value
CONSTANT	-0.037	0.773	CONSTANT	-0.034	0.782
SoVI	-0.193	0.010**	SoVI	-0.188	0.011**
BRIC	-0.078	0.227	BRIC	-0.078	0.223
Environmental Hazard	0.165	0.013**	Environmental Hazard	0.193	0.003**
LAMBDA	0.592	0.000**	LAMBDA	0.578	0.000**
GWR (450 mm + Debris flow)			GWR (600 mm + Debris flow)		
R^2	R^2-ADJ	AIC	R^2	R^2-ADJ	AIC
0.567	0.437	571.637	0.567	0.436	571.758
Variable	Coeff_MAX	Coeff_MIN	Variable	Coeff_MAX	Coeff_MIN
SoVI	0.943	-0.877	SoVI	1.045	-0.876
BRIC	0.379	-0.673	BRIC	0.338	-0.673
Environmental Hazard	1.212	-0.357	Environmental Hazard	1.215	-0.119

$0.05 \leq P < 0.1$ = *; $P < 0.05$ = **

Table 4.18 and 4.19 demonstrate the summary of all regressions of the floodplain areas. The R^2 and R^2-ADJ of OLS in all scenarios are approximately 0.2. The goodness of fit of OLS is substandard. After solving the spatial dependence of authentic flood events by SLM and SEM, the goodness of fit of regression has been improved dramatically. The R^2 and R^2-ADJ rise to approximately 0.5, while the AIC also has a dramatic change, meaning the goodness of fit of regression increased.

Although the coefficient shows the relationship between the SoVI correlates with authentic floods negatively, the *p*-value shows only the scenario of 200 mm of daily precipitation is significant. Most of the negative correlations between SoVI and authentic flood events are insignificant. The BRIC, on the other hand, shows a negative correlation between authentic flood events, meaning a higher BRIC value, with fewer flood events. Although the majority of BRIC coefficients show a negative correlation and fit with our presumption, based on the *p*-value, only the result of OLS shows a statistically significant negative correlation. The coefficient of the spatially lagged dependent variable (SL_EnvironmentalHazard and SL_Flood) and the spatially correlated errors (LAMBDA) also positively correlate with the authentic flood.

Based on the R^2 and R^2-ADJ, the goodness of fit of GWR has a better outcome compared to SLM and SEM. The goodness of fit has improved since the spatial nonstationarity has been solved. The R^2 of 350 mm is 0.725. In general, the R^2 is higher than SLM and SEM, while AIC has also dropped.

Table. 4.18 Summary of OLS, SLM, SEM, and GWR of floodplain areas (SERV)-1.

Floodplain areas					
OLS (200 mm)			OLS (350 mm)		
R^2	R^2-ADJ	AIC	R^2	R^2-ADJ	AIC
0.113	0.097	490.888	0.226	0.213	466.535
Variable	Coefficient	*p*-value	Variable	Coefficient	*p*-value
CONSTANT	-0.014	0.848	CONSTANT	-0.004	0.949
SoVI	-0.160	0.056*	SoVI	-0.049	0.527
BRIC	-0.141	0.054*	BRIC	-0.147	0.031**
Potential of Flood	0.226	0.006**	Potential of Flood	0.447	0.000**
TEST	VALUE	*p*-value	TEST	VALUE	*p*-value
Robust LM (lag)	1.223	0.269	Robust LM (lag)	1.975	0.160
Robust LM (error)	2.033	0.154	Robust LM (error)	1.523	0.217
SLM (200 mm)			SLM (350 mm)		
R^2	R^2-ADJ	AIC	R^2	R^2-ADJ	AIC
0.501	0.487	413.958	0.523	0.509	401.954
Variable	Coefficient	*p*-value	Variable	Coefficient	*p*-value
SL_EnvironmentalHaz	0.702	0.000**	SL_EnvironmentalHaz	0.653	0.000**
CONSTANT	-0.052	0.336	CONSTANT	-0.043	0.412
SoVI	-0.093	0.134	SoVI	-0.028	0.646
BRIC	-0.042	0.440	BRIC	-0.055	0.297
Potential of Flood	0.080	0.192	Potential of Flood	0.232	0.000**
SEM (200 mm)			SEM (350 mm)		
R^2	R^2-ADJ	AIC	R^2	R^2-ADJ	AIC
0.504	0.489	412.764	0.540	0.527	397.446
Variable	Coefficient	*p*-value	Variable	Coefficient	*p*-value
CONSTANT	-0.142	0.452	CONSTANT	-0.106	0.533
SoVI	-0.145	0.056*	SoVI	-0.105	0.151
BRIC	-0.003	0.956	BRIC	0.003	0.957
Potential of Flood	0.102	0.189	Potential of Flood	0.352	0.000**
LAMBDA	0.721	0.000**	LAMBDA	0.702	0.000**
GWR (200 mm)			GWR (350 mm)		
R^2	R^2-ADJ	AIC	R^2	R^2-ADJ	AIC
0.590	0.457	434.903	0.725	0.568	423.265
Variable	Coeff_MAX	Coeff_MIN	Variable	Coeff_MAX	Coeff_MIN
SoVI	0.630	-0.979	SoVI	0.921	-0.669
BRIC	0.273	-0.612	BRIC	0.452	-0.719
Potential of Flood	1.150	-1.135	Potential of Flood	1.559	-1.574

$0.05 \leq P < 0.1$ = *; $P < 0.05$ = **

Table. 4.19 Summary of OLS, SLM, SEM, and GWR of floodplain areas (SERV)-2.

Floodplain areas					
OLS (450 mm)			OLS (600 mm)		
R^2	R^2-ADJ	AIC	R^2	R^2-ADJ	AIC
0.239	0.226	463.520	0.276	0.264	454.534
Variable	Coefficient	*p*-value	Variable	Coefficient	*p*-value
CONSTANT	-0.004	0.956	CONSTANT	-0.002	0.978
SoVI	-0.042	0.587	SoVI	-0.021	0.785
BRIC	-0.142	0.035**	BRIC	-0.147	0.025**
Potential of Flood	0.464	0.000**	Potential of Flood	0.513	0.000**
TEST	VALUE	*p*-value	TEST	VALUE	*p*-value
Robust LM (lag)	3.380	0.066*	Robust LM (lag)	3.761	0.052*
Robust LM (error)	2.110	0.146	Robust LM (error)	2.420	0.120
SLM (450 mm)			SLM (600 mm)		
R^2	R^2-ADJ	AIC	R^2	R^2-ADJ	AIC
0.527	0.513	400.160	0.538	0.524	394.790
Variable	Coefficient	*p*-value	Variable	Coefficient	*p*-value
SL_EnvironmentalHaz	0.647	0.000**	SL_EnvironmentalHaz	0.628	0.000**
CONSTANT	-0.042	0.419	CONSTANT	-0.040	0.440
SoVI	-0.023	0.708	SoVI	-0.008	0.894
BRIC	-0.053	0.308	BRIC	-0.059	0.254
Potential of Flood	0.247	0.000**	Potential of Flood	0.287	0.000**
SEM (450 mm)			SEM (600 mm)		
R^2	R^2-ADJ	AIC	R^2	R^2-ADJ	AIC
0.546	0.533	395.037	0.560	0.548	388.950
Variable	Coefficient	*p*-value	Variable	Coefficient	*p*-value
CONSTANT	-0.100	0.555	CONSTANT	-0.089	0.586
SoVI	-0.100	0.171	SoVI	-0.084	0.244
BRIC	0.006	0.919	BRIC	0.005	0.933
Potential of Flood	0.375	0.000**	Potential of Flood	0.425	0.000**
LAMBDA	0.701	0.000**	LAMBDA	0.696	0.000**
GWR (450 mm)			GWR (600 mm)		
R^2	R^2-ADJ	AIC	R^2	R^2-ADJ	AIC
0.648	0.534	407.983	0.624	0.520	407.689
Variable	Coeff_MAX	Coeff_MIN	Variable	Coeff_MAX	Coeff_MIN
SoVI	0.617	-0.621	SoVI	0.552	-0.554
BRIC	0.337	-0.649	BRIC	0.296	-0.559
Potential of Flood	1.273	-0.725	Potential of Flood	1.223	-0.104

$0.05 \le P < 0.1$ = *; $P < 0.05$ = **

Table 4.20 demonstrates the result of the multivariate regression of mountain areas. The dependent variable used in the regression is authentic debris flows. Based on the coefficient, the result of the mountain areas seems to fit our expectations. The SoVI is positively correlated to an authentic debris flow in all regressions, meaning the individuals or groups with poor socioeconomic status encounter more debris flows. The BRIC, on the other hand, shows a negative correlation to authentic debris flows in all regressions. In other words, the individuals or groups with better socioeconomic status encounter fewer debris flows. Moreover, based on the *p*-value, the relationships between SoVI, BRIC, and authentic debris flows are statistically significant. However, the R^2 and R^2-ADJ show the goodness of fit of all regressions is extremely low; none of them can reach 0.2, except for GWR. AIC also indicates the same result.

Table. 4.20 Summary of OLS, SLM, SEM, and GWR in mountain areas (SERV).

Mountain areas					
OLS			SEM		
R^2	R^2-ADJ	AIC	R^2	R^2-ADJ	AIC
0.120	0.094	158.240	0.114	0.025	158.189
Variable	Coefficient	*p*-value	Variable	Coefficient	*p*-value
CONSTANT	0.000	1.000	CONSTANT	0.000	0.997
Potential of DF	-0.041	0.762	Potential of DF	-0.027	0.838
SoVI	0.268	0.048**	SoVI	0.281	0.027**
BRIC	-0.250	0.074*	BRIC	-0.267	0.044**
TEST	VALUE	*p*-value	LAMBDA	-0.058	0.733
Robust LM (lag)	12.284	0.000**			
Robust LM (error)	12.013	0.001**			
SLM			GWR		
R^2	R^2-ADJ	AIC	R^2	R^2-ADJ	AIC
0.121	0.033	159.863	0.275	0.154	156.437
Variable	Coefficient	*p*-value	Variable	Coeff_MAX	Coeff_MIN
SL_Debris	0.113	0.477	SoVI	0.362	0.104
CONSTANT	0.007	0.957	BRIC	-0.088	-0.337
Potential of DF	-0.063	0.630	Potential of DF	0.037	-0.215
SoVI	0.258	0.041**			
BRIC	-0.242	0.066*			

$0.05 \le P < 0.1$ = *; $P < 0.05$ = **

CHAPTER 5
CONCLUSION

Due to the location of Taiwan, environmental hazards such as debris flows and floods are remarkably common. As a result, nowadays, disaster management has become an extremely crucial task for Taiwan's government. Environmental hazards generally cause more damage to individuals or groups who are more vulnerable. The effects of environmental hazards are not random. As a result, the concept of social vulnerability was developed based on the hazard-of-place model. According to the hazard-of-place model, vulnerability represents potential losses dues to environmental hazards. Both the geographic context and social vulnerability to environmental hazards contribute to the damage of environmental hazards. In order to measure the social vulnerability to environmental hazards, SoVI is created. Based on the disadvantageous aspects of socioeconomic variables, SoVI can be calculated and stand for social vulnerability to environmental hazards.

On the other hand, according to the theory of resilience proposed by Holling (1973), after encountering an environmental hazard, recovery is necessary for the system, society, and community to move on. Based on experience and learning, humans have co-evolved with environmental hazards. Therefore, each time a human encounters an environmental hazard, it is an opportunity to move forward. Therefore, the ability to recover and co-evolve are notable elements of how humans face environmental hazards. However, the extent of recovery and co-evolution with the environmental hazards are strongly correlated to the inherent resilience. In order to measure the inherent resilience, BRIC was developed based on the DROP model. Through the specific positive aspects of socioeconomic variables, BRIC can be computed and can represent a community's inherent resilience to environmental hazards.

Based on the theory of vulnerability and resilience, we have collected particular socioeconomic variables and constructs, i.e., SoVI and BRIC. Through GIS technology, we can not only visualize the SoVI and BRIC but explore the patterns of spatial distribution. In the scope of the entire Yilan County, mountain areas not only have H-H clusters of SoVI values but also L-L clusters of BRIC. In other words, the mountain areas might be the most vulnerable areas to environmental hazards. Moreover, for mountain areas, it is comparatively challenging to recover from environmental hazards since the value of BRIC is relatively mediocre compared to other areas in Yilan County.

In the floodplain areas, the center areas have L-L clusters of SoVI. This distribution pattern means the central floodplain areas are less vulnerable to environmental hazards compared to other floodplain areas. Moreover, among the central floodplain areas, two of the most prosperous urban areas, Yilan City and Luodong Township, are the H-H clusters according to BRIC. In other words, Yilan City and Luodong Township have higher inherent resilience. Generally speaking, the center of the floodplain areas seems to be less vulnerable to environmental hazards and might recover from environmental hazards more easily.

In the mountain areas, the spatial patterns of SoVI and BRIC are relatively insignificant. Although Moran's *I* of SoVI shows a statistically significant cluster, the result of LISA shows the majority of mountain areas do not have a specific cluster. That is to say, most of the mountain areas have comparatively similar SoVI values. On the other hand, Moran's *I* of BRIC shows a relatively random distribution, meaning the BRIC values in mountain areas do not have a particular distribution pattern. The LISA result of BRIC also shows a similar result.

Based on the hazard-of-place model, the vulnerability to environmental hazards is composed of geographic context and social vulnerability to environmental hazards. The matrix of risk is applied in order to combine the geographic context and social vulnerability to environmental hazards. Based on the literature review, this research takes the potential for flooding and debris flows as the geographic context terms. As for the social vulnerability to environmental hazards, SoVI is applied. We use the matrix of risk to combine environmental hazard potential and SoVI. The Moran's *I* of risk on the county-wide scale shows a statistically significant cluster in four different levels of potential for environmental hazards. Through LISA, we found that on the county-wide scale, mountain areas have the largest H-H cluster of risk, while the areas in the northwest floodplain areas have the largest L-L cluster of risk.

In floodplain areas, the Moran's *I* of risk shows four significant clusters under four different levels of potential for floods. According to LISA, the northern and southern areas of the floodplain are generally H-H clusters of risk. In other words, in these two areas, the risk is higher than in other areas in the floodplain. Most of the southwestern floodplain areas are L-L clusters due to the location.

In the mountain areas, Moran's *I* of risk also shows a statistically significant cluster. The result of LISA shows there are two H-H clusters in the mountain areas. The larger one is located in the southwestern part of the mountain areas, while the second H-H cluster is close to the eastern part of the mountain areas.

To combine the potential for environmental hazards, SoVI, and BRIC, the SERV model is applied. By integrating these three indices, we can offer a holistic index to evaluate vulnerability and resilience. On a county-wide scale, Moran's *I* of SERV shows the SERV is significantly clustered no matter under which extent of environmental hazard potential. LISA shows the H-H cluster of SERV is located in the mountain areas, while the L-L cluster is located around Yilan City and Luodong Township. This distribution means the mountain areas have a higher vulnerability and lower inherent resilience. As for the Yilan City and Luodong Township, the vulnerability is lower, and the inherent resilience is higher than in the mountain areas.

In the floodplain areas, Moran's *I* indicates the SERV is significantly clustered. According to the result of LISA, the northern parts of the floodplain areas are H-H clusters, while some of the southern parts are also H-H clusters. The areas around Yilan City and Luodong Township are still L-L clusters. In other words, the northern part of the floodplain areas has higher vulnerability and lower inherent resilience. The areas around Yilan City and Luodong Township have less vulnerability but higher inherent resilience.

In the mountain areas, the Moran's *I* of SERV shows the distribution is relatively random. Also, the result of LISA shows no significant clusters, only some outliers. It seems the distribution of SERV in mountain areas is relatively random compared to the distribution in floodplain areas.

In order to validate the effectiveness of the indices, we apply multivariate regression. Generally speaking, most of the components of SoVI show a negative correlation with authentic environmental hazards. The goodness of fit of floodplain areas is the best among the three different areas. The R^2 and R^2-ADJ of OLS are not ideal; after solving the spatial dependence and spatial nonstationarity through SLM, SEM, and GWR, the goodness of fit of regression is improved and acceptable. The R^2 and R^2-ADJ of GWR reach 0.7 and 0.6

As for BRIC, the majority of components fit our expectations. The individuals or groups with higher socioeconomic status are negatively correlated with environmental hazards. Also, after solving the spatial dependence and spatial nonstationarity through SLM, SEM, and GWR, the goodness of fit of regression is improved and acceptable.

The regression of risk shows that the potential for environmental hazards has a significantly positive correlation with authentic hazards. However, SoVI shows a negative correlation with environmental hazards, meaning that individuals or groups with poor socioeconomic status have less chance of encountering environmental hazards. This result does not fit our expectations. Moreover, the goodness of fit of SLM, SEM, and GWR are acceptable since the spatial dependence and spatial nonstationarity have been resolved.

Last but not least, the regression of SERV, through the coefficients, shows that both SoVI and BRIC present negative correlations with environmental hazards.

Although the SoVI does not fit with our expectations, the BRIC does coincide with our expectations. However, the result of GWR of the floodplain areas has the second-highest R^2 and R^2-ADJ, 0.7 and 0.5, respectively. The results of SLM, SEM, and GWR are acceptable.

REFERENCES

Adger W.N., Brooks N., Bentham G., Agnew M., and Eriksenet S. (2004). *New indicators of vulnerability and adaptive capacity.* Tyndall Centre for Climate Change Research, Norwich, United Kingdom.

Adger W. N. (2006). Vulnerability. *Global Environmental Change*, 16(3):268-281.

Anselin, L. (1988). *Spatial Econometrics: Methods and Models.* Kluwer Academic Publishers*,* Dordrecht, Netherlands.

Anselin, L. (1995). Local indicators of spatial association-lisa. *Geographical Analysis*, 27:93-115.

Anselin, L. (2005) *Exploring Spatial Data with DeoDa: A Workbook.* Center for Spatially Integrated Social Science, Santa Barbara, United States.

Bakkensen, L. A., Lent, C. F., Read, L. K., and Linkov, I. (2016). Validating Resilience and Vulnerability Indices in the Context of Environmental Disasters. *Risk Analysis*, 37(5):982-1004.

Balica, S. F., Wright, N. G., and van der Meulen, F. (2012). A Flood Vulnerability Index for Coastal Cities and Its Use in Assessing Climate Change Impacts. *Environmental Hazards*, 64(1):73-105.

Burton, C. G. (2015). A Validation of Metrics for Community Resilience to Environmental Hazards and Disasters Using the Recovery from Hurricane Katrina as a Case Study. *Annals of the Association of American Geographers*, 105(1):67-86

Carpenter, S., Walker, B., Anderies, J. M., and Abel. N. (2001). From Metaphor to Measurement: Resilience of What to What? *Ecosystems*, 4(8):765-781.

Chang, L. F., and Huang, S. Li. (2015). Assessing urban flooding vulnerability with an emergy approach. *Landscape and Urban Planning*, 143:11-24.

Costa, L., and Kropp, J. P. (2013). Linking Components of Vulnerability in Theoretical Frameworks and Case Studies. *Sustainability Science*, 8(1):1-9.

Cutter, S. L. (1996). Vulnerability to environmental hazards. *Progress in Human Geography*, 20(4):529-539.

Cutter, S. L. (2016). The landscape of disaster resilience indicators in the USA. *Environmental Hazards*, 80:741-758.

Cutter, S. L., and Emrich, C. T. (2006). Moral hazard, social catastrophe: The changing face of vulnerability along the hurricane coasts. *The Annals of the American Academy of Political and Social Science*, 604(1):102-112.

Cutter, S. L., and Finch, C. (2008). Temporal and spatial changes in social vulnerability to environmental hazards. *Proceedings of the National Academy of Sciences*, 105(7):2301-2306.

Cutter, S. L., Ash, K. D., and Emrich, C. T., (2014). The geographies of community disaster resilience. *Global Environmental Change*, 29:65-77.

Cutter, S. L., Ash, K. D., and Emrich, C. T., (2016). Urban-Rural Differences in Disaster Resilience. *Annals of the American Association of Geographers*, 106(6)1236-122.

Cutter, S. L., Barnes, L., Berry, M., Burton, C. G., Evans, E., Tate, E., and Webb, J., (2008). A place-based model for understanding community resilience to environmental disasters. *Global Environmental Change*, 18:598-606.

Cutter, S. L., Boruff, B. J., and Shirley, W. L. (2003). Social vulnerability to environmental hazards. *Social Science Quarterly*, 84(2):242-261.

Cutter, S. L., Burton, C. G., and Emrich, C. T. (2010). Disaster resilience indicators for benchmarking baseline conditions. *Journal of Homeland Security and Emergency Management*, 7(1):1-22

Cutter, S. L., Emrich, C. T., Webb, J. J., and Morath, D. (2009). Social vulnerability to climate variability hazards: A review of the literature, *Final Report to Oxfam America*, 5.

Doorn, N. (2015). Resilience indicators: opportunities for including distributive justice concerns in disaster management. *Journal of Risk Research*, 20(6):711-731.

Działek, J., Biernacki, W., Fiedeń, Ł., Franczak, K. L., and Franczak, P. (2016). Universal or context-specific social vulnerability drivers - Understanding flood preparedness in southern Poland. *International Journal of Disaster Risk Reduction*, 19:212-223.

Fekete, A. (2009). Validation of a social vulnerability index in context to river-floods in Germany. *Environmental Hazards and Earth System Sciences*, 9:393-403

Fotheringham, A. S., Charlton, M. E., and Brunsdon, C. (1998). Geographically weighted regression: a environmental evolution of the expansion method for spatial data analysis. *Environment and Planning A,* 30:1905-1927.

Frazier, T. G., Thompson, C. M., Dezzani, R. J., and Butsick, D. (2013). Spatial and temporal quantification of resilience at the community scale. *Applied Geography*, 42:95-107.

Frazier, T. G., Thompson, C. M., and Dezzani, R. J. (2014). A framework for the development of the SERV model: A Spatially Explicit Resilience-Vulnerability model. Applied Geography, 52:158-172.

Frigerio, I., and Amicis, M. D. (2016). Mapping social vulnerability to environmental hazards in Italy: A suitable tool for risk mitigation strategies. *Environmental*

Science & Policy, 63:187-196.

Frigerio, I., Ventura, S., Strigaro, D., Mattavelli, M., Amicis, M. D., Mugnano, S., and Boffi, M. (2016). A GIS-based approach to identify the spatial variability of social vulnerability to seismic hazard in Italy. *Applied Geography*, 74:12-22.

Holling, C.S. (1973). Resilience and Stability of Ecological Systems. *Annual Review of Ecology and Systematics*, 4:1-23.

Hung, L. S., Wang, C., and Yarnal, B. (2016). Vulnerability of families and households to environmental hazards: A case study of storm surge flooding in Sarasota County, Florida. *Applied Geography*, 76:184-197.

IPCC. (2007). *Technical Summary: Chap. 20 in Climate Change 2007: Impacts, Adaptation and Vulnerability. Contribution of Working Group II to the Fourth Assessment Report of the Intergovernmental Panel on Climate Change*. Cambridge University, Cambridge, United Kingdom.

Jordan, E., and Javernick, W. A. (2013). Indicators of Community Recovery: Content Analysis and Delphi Approach. *Environmental Hazards Review*, 14(1):21-28.

Khan, S. (2012). Vulnerability assessments and their planning implications: a case study of the Hutt Valley, New Zealand. *Environmental Hazards*, 64(2):1587-1607.

Klein, R. J. T., Nicholls, R. J. and Thomalla, F. (2003). Resilience to Environmental Hazards: How Useful is This Concept? *Environmental Hazards*, 5(1):35–45.

Lee, Y.J. (2014). Social vulnerability indicators as a sustainable planning tool. *Environmental Impact Assessment Review*, 44:31-42.

Mayunga, J.S. (2007). *Understanding and Applying the Concept of Community Disaster Resilience: A Capital-Based Approach*. Draft working paper prepared for the summer academy, Megacities as Hotspots of Risk: Social Vulnerability and Resilience Building, Munich, German.

McCarthy, J.J., Canziani, O.F., Leary, N.A., Dokken, D.J. and White, K.S. (2001). *Climate change 2001: impacts, adaptation, and vulnerability.* Cambridge University, Cambridge, United Kingdom.

McLaughlin, S., and Cooper, J. A. G. (2010). A Multi-scale Coastal Vulnerability Index: A Tool for Coastal Managers? *Environmental Hazards-Human and Policy Dimensions*, 9(3):233-248.

Moran, P.A.P. (1948). The interpretation of statistical maps, *Journal of the Royal Statistics Society, Series B (Methodological),* 10(2):243-251.

Moran, P.A.P. (1950). Notes on continuous stochastic phenomena, *Biometrika*, 37:17-23.

Norris, F. H., Stevens, S. P., Pfefferbaum, B., Wyche, K. F., and Pfefferbaum, R. L.

(2008). Community Resilience as a Metaphor, Theory, Set of Capacities, and Strategy for Disaster Readiness. *American Journal of Community Psychology*, 41(1-2):127-150.

Peacock, W.G., Brody, S. D., Seitz, W. A., Merrell, W. J., Vedlitz, A., Zahran, S., Harriss, R.C., and Stickney. R. (2010). *Advancing Resilience of Coastal Localities: Developing, Implementing, and Sustaining the Use of Coastal Resilience Indicators: A Final Report.* Final report for NOAA CSC grant no. NA07NOS4730147. College Station, TX: Hazard Reduction and Recovery Center, Houston, United States.

Prior, T., and Hagmann, J. (2014). Measuring Resilience: Methodological and Political Challenges of a Trend Security Concept. *Journal of Risk Research*, 17(3):281-298.

Rygel, L., O'sullivan, D., and Yarnal, B. (2006). A method for constructing a social vulnerability index: An application to hurricane storm surges in a developed country. *Mitigation and Adaptation Strategies for Global Change*, 11(3):741－764.

Sherrieb K., Norris F, and Galea, S. (2010). Measuring capacities for community resilience. *Social Indicators Research*, 99:227-247.

Siagian, T.H., Purhadi, P., Suhartono, S. and Ritonga, H. (2014). Social vulnerability to environmental hazards in Indonesia: driving factors and policy implications. *Environmental Hazards*, 70: 1603-1617.

Tate, E. (2012). Social vulnerability indices: a comparative assessment using uncertainty and sensitivity analysis. *Environmental Hazards*, 63(2):325-347.

Thomalla, F., Downing, T., Spanger, S. E., Han, G. Y., and Rockström. J. (2006). Reducing Hazard Vulnerability: Towards a Common Approach between Disaster Risk Reduction and Climate Adaptation. *Disasters*, 30(1):39-48.

Twigger-Ross, C., Kashefi, E., Weldon, S., Brooks, K., Deeming, H., Forrest, S., and Tapsell, S. M. (2014). *Flood Resilience Community Pathfinder Evaluation: Rapid Evidence Assessment*. Department for Environment Food & Rural Affairs, London, United Kingdom.

Uitto, J.I. (1998). The geography of disaster vulnerability in megacities: A theoretical framework. *Applied Geography,* 20(1): 7-16.

UNDP (2014). *Understanding community resilience: findings from community-based resilience analysis (CoBRA) assessments*. Drylands Development Centre, UNDP, Nairobi, Kenya.

Wang, C.K. (2004). Features of Monsoon, Typhoon and Sea Waves in the Taiwan Strait. *Marine Georesources & Geotechnology*, 22(3):133-150.

Wang, C., and Yarnal, B. (2012). The vulnerability of the elderly to hurricane hazards in Sarasota, Florida. *Environmental Hazards*, 63:349-373.

Wardekker, J. A., Jong, A. D., Knoop, J. M., and Van der Sluijs, J. P. (2010). Operationalising a Resilience Approach to Adapting an Urban Delta to Uncertain Climate Changes. *Technological Forecasting & Social Change*, 77(6):987-998.

Winderl, T. (2014). *Disaster resilience measurements: stocktaking of ongoing efforts in developing system for measuring resilience.* UNDP.

Wood, N. J., Burton, C. G., and Cutter, S. L. (2010). Community variations in social vulnerability to Cascadia-related tsunamis in the U.S. Pacific Northwest. *Environmental Hazards*, 52(2):369-389.

Yoon, D. K., Kang, J. E., and Brody, S. D. (2016). A measurement of community disaster resilience in Korea. *Journal of Environmental Planning and Management,* 59(3):436-460.

Zebardast, E. (2013). Constructing a social vulnerability index to earthquake hazards using a hybrid factor analysis and analytic network process (F’ANP) model. *Environmental Hazards*, 65(3):1331-1359.

謝　　辭

感謝恩師 廖學誠教授從碩士時期開始的栽培與教導。拜入老師門下近 10 年，不論是在學術、待人接物及人生規劃上均受益良多，承蒙老師的指導、啟蒙與教育，讓學生的論文得以順利開展與發表，在老師的鼓勵下讓學生能夠直面每個博士班學生均會面對的就業難題，並順利的在入學第二年即取得一份安穩、收入不斐的公職。感謝老師的幫忙，讓我取得科技部千里馬計畫及前往 UBC 森林學院研究的機會，赴外研究期間著實認識了自身的不足、缺陷以及與國外博士生的巨大差距，未來更需要努力精進自己，就如同老師常與學生分享的那句話：「百尺竿頭，更進一步。」。

感謝國立政治大學地政學系詹進發老師、逢甲大學都市計畫與空間資訊學系莊永忠老師、本系郭乃文老師以及本系王聖鐸老師，在一發、二發以及口試時精闢的建議與指導，多虧老師們的建議與指導，讓論文能夠順利地刊登在三篇不同的 SCI/SSCI 期刊上。感謝本系周學政老師、陳哲銘老在相關技術上的幫忙與支持；感謝林和駿博士、謝偉民博士、哈勇·諾幹博士與翁淑娟博士所提供的所有幫忙與陪伴；特別感謝莊永忠老師以及詹進發老師，在學生於 UBC 訪問研究時提供許多遙航測之建議、幫助以及相關資料。

感謝雲林縣北港地政事務所主任楊昆庭、課長吳明權、劉浚育測量員、吳伯貞測量員、陳彥廷測量員、陳�羽測量員、時任技佐郭家宏在工作業務上、案件分配以及相關行政流程上許多的幫忙與支持。特別感謝劉浚育測量員、吳伯貞測量員於論文投稿時圖案美編、圖幅整飾的相關專業知識、技術。

感謝父親、母親、兄長與家族成員在我就學期間的幫忙，感謝我的妻子王憶婷女士給予的幫忙與鼓勵，更感謝她在我就讀博士期間的包容，無私的付出讓我能夠順利的完成學業。

沒有老師們、同事們及學長姐們的鼎力相助，完成此文勢必困難重重，感謝一路上曾幫助過我的您們，僅以此文獻上我對您們無上的感激與祝福。20 年後，若有幸我的女兒能夠讀到這篇論文，希望您能夠將「百尺竿頭，更進一步。」奉為您人生中的圭臬，這句話曾經激勵即將初為您父親的我無數次，希望您能將這句話謹記於心頭。

宋健豪 謹誌於 師大地理學系

2022 年　夏